Performance of micro and nano engineered high volume fly ash cement composite

A thesis submitted in fulfilment of the requirements for the degree of

Doctor of Philosophy

by

Rajeev Roychand

School of Engineering

College of Science Engineering and Health

RMIT University, Melbourne, Australia

March 2017

Declaration

I certify that except where due acknowledgement has been made, the work is that of the author alone; the work has not been submitted previously, in whole or in part, to qualify for any other academic award; the content of the thesis is the result of work which has been carried out since the official commencement date of the approved research program; any editorial work, paid or unpaid, carried out by a third party is acknowledged; and, ethics procedures and guidelines have been followed. I acknowledge the support I have received for my research through the provision of an Australian Government Research Training Program Scholarship

Rajeev Roychand

March 2017

Acknowledgements

I would like to express my sincere and deep gratitude to my supervisors, Dr Saman De Silva and Prof. Sujeeva Setunge who gave me an opportunity to do a PhD under their expert guidance and have supported me throughout my PhD. I will always be indebted to them for the intellectual, moral and financial support they provided during the course of my PhD candidature. I would also like to express my gratitude to Dr. David Law for his expert guidance, critical feedback and dedicated support at every stage of my PhD candidature. I am extremely happy that because of their support I am able to submit my thesis on time, in spite of various challenges I had to go through during my PhD candidature.

I would like to thank the civil engineering laboratory staff: Mr Pavel Ryjkov, Mr Xiang Gao and Mr Shamir Bhuiyan for their great help and support in using various laboratory instruments and materials. I would also like to thank Mr Frank Antolasic (x-ray facility), Dr Muthu Pannirselvam (rheology and material characterisation facility), Mr Phil Francis and other laboratory staff (microscopy and microanalysis facility) for their technical support in using the advanced material characterisation instruments and techniques.

Many thanks to my fellow colleagues: Biplob Kumar Pramanik, Sivanandan Balakrishnan, Muhammad Wasim, Arie Wardhono and Rahmat Dirgantara for their great friendship and for making the research environment full of fun and learning.

I wish to extend my deepest gratitude and dedicate my thesis to my parents, my wife and my little daughter Sara. My family has been of tremendous support during the various challenging times of my PhD candidature. I am indebted to their support, sacrifice and understanding. The naughty and cheerful welcome by my little daughter has always been my biggest stress relievers after my daylong strenuous research activities. Thanks to my whole family for all their love and support. Last but not the least; I thank the almighty god who always paved the way for me whenever I faced the most challenging circumstances with strong determination and perseverance.

List of Publications

1. **Rajeev Roychand**, Saman De Silva, David Law and Sujeeva Setunge (2016). Micro and nano engineered high volume ultrafine fly ash cement composite with and without additives. International journal of concrete structures and materials 10(1), 113–124 http://link.springer.com/article/10.1007/s40069-015-0122-7

2. **Rajeev Roychand**, Saman De Silva, David Law and Sujeeva Setunge (2016). High volume fly ash cement composite modified with nano silica, hydrated lime and set accelerator. Materials and Structures 49(5), 1997–2008 http://link.springer.com/article/10.1617/s11527-015-0629-z

3. **Rajeev Roychand**, Saman De Silva, Sujeeva Setunge and David Law (2017). A quantitative comparative study on the effect of nano SiO_2, nano Al_2O_3 and nano $CaCO_3$ on the physicochemical properties of very high volume fly ash cement composite. (Under peer review process)

4. **Rajeev Roychand**, Saman De Silva and Sujeeva Setunge (2017). Nano engineered zero cement composite. (Under peer review process)

Table of Contents

List of Figures

List of Tables

List of Abbreviations

Materials

CNS	Colloidal nano silica
FA	Fly ash
GGBFS	Ground granulated blast furnace slag
HL	Hydrated lime
HVFA	High volume fly ash
HV-UFFA	High volume ultra fine fly ash
nA	Nano alumina
nCC	Nano calcium carbonate
nS, NS	Nano silica
OPC	Ordinary portland cement
SA	Set accelerator
SCM	Supplementary cementitious material
SF	Silica fume
SP	Superplasticizer

Material Characterisation Techniques

TGA	Thermogravimetric analysis
DTG	Derivative thermogravimetry
SEM	Scanning electron microscopy
XRD	X-ray diffraction

Mineral Phases

AFm	Al_2O_3 - Fe_2O_3 - mono (family of hydrated calcium aluminate phases)
C_3A	Tri calcium Aluminate
C_4AF	Tetra calcium Aluminoferrite
C-A-H	Calcium alumino hydrate
C_3AH_6	Tri calcium alumino hydrate
C-A-S-H	Calcium alumino silicate hydrate
CC	Calcium carbonate

CH	Calcium hydroxide
C_2S	Di calcium silicate
C_3S	Tri calcium silicate
C-S-H	Calcium silicate hydrate
Hc	Hemi-carboaluminate
Mc	Mono-carboaluminate

Measurement units

℃	degree celcius
g	gram
kV	kilo volt
mA	milli ampere
mg	milli gram
mL	milli litre
mL Kg^{-1}	milli litre per kilogram
mm	millimeter
MPa	Mega pascal
nm	nano meter
μm	micro meter
2θ	2-theta

Other abbreviations

Cu-Kα	Copper - K alpha
S/B :	Sand to binder ratio
W/B :	Water to binder ratio

Thesis outline

This thesis is organized into the following sections, as described below:

Thesis summary briefly describes; the real world problem that forms the focus of this research, the status of past research undertaken to address this problem, then formulates the aim, identifies the research gap and finally presents the overview of the results of various experiments undertaken to fill up the researchgap.

Chapter 1 is an introductory chapter which presents the background of the research, develops research aim that broadly defines the research area and outlines the scope of research.

Chapter 2 presents the detailed literature review on the broadly defined research area and identifies the research gap.

Chapter 3 presents the design, methodology and the results of the first experiment on the identified research gap. The first experiment looks at the effect of silica fume, nano silica, set accelerator and hydrated lime on high volume ultrafine fly ash cement composites replacing 80% of ordinary Portland cement. Raw fly ash was micronized using Sturtevant jetmill micronizer to produce ultrafine fly ash.

Chapter 4 presents the design, methodology and the results of the second parallel experiment on the effect of different concentrations of nano silica on high volume fly ash cement composites with and without the use of set accelerator and hydrated lime. The cement replacement level in this experiment was 70% and the fly ash used was raw fly ash.

Chapter 5 presents the design, methodology and the results of the third experiment on the quantitative comparative study of the effect of different nano materials on high volume fly ash cement composites, replacing 80% of OPC. The various nano materials used were nano silica, nano alumina and nano calcium carbonate. To investigate the physicochemical behaviour of various nano engineered mix designs in detail, the quantitative phase analysis was undertaken with the help of thermogravimetric analysis in conjunction with the XRD quantitative rietveld analysis (external standard method). In addition, nitrogen adsorption/desorption analysis was undertaken to study the effect of different nano materials on the porosity of the cement matrix of various mix designs.

Chapter 6 presents the design, methodology and the results of the fourth experiment on zero cement composite. This experiment was designed to replace 100% of ordinary Portland cement. Based on the previous experiments, nano silica proved to be the most effective in improving the properties of high volume fly ash cement composites, therefore nano silica was used in different concentrations in this experiment. The other materials used were high volume raw fly ash, ground granulated blast furnace slag and hydrated lime. Various material characterisation techniques used were (i) SEM for the microstructure studies and (ii) thermogravimetric analysis in conjunction with XRD analysis using rietveld refinement external standard method to study the quantitative phase analysis of the various phases formed within the cement matrix of various mix designs.

Chapter 7 presents the overall conclusion of the whole experimental program undertaken in this research and provides the recommendations for future research that can be undertaken as an extension of the present work.

Summary

Fly ash, a byproduct of coal-fired thermal power plants is considered an environmental pollutant if it is to be disposed of and requires considerate financial liabilities on fly ash producers for its safe disposal. But fortunately, because of its physical and chemical properties, it has found applications in many fields; like mineral extraction, soil stabilization, waste treatment and as a supplementary cementitious material. As cement industry is responsible for 5-7% of global greenhouse gas emissions, application of fly ash as a cement replacement material provides the dual benefit of cutting down the greenhouse gas emissions and in increasing the utilization rate of fly ash produced worldwide. The majority of global fly ash production falls under class F low calcium category, which has low reactivity. Therefore to improve the performance of fly ash blended cement composites, the researchers have looked at many ways like; reducing the particle size, making use of hydrated lime, silica fume, and Metakaolin, etc. Recently, the use of nanomaterials has been gaining widespread attention of the research community due to their small particle size and high reactivity that help in improving the properties of the concrete at the nanoscale level. The majority of the past research on low calcium, class F fly ash cement composites, concentrated on 60% or less of fly ash content and there is a great potential for the further improvement in replacement levels. Therefore, our research aimed at developing a cement composite that not only increases the percentage of fly ash content but also considerably increases the cement replacement level having comparable mechanical properties to that of ordinary portland cement (OPC).

Based on the review of existing literature, there appeared to be no research available that investigates the effect of micro (silica fume) and nano silica in combination with hydrated lime and set accelerator on high volume fly ash (HVFA) cement composite replacing 80% of cement. Therefore, our first study was undertaken to fill up this knowledge gap. The fly ash used in this study was micronised using Sturtevant jet mill micronisер to produce ultra fine fly ash (UFFA). The research findings show that when UFFA is partially replaced with silica fume (SF) and used in combination with both the set accelerator (SA) and hydrated lime (HL), there is a considerable improvement in its pozzolanic activity resulting in large improvement in its 7 and 28 day compressive strength. On the contrary, nano silica (nS)

modified HV-UFFA performed better when used without the SA and HL, resulting in significantly improving its 7 and 28 day compressive strength. The strength achieved at 28 days was at par with that of OPC. The addition of SA and HL to nS modified HV-UFFA blend resulted in the development of high early age microcracking, thereby considerably reducing its 28 day strength compared to that of nS, HV-UFFA and OPC blend not containing HL and SA.

The second experiment was planned to look at the effect of different concentrations of nS on raw HVFA cement blends with and without SA and HL, replacing 70% of cement. The difference in experiment 2 compared to experiment 1 were (i) raw fly ash was used in experiment 2 in lieu of UFFA as micronising fly ash consumes electricity that adds to the carbon footprint (ii) two concentrations of nano silica were used i.e. 5 and 7.5% to study the effect of increase in nano silica content on HVFA cement composite. The fly ash content was partially replaced with 5 and 7.5% of nS and 5% HL. The results show that the 7 day strength increased with the increasing amount of nano silica. However, at 28 days both the samples showed approximately the similar improvement in strength. With the addition of set accelerator to nano silica modified HVFA cement blends, there was a considerable reduction in 7 and 28 day compressive strength results. Addition of HL to HVFA cement blend, containing 5% nS showed no effect on its further strength development. However, when HL was added to the 7.5% nS modified HVFA cement coposite, a considerable reduction in its 7 and 28 day compressive strength results were observed. This shows that nS is highly effective in improving the strength of HVFA cement composites when used alone without any additives, but when it is used in combination with either HL or SA, shows no or negative effect on the development of compressive strength of raw fly ash blended cement composites.

Looking at the significant improvement in the strength results of HVFA cement composites by incorporating nano silica, the next experiment was planned to looking at the effect of other nano materials on HVFA cement composites. As the major elemental oxides present in OPC are SiO_2, CaO and Al_2O_3. This experiment was planned to incorporate the nano sized sources of these elemental oxides. Since the reaction of pure CaO is highly thermal in nature and addition of nano CaO would have been highly exothermic and could have introduced high thermal stresses at early ages of curing, nano $CaCO_3$ was used as a source of CaO. Therefore, the third experiment plan looked at a quantitative comparative study of the effect

of 5% and 7.5% of nano silica, 2.5% and 5% of nano alumina (nA) and 2.5% and 5% of nano calcium carbonate (nCC), on the properties of HVFA cement composites, replacing 80% of cement. The results show that the addition of nS significantly improves the compressive strength of HVFA cement composites and considerably increases the formation and thermal stability of silica-rich hydrogarnet phase, which increases with the increase in nS content. The addition of nCC to HVFA cement composite does not show any effect on the pozzolanic reaction at 7 days of curing but at 28 days considerably improves its pozzolanic reaction, which increases with the increase in nCC content. The performance of nCC in improving the mechanical properties is less pronounced than that of nS. The addition of nA though improves the hydration/pozzolanic reaction of HVFA cement composite, resulting in the improvement in compressive strength, but only if added in small quantities (2.5% or less). If it is added in higher amounts, it promotes the formation of $Al(OH)_3$ gel that severely inhibits the hydration/pozzolanic reaction within the cement matrix.

Based on the knowledge gained from the previous experiments, we found that the amorphous nano silica holds a great potential for the development of zero cement composite. That motivated us to design our fourth experiment, replacing 100% of cement. In the fourth experiment we replaced OPC with slag, which is another industrial by product. Zero cement mix designs were developed incorporating slag, HVFA and various concentrations of nano silica and hydrated lime. The results show that the optimum content of nano silica in a high volume fly ash, slag and HL blend is 5%. With a further increase in nano silica content although the pozzolanic reaction and the resulting C-S-H/C-A-S-H gel formation increases but it also increase the micro-cracking within the cement matrix, resulting in negatively impacting the strength development. The portlandite added externally in the form of $Ca(OH)_2$ powder, to the nS modified SCM blend, activates the pozzolanic reaction which increases with the increase in portlandite content. The best mix design containing 5% nS, 70% FA and 25% slag in combination with 15% HL as an additive, achieved a 28 day compressive strength of 70% compared to that of OPC.

It is to be noted that though this research aimed at minimising the carbon footprint of the cement composites, it was not completely eliminated. The various raw materials that have CO_2 emissions associated with their production are listed below:

Nano silica – As per the information provided by the supplier of Nano silica, it was produced by pyrogenic method, which is highly energy intensive process. It is produced from the flame hydrolysis of silicon tetrachloride ($SiCl_4$) at ~1800 °C temperature.

Calcium hydroxide – Calcium hydroxide is produced commercially by treating lime (CaO) with water (H_2O). The CaO used in this process is produced by the de-carbonation of limestone ($CaCO_3$), which releases CO2 into the atmosphere during production.

Ultrafine fly ash (UFFA) – Though fly ash is a by-product of thermal power plants using coal as a fuel, micronizing the fly ash (i.e. reducing the particle size of the raw fly ash) is an energy intensive process. The Sturtevant jet mill microniser used to reduce the particle size of the raw fly ash runs on electricity which otherwise is produced primarily by the thermal power plants in Australia.

Chapter 1

1. Introduction

1.1. Research Background

The cement manufacturing industry is estimated to be responsible for 5 - 7% of the global anthropogenic greenhouse gas emissions [1]. Extensive research studies have been going on to cut down these emissions by making use of various industrial by-products such as fly ash, silica fume, slag etc. as cement replacement materials [2-4]. Of these various industrial by products, fly ash is the most abundantly available and least utilised material worldwide [5, 6] with an estimated production of 750 million tonnes per year [7]. This industrial by-product produced by the thermal power plants used to be considered a waste material is slowly transforming into a resource, which is yet to be fully utilized. The producers of fly ash are constantly looking for ways to exploit this resource. Since it has pozzolanic properties and can be used as a supplementary cementitious material, it attracts a major focus of the research community to increase its use as a cement replacement material. This would provide dual benefit of cutting down greenhouse has emissions associated with the cement production and would increase the utilisation rate of fly ash produced annually.

Fly ash is broadly categorised into two classes; class F and class C. In class F, the total minimum amount of SiO_2, Al_2O_3, and Fe_2O_3 is 70%, whereas, in class C it is between 50% and 70% [8]. The class F fly ash has low calcium oxide content, generally less than 10%, whereas class C fly ash generally contains more than 10% and is often found to contain 15-20%. The majority of global fly ash production falls under low calcium class F category [9] which has low reactivity [10]. To improve its low reactivity and to improve the early strength

properties of high volume fly ash cement composites, researchers have looked at many ways like reducing its particle size [11], making use of hydrated lime [2], lime water [12] set accelerator [13], silica fume [2], and metakaoline [14]. Particle size of fly ash is one of the important factors on which mechanical properties of the blended concrete depends [11]. Smaller the particle size higher is the surface area available to react with the portlandite, resulting in the increase in formation C-S-H gel that is responsible for strength development. Pozzolanic reaction of fly ash can be improved by adding hydrated lime powder. It accelerates the pozzolanic reaction of fly ash resulting in the improvement of strength

properties of fly ash blended concrete [2]. Addition of saturated lime water has also proved to be highly beneficial in improving the reactivity of fly ash which increases with the increase in pH value of lime water [12]. Incorporation of highly amorphous silica fume [2] and metakaolin [15] are also highly effective in improving the early strength properties of high volume fly ash cement composites. They help in counterbalance the effect of low reactivity of fly ash by actively reacting with the available lime to produce additional C-S-H gel thereby imparting high early strength properties to the fly ash blended mixes. Also, metakaolin shows better performance in improving the early strength properties of HVFA cement compostites compared to that of silica fume [15]. Recently, there has been a strong inclination towards the use of nano silica in improving the properties of plain cement [16] and high volume fly ash blended cement composites [17, 18] because of its highly amorphous characteristics and nano sized particles. Nano silica readily reacts with the free lime available in the mix to produce additional calcium silicate hydrate (C-S-H) gel, resulting in a considerable improvement in the early strength properties [19]. Though nano silica has shown to improve the mechanical properties of high volume fly ash cement blends but the available studies show a significant variation in their respective strength improvements from one researcher to the other [17, 18, 20].

Based on the review of past literature, we find that in spite of many decades of research on the use of low calcium class F fly ash in concrete, the majority of studies concentrated on 50-60% of FA content as a cement replacement material [21-23]. Very few studies are available that report the properties of class F high volume fly ash cement composite replacing 80% of cement [24, 25].

1.2. Aim of Research

The aim of this research project was to develop a cement composite replacing 70% or above of cement, incorporating high volume fly ash as a major supplementary cementitious material, having mechanical properties at par with that of OPC. This research also aimed at developing a cement composite, replacing 100% of cement, incorporating fly ash in combination with other supplementary cementitious materials and chemical additives. In addition this study aimed at understanding the various physicochemical changes occurring withing the cement matrix of various cement composites, using advanced materials chanracterisation techniques and quantitative analysis to formulate strategies for further development.

1.3. Scope of Research

The scope of this research covered the development of micro and nano engineered cement composites incorporating low calcium class F high volume fly ash at cement replacement levels of 70% and above. The research was focussed on the improvement of the mechanical properties of cement composites, by making use of the chemical reactivity potential of various supplementary cementitious materials and chemical additives, without the use of heat treatment method. It covers the study of compressive strength properties of the blended mortar samples. In addition it covers the investigation of physicochemical properties of various cement composites with the advanced material characterisation techniques like thermogravimetric analysis, x-ray diffraction analysis and scanning electron microscopy, to understand the reasoning behind the physicochemical changes taking place within the cement matrix.

1.4. Experimental plan and justification

Experiment Number	**Raw materials used**	**Justification for the use of raw materials**
Experiment 1	i) NS (5%) ii) SF (15%) iii) HL (5%) iv) SA v) UFFA (65 – 75%)	Since, the aim of this research was to replace OPC with the maximum possible percentage of SCM and additives to cut down the carbon footprint. The first replacement level was chosen as 80% as the majority of the previous studies concentrated on less 70%. The trial experiment conducted on the 80% OPC replaced raw fly ash and cement composite showed a significant reduction in 7 and 28 day compressive strength. Since low calcium class F fly ash typically has low reactivity. I undertook extensive literature review to look for ways to improve the early strength properties of the cement composites. Since amorphous silica plays an important role in the formation of C-S-H gel that is responsible for the development of compressive strength. I looked at studying the effect of (i) nano silica (ii) silica fume (micro silica). Nano silica used in existing literature varied between 1–10% with varying digrees of optimum

		contents depending upon the mix design. To study the effect of nano silica I chose 5% for my first experiment. Similarly, in the previous studies silica fume was used at cement replacement levels of 5–20% with varying degrees of optimum contents depending upon the mix design. I chose 15% of SF content for my first experiment. The reason for a large difference in the chosen percentage of nano silica and silica fume in the mix designs was because of the large difference in their respective particle size and their surface areas. Since silica fume and nano silica had zero lime content and fly ash contained a negligible amount of lime, therefore it was decided to add additional lime into the mix design. Therefore, for first experiment the 5% HL was used in the mix design. Also, set accelerators proved to accelerate the pozzolanic/hydration reactions, we also studied the effect of the addition of SA to the mix designs. Based on the past literature it was clearly evident that the particle size of the fly ash plays a significant role on its reactivity. Therefore, it was decided to micronize the raw fly ash to reduce its particle size to produce UFFA.
Experiment 2	i) NS (5 – 7.5%) ii) HL (5%) iii) SA iv) FA (62.5–65%)	The results of the first experiment were taken as a basis for the design of the second experiment. It was identified in the first experiment that the nano silica played a significant role in the improvement of compressive strength of HVFA cement composites. Therefore, I decided to study the effect of higher concentration of nano silica and used 5 and 7.5% of nano silica content for the mix designs. HL and SA content were kept the same as that in experiment 1 to study if their effect varies with that of experiment 1. Since, the main aim of my research was to cut down the carbon footprint to the

		maximum possible level, I decided to use raw fly ash in my second experiment in place of UFFA. The reason being that micronising fly ash is an energy intensive process and it adds to the carbon footprint of the mix design.
Experiment 3	i) NS (5 – 7.5%) ii) NA (2.5 – 5%) iii) NCC (2.5 – 5%) iv) FA (80%)	From the results of experiments 1 and 2, I found that nano silica is highly effecting in improving the mechanical properties of HVFA cement composites because of its nano sized particles and very high surface area. As the major elemental oxides present in OPC are SiO_2, CaO and Al_2O_3. Therefore, the next experiment was planned to undertake a comparative study of the nano sized sources of these elemental oxides. Since the reaction of pure CaO is highly thermal in nature and addition of nano CaO would have been highly exothermic and could have introduced high thermal stresses at early ages of curing, nano $CaCO_3$ was used as a source of CaO. The percentage of nano silica was kept the same as that in experiment 2. But nano alumina and nano calcium carbonate were chosen as 2.5 and 5% concentration based on the past studies, though they showed a varying degree of results in the existing published literature depending upon the mix designs used.
Experiment 4	i) OPC/GGBFS (25%) ii) NS (2.5 – 7.5%) iii) FA (67.5 – 75%) iv) HL (10 – 15%)	The fourth experiment was designed to look at replacing 100% of OPC. The experiment was designed with the initial mix designs having 25% of OPC content. In the subsequent mix designs OPC was replaced with GGBFS which is another industrial by product. To look at the upper limit, lower limit and the optimum content of NS, its concentration was varied as 2.5, 5 and 7.5%. Remaining concentration was that of FA that varied

		between 67.5 – 75%. Since, GGBFS and NS don't have any free lime and FA contains negligible amount of it, additional source of lime was required for the pozzolanic reaction. Therefore, HL powder was added externally at 10 and 15% of the total cementitious material (i.e. GGBFS, NS and FA).

References

[1] Benhelal E, Zahedi G, Shamsaei E, Bahadori A. Global strategies and potentials to curb CO_2 emissions in cement industry. Journal of Cleaner Production. 2013;51:142-61.

[2] Barbhuiya S, Gbagbo J, Russell M, Basheer P. Properties of fly ash concrete modified with hydrated lime and silica fume. Construction and Building Materials. 2009;23(10):3233-9.

[3] Şahmaran M, Yaman İÖ, Tokyay M. Transport and mechanical properties of self consolidating concrete with high volume fly ash. Cement and concrete composites. 2009;31(2):99-106.

[4] Hannesson G, Kuder K, Shogren R, Lehman D. The influence of high volume of fly ash and slag on the compressive strength of self-consolidating concrete. Construction and Building Materials. 2012;30:161-8.

[5] Heidrich C, Feuerborn H-J, Weir A. Coal Combustion Products: a Global Perspective. WOCA; 2013.

[6] Joshi RC, Lohita R. Fly ash in concrete: production, properties and uses: CRC Press; 1997.

[7] Blissett R, Rowson N. A review of the multi-component utilisation of coal fly ash. Fuel. 2012;97:1-23.

[8] ASTM C618-15 : Standard Specification for Coal Fly Ash and Raw or Calcined Natural Pozzolan for Use in Concrete. American society for testing and materials; 2015.

[9] Rangan BV. Fly ash-based geopolymer concrete. Your Building Administrator. 2008;2.

[10] Wang S, Li VC. Engineered cementitious composites with high-volume fly ash. ACI Materials Journal. 2007;104(3).

[11] Paya J, Monzo J, Peris-Mora E, Borrachero M, Tercero R, Pinillos C. Early-strength development of Portland cement mortars containing air classified fly ashes. Cement and concrete research. 1995;25(2):449-56.

[12] Ling X, Setunge S, Patnaikuni I. Effect of different concentrations of lime water on mechanical properties of high volume fly ash concrete. 22nd ACMSM: Materials to Structures: Advancement through Innovation: CRC Press/Balkema; 2012. p. 1135-41.
[13] Thomas MD. Optimizing Fly Ash Content for Sustainability, Durability, and Constructability. Proc of Coventry University and The University of Wisconsin, Milwaukee Centre for By-Products Utilization Second International Conference on Sustainable Construction Materials and Technologies, Universita Politecnica Delle Marche, Ancona, Italy Np: np, nd N pag2010.
[14] Güneyisi E, Gesoğlu M. Properties of self-compacting mortars with binary and ternary cementitious blends of fly ash and metakaolin. Materials and Structures. 2008;41(9):1519-31.
[15] Wei X, Zhu H, Li G, Zhang C, Xiao L. Properties of high volume fly ash concrete compensated by metakaolin or silica fume. Journal of Wuhan University of Technology-Mater Sci Ed. 2007;22(4):728-32.
[16] Björnström J, Martinelli A, Matic A, Börjesson L, Panas I. Accelerating effects of colloidal nano-silica for beneficial calcium–silicate–hydrate formation in cement. Chemical Physics Letters. 2004;392(1):242-8.
[17] Zhang M-H, Islam J. Use of nano-silica to reduce setting time and increase early strength of concretes with high volumes of fly ash or slag. Construction and Building Materials. 2012;29:573-80.
[18] Shaikh F, Supit S, Sarker P. A study on the effect of nano silica on compressive strength of high volume fly ash mortars and concretes. Materials & Design. 2014;60:433-42.
[19] Li H, Xiao H-g, Yuan J, Ou J. Microstructure of cement mortar with nano-particles. Composites Part B: Engineering. 2004;35(2):185-9.
[20] Hou P, Wang K, Qian J, Kawashima S, Kong D, Shah SP. Effects of colloidal nanoSiO_2 on fly ash hydration. Cement and Concrete Composites. 2012;34(10):1095-103.
[21] Ibrahim A, El-Chabib H, Eisa A. Ultrastrength Flowable Concrete Made with High Volumes of Supplementary Cementitious Materials. Journal of Materials in Civil Engineering. 2012;25(12):1830-9.
[22] Ibrahim A, Mahmoud E, Ali T. Investigation of relationships between high strength self consolidating concrete compressive strength and macroscopic internal structure. Construction and Building Materials. 2013;38:1161-9.

[23] Hou P-k, Kawashima S, Wang K-j, Corr DJ, Qian J-s, Shah SP. Effects of colloidal nanosilica on rheological and mechanical properties of fly ash–cement mortar. Cement and Concrete Composites. 2013;35(1):12-22.
[24] Huang C-H, Lin S-K, Chang C-S, Chen H-J. Mix proportions and mechanical properties of concrete containing very high-volume of Class F fly ash. Construction and Building Materials. 2013;46:71-8.
[25] Liu M. Self-compacting concrete with different levels of pulverized fuel ash. Construction and Building Materials. 2010;24(7):1245-52.

Chapter 2

2. Literature Review

2.1. Supplementary cementitious materials

Supplementary cementitious materials (SCMs) have been extensively used by the cement industry all over the world due to their economic and environmental benefits**.** They originate from various sources like industrial by-products or ashes generated by agricultural waste. The various industrial by-products which are rich in amorphous silica are fly ash, ground granulated blast furnace slag and silica fume**.** The ashes generated from the agriculture waste which are rich is amorphous silica are, rice husk ash, and palm oil fuel ash. The utilization of these materials in partially replacing cement can contribute towards the reduction in greenhouse gas emissions associated with cement production. In addition they can help in converting the industrial waste into an economic resource and even contribute towards the reduction in construction cost. Depending upon their availability, chemical properties and the desired results, these supplementary cementitious materials can either be used independently or can be used in a binary or ternary blend by the concrete producers. Some of these supplementary cementitious materials having good hydraulic properties can be used individually, such as slag or high calcium fly ash containing high amorphous content. However purely pozzolanic materials like low calcium class F fly ash or silica fume, cannot chemically react with water unless that water is rich in portlandite, either released by the cement or added externally. Of the various supplementary cementitious materials vailable, fly ash is the most abundantly available and least utilised material worldwide [1, 2].

2.1.1. Fly ash as a supplementary cementitious material

Fly ash is a combustion by-product of pulverized coal in thermal power plants and is also known as pulverised fuel ash. It is composed of very fine spherical glassy particles, that are driven out of the boiler along with the exhaust gasses and are generally captured by electrostatic precipitators before they are discharged into the atmosphere. The size of the fly ash particles range from 1 – 150 μm**,** and the range of the particle size collection and separation largely depend upon the type of dust collection system in place. Based on the major chemical composition fly ash is categorised into two classes i.e. class F and class C. In class F the total minimum amount of SiO_2, Al_2O_3, and Fe_2O_3 is 70%, whereas in class C it is between 50% and 70% [3]. In addition, it also contains calcium oxide (CaO), magnesium

oxide (MgO), sulfur trioxide (SO_3) and alkali oxides (Na_2O and K_2O). The class F fly ash has low calcium oxide content and since it is rich in reactive silica and alumina, it has high pozzolanic. Whereas, the class C fly ash generally contains more than 10% of calcium oxide which often ranges between 15-20%, show both cementitious and pozzolanic properties. The total estimated production of fly ash worldwide is 750 million tons per year [4]. The majority of global fly ash production falls under low calcium class F category [5] which has low reactivity [6].

Fly ash or volcanic ash has been in use as a pozzolanic material since ancient times, as evident in roman structures such as aqueducts and the Pantheon [7] but this technology was lost with the fall of roman empire. The interest in the use of fly ash in concrete got focus as early as in 1914, although the first available record of research studies was published in late 1930's [8].

Review of the past literature shows that fly ash not only enhances the properties of fresh concrete [9] but also improves its mechanical [10, 11] and durability [12, 13] properties. Its spherical particle size provides a ball bearing effect, thereby improving the workability of the concrete [14]. As per Sata et al. [15], to improve the workability of fly ash blended concrete, the requirement of superplasticizer decreases with the increasing amount of fly ash content Replacement of cement with fly ash in concrete results in very low to negligible bleeding [16]. Due to its high surface area as compared to the cement and reduction in water requirement the ratio of water to the volume of cementitious material is decreased [9], thereby considerably increasing its cohesive and strength properties [17].

Fly ash reacts with calcium hydrate released during the cement hydration process to produce additional calcium silicate hydrate gel that adds to the strength of the concrete. Li et al. [18] studied the long-term behaviour of fly ash concrete and found that the long-term strength of fly ash concrete was higher than that of normal cement concrete. They found that the mix design having 53% fly ash content with mean particle size of 18.8 μm had 18% higher compressive strength than the control mix (100% cement concrete) at 120 days. The strength further increased to 34% higher than the control mix when the mean particle size of the fly ash was 2.8 μm.

Though fly ash has numerous benefits it has few limitations as well. The major limitations of using fly ash as cement replacement material are the reduction in early strength and increased carbonation. Class F low calcium fly ash has low reactivity and therefore results in slower strength gain in fly ash blended cements as compared to ordinary portland cement [19]. Liu [20] investigated the effect of various percentages of fly ash in blended cement concrete on the strength development. He found that 7 & 28 day strength of all levels of fly ash blended cement concrete had lower strength than the reference portland cement concrete. Moreover, the strength gain decreased with the increasing amount of fly ash content.

There have been numerous researches conducted in the past to look at various ways to improve the mechanical properties of high volume fly ash cement composite. Particle size of fly ash is one of the important factors on which mechanical properties of the concrete depends. Smaller the particle size higher is the surface area available to react with lime, resulting in the improvement of the mechanical properties [21]. Paya et al. [21] looked at the effect of reduction in particle size on the reactivity of fly ash blended cement concrete. They prepared fly ash concrete samples having particle size ranging between 10 μm to 55 μm and fly ash content of 60% as cement replacement. They found that a linear relation between the particle size and compressive strength existed in fly ash blended cement concrete. Compressive and flexural strength of fly ash concrete increased with the decrease in particle size of fly ash.

Pozzolanic reaction of fly ash can be improved by adding hydrated lime. Bharbhuia et al. [22] studied the effect of hydrated lime on the reactivity of fly ash. They observed that the hydrated lime accelerated the hydration reaction and the compressive strength of fly ash blended concrete modified with hydrated lime was higher than that of fly ash concrete without hydrated lime. The difference in strength gain between hydrated lime modified and non-modified fly ash concrete increased with the increase in fly ash content.

Various salts of calcium and sodium have been used to accelerate the pozzolanic reaction of fly ash. Hill et al. [23] investigated the effect of calcium nitrate and calcium formate set accelerators at 2.5, 5 and 10% dosage, on the pozzolanic reaction of fly ash. They found that both calcium nitrate and calcium formate accelerated the pozzolanic reaction. The increase in the dosage of calcium nitrate had a positive effect on the improvement in reactivity, setting

time and the compressive strength of fly ash, however, they didn't observe the similar trend with the increase in the dosage of calcium formate, which showed little effect on the improvement in reactivity of fly ash. A. M. Paillere [24] investigated the effect of calcium nitrate and sodium thiocyanate on the reactivity of fly ash and found that calcium nitrate accelerates the setting time and moderately accelerates hardening whereas sodium thiocyanate accelerates the strength gain. Another study reported by Rettvin and Dalen and cited by Cabrera et al. [25] shows that when calcium nitrate is used in combination with sodium thiocyanate, calcium nitrate starts the hydration/pozzolanic reaction earlier which is then hastened by sodium thiocyanate.

Ling et al. [26] studied the effect of lime water having pH values ranging between 10.5 and 12.5 on 65% ultra-fine fly ash blended concrete. They micronized the raw fly ash in Sturtevant jet mill to produce ultra-fine fly ash. They observed that the lowest pH concentration (i.e. 10.5 – 11.0) of limewater provided the best results in improving the 28 and 56 day compressive strengths of HVFA concrete and the strength results were comparable to that of OPC.

Cement hydration is an exothermic chemical reaction which can lead to thermal cracking in large concrete pours due to temperature differential between the interior and the surface of the concrete in the initial curing period [27]. Turanli et al. [28] investigated the effect of fly ash in the blended cement concrete on heat of hydration. They observed that fly ash blended cement showed lower heat of hydration as compared the ordinary portland cement. Moreover, heat of hydration decreased with the increasing amount of fly ash content as cement replacement.

Carbonation is considered a potential problem with high volume fly ash concrete. CO_2 that is available in the atmosphere, diffuses in concrete pores and reacts with $Ca(OH)_2$ and C-S-H [29]. This process leads to the reduction in concrete's pH value to less than 9. The decrease of concrete's pH leads to de-passivation of steel reinforcement resulting in corrosion [30]. Jiang et al. (2000) studied the effect of carbonation on high volume fly ash concrete having 55 and 70% fly ash content. They found that the carbonation depth of HVFA was higher than that of ordinary portland cement concrete and increased with the increase in the percentage of

fly ash content. He further observed that increase in curing period decreased the effect of carbonation in HVFA concrete [29].

Drying Shrinkage of high volume fly ash concrete is significantly lower than that of ordinary Portland cement concrete. Lower drying shrinkage is due to the reduction in water requirement for the same slump and because of the reduction in the volume of Portland cement used [31]. Nakarai et al. [32] reported the results of Nawa (2001) on drying shrinkage. They found that the fly ash concrete has lower drying shrinkage at all replacement levels compared to that of OPC. In addition, increase in fly ash content leads to further reduction in drying shrinkage.

Fly ash concrete has lower permeability as compared to that of ordinary portland cement concrete. This is because of lower water requirement and the refinement of pore structure due to the formation of additional calcium silicate hydrate gel [33]. Sahmaran et al. [19] studied the effect of fly ash on the permeability of concrete and found that volume of penetrable pores of fly ash concrete samples, having various cement replacement levels were significantly lower than that of ordinary portland cement concrete. Addition of fly ash results in the reduction of pore size and thickness of transition zone between aggregate and surrounding cementitious matrix, thereby reducing the chloride ion permeability [34, 35]. Dinakar et al. [36] did a study on chloride permeability of concrete having cement replacement levels ranging between 30 – 85% with fly ash. They found that chloride permeability of all the samples containing fly ash had low to very low chloride ion permeability.

Sulfate salts that can come from external or internal sources can attack hardened concrete to form expansive compounds resulting in the deterioration of concrete [37]. As per Mehta [38] sulfate salts react with calcium hydroxide to form gypsum which further reacts with calcium aluminate hydrate to produce ettringite which increases in volume and leads to cracking and loss of strength. Turanli et al. [28] studied the effect of sulfate attack on blended cement concrete containing various percentages of fly ash. They observed that the fly ash blended cement concrete exhibited much higher resistance to the sulfate attack as compared to ordinary portland cement concrete. They also studied the effect of alkali-silica reactivity on the fly ash blended concrete samples with the same cementitious material combination. They

found that there was a significant reduction in the expansion of concrete due to alkali-silica reactivity as compared to the reference portland cement concrete.

2.1.2. Silica fume as a supplementary cementitious material

Silica fume or micro silica is a byproduct of the production of silicon metal and the ferrosilicon alloys. It has very high amorphous silica content and very fine particle size that makes it a highly reactive pozzolanic material. The physicochemical activity of silica fume in a blended cement composite helps in refining the pore structure, densifying the cement matrix, pozzolanic reaction with portlandite to produce additional C-S-H gel, and provides a stronger cement paste–aggregate interfacial zone. This combined effect results in enhancing the mechanical and durability properties of silica fume modified concrete.

The addition of silica fume increases the water demand to maintain the required slump. Wong et al. [39] studied the effect of 5, 10, and 15% of silica fume on the workability of blended concrete samples. They found that with the constant w/c ratio and superplasticiser dosage the slump values decreases with the increase in silica fume content. Similar results were reported by Mazloom et al. [40]. They attributed the reduction in the workability or the slump values of silica fume modified concrete to its very fine particle size that adsorbs some of the superplasticizer on its surface.

The addition of silica fume to a blended cement composite helps in refining the pore structure. Igarashi et al. [41] studied the effect of the addition of 10% silica fume on the porosity and pore size distribution of the blended concrete at early ages. They found that the silica fume modified concrete had fewer coarse pores than that of the OPC. Khan [42] investigated the effect of inclusion of 0, 5, 10 and 15% of silica fume to fly ash blended cement composites. They observed that the addition of silica fume resulted in a significant reduction in porosity of the blended mixes, and the reduction in the porosity increased with the increase in SF content up to 10%, beyond which the reduction was marginal or reversed. Rossignolo [43] studied the effect of silica fume on the microstructure of the interfacial transition zone (ITZ) between the portland cement paste and basalt aggregates. He observed that the addition of 10% of silica fume as a cement replacement material in the blended concrete, caused a reduction of 36% in the thickness of the ITZ, compared to that of the OPC concrete.

The combined effect of refinement of pore structure, densification of ITZ and the production of additional C-S-H gel helps in significantly improving the compressive strength of the silica fume blended concrete. Wong et al. [39] studied the effect of 5, 10 and 15% of silica fume on the compressive strength results of the blended concrete.They observed that the addition of silica fume at all replacement level did not produce any strength enhancement until 7 days of curing. From 7 day onwards the strength results of silica fume blended concretes encreased with the increase in SF content and were considerably higher than that of the control mix. They attributed the strength loss at early ages, to possibly the dilution effect and the slow pozzolanic activity of silica fume. Barbhuiya et al. [22] studied the effect of silica fume on the reactivity of fly ash. They found that silica fume improves the reactivity of fly ash and accelerates the pozzolanic reaction due to its very fine particle size and high amorphous silica content. They observed that the compressive strength of fly ash blended concrete modified with silica fume was higher than that of fly ash concrete sample prepared without silica fume. They also observed that the difference in strength gain between silica fume modified and non-modified fly ash concrete increased with the increase in fly ash content.

G. Appa Rao [44] studied the effect of 0, 10, 15 and 20% of silica fume on the drying shrinkage of the blended mortar samples. They observed that the addition of silica fume has a dominating influence on the 28 days drying shrinkage, which increases with the increase in silica fume content. The increase in drying shrinkage in the silica blended cement composites was also reported by other researchers [45, 46]. They attributed the increase in the drying shrinkage of mortar to the pozzolanic reaction and pore size refinement mechanism of silica fume. They observed that the long-term drying shrinkage of mortar after 365 days was not affected significantly with the addition of silica fume. The rate of increase in the drying shrinkage of mortar was high up to the age of 365 days and after that the increase in the drying shrinkage decreased with the age of mortar.

The addition of silica fume reduces the chloride ion permeability of the concrete, which protects the reinforcing steel from corrosion. Ramezanianpour and Malhotra [47] studied the effect of 10% silica fume on the resistance to chloride ion permeability and the porosity of the concrete. They found that the addition of silica fume significantly reduced the chloride ion permeability, indicating very low permeability of the blended concrete. They attributed

the decrease in the permeability of the silica fume blended concrete to the refinement of pore structure of the cement matrix, due to the addition of highly amorphous and very fine particle size silica fume.

Carbonation in reinforced concrete decreases its pH value resulting in the depassivation of the steel reinforcement leading to the corrosion in reinforcement. Skjolsvold [48] studied the effect of silica fume on the carbonation depths of the blended concrete. They observed that the silica fume blended concrete had higher carbonation rates than that of the control mix not containing silica fume. Schubert [49] believed that the consumption of portlandite in the pozzolanic reaction, with the addition of silica fume, increases the rate of carbonation, but the refinement of capillary pores tends to decrease the effect of carbonation.

The addition of silica fume helps in considerably reducing the resistance to the sulphate attack in the blended concrete, due its effect on the reduction in concrete permeability. Mangat and Khatib [50] studied the effect of 0%, 5%, 9%, and 15% silica fume on the sulphate resistance of concrete. They observed that the addition of silica fume increased its resistance to the sulphate attack, which increases with the increase in silica fume content. They attributed the increase in sulphate resistance to (i) the refinement of pore structure of silica fume incorporated mixes and (ii) the reduction in calcium hydroxide content due to the addition of silica fume, which reduces the tendency of gypsum formation resulting in the increase in sulphate resistance.

2.1.3. Ground granulated blast furnace slag as a supplementary cementitious material

Ground-granulated blast-furnace slag (GGBFS) is a by-product of iron and steel industry. It is produced by rapidly quenching molten iron slag in water that forms a glassy sand like granulated material, which is further ground to less than 45 microns, to produce GGBFS. The rough and angular-shaped slag particles react with the available portlandite, produced by the hydrated cement or added externally, in presence of water to produce calcium silicate hydrate gel, which is responsible for the strength improvement. GGBFS was first developed in Germany in 1853 [51]. It has been used as a cementitious material in concrete since the beginning of the 1900s [52]. The utilisation of GGBFS as a partial cement replacement material is well recognized and there is a large number of research studies available in the literature [53-55].

GGBFS has angular particle shape and high surface area that increases the water demand of a blended concrete mix. Studies show that the workability of GGBFS blended concrete decreases with the increase in GGBFS content [56, 57].

The glass content of GGBFS is considered to be an important factor that is critical to its hydraulic properties responsible for strength development. Although a glassy structure is essential to its reactivity as reported by some researchers [58] but it has no exact correlation with its hydraulic properties, and therefore, there is no guarantee that high glass content will produce a highly reactive slag [59]. Paul et al. [59] found that the reactivity of GGBFS depends not only on the glass content but also depends upon its chemical composition and Blaine's fineness.

Oner et al. [60] studied the effect of GGBFS on blended concrete at various cement replacement levels. They found that the early age strengths of all replacement levels were lower than that of the control mix because of the low pozzolanic activity of GGBFS. However, they found that with the increase in the curing age, the compressive strength of GGBFS concrete increases with the increase in GGBFS content up to an optimum replacement level. With the further increase in GGBFS beyond the optimum content, the strength decreases with the increase in GGBFS content. They found that 55–59% of GGBFS was the optimum content that provided the maximum improvement in compressive strength. Another study by Hogan et al. [61] reports the similar slow strength development of GGBFS blended concrete during the first three days of hydration. However, they found the optimum content of GGBFS to be 40%. This reinforces the earlier observation by Pal et al. [62] that the reactivity of GGBFS depends on many factors like glass content, chemical composition and Blaine's fineness which varies with the source of GGBFS. Blended cement containing GGBFS shows lower heat of hydration as compared the ordinary portland cement which is highly beneficial for the projects requiring mass concreting.

Addition of GGBFS as a cement replacement material is highly beneficial in reducing the drying shrinkage of concrete which is one of the major reasons of concrete deterioration. Güneyisi et al. [63] studied the effect of GGBFS on drying shrinkage of the blended concrete replacing cement with 20, 40 and 60% of GGBFS. They observed that the shrinkage strains

were somewhat similar at early age i.e. 3 days of curing, but the difference increased considerably at the later ages of curing. The shrinkage strains were lower than the control mix at all replacement levels with GGBFS and reduction in drying shrinkage increased with the increase in GGBFS content. Also, blended concretes containing GGBFS exhibit low expansion levels compared to that of OPC [64]. Arano and Kawamurai (2005) conducted a study on the expansion of concrete containing 5%, 10%, 20%, 30% and 60% of GGBFS and they found that the expansion levels decreased with the increase in the GGBFS content [65].

Generally, partial replacement of ordinary Portland cement with GGBFS improves the sulphate resistance of concrete but its effectiveness largely depends upon the chemical composition, glass content and the fineness of GGBFS [61, 66, 67]. Replacing cement with more than 65% of GGBFS tends to improve the sulphate resistance of concrete regardless of the Al_2O_3 contents of GGBFS and OPC. However, concrete made with lower content of GGBFS tends to resist sulphate only if OPC is low in C_3A [68]. Mehta [67] suggested that the improvement in sulphate resistance is not only due to the reduction in free lime and reactive alumina content, but it also because of the reduction in permeability associated with pore refinement which hinders the ingress of sulphate ions. Blended concretes containing 50% of GGBFS content achieved similar resistance to carbonation to that of normal OPC concrete. However, the blended mix containing 70% GGBFS showed higher carbonation compared to that of OPC [69]. Also, the presence of GGBS in blended concrete increases the resistance to chloride ion ingress, mainly due to the refinement in pore structure [70].

2.2. Nanomaterials in concrete

Application of nanomaterials in concrete presents an innovative approach to improve its mechanical and durability properties at nano scale level. Nanosized particles have a very high surface to volume ratio that helps in improving their chemical reactivity within the cement matrix. In recent years, researchers have been showing high interest in the use of nano-materials in concrete. Review of the past literature shows that the researchers have not only looked at the effect of nano forms of the primary elemental oxides of the cement i.e. nano silica [71, 72], nano alumina [73, 74], nano calcium carbonate [75, 76], but they have also investigated the effect of nano iron oxide [71, 74], nano zinc oxide [77] and nano titanium dioxide [78], on the physicochemical properties of concrete. All of these nano materials have helped in improving the properties of the blended cement composites in their

individual capacity but nano silica has proved to be most effective providing a significant improvement the mechanical and durability properties.

2.2.1. Nano silica

Addition of nano silica to a cement composites can help in improving both the mechanical and the durability properties because of its highly amorphous characteristic and nano sized particles. However, it significantly decreases the workability of the cement composite and requires higher water cement ratio or significant increase in the superplasticizer content to maintain the similar slump [79, 80]. It also reduces the flow spread, increases cohesion and yield stress of the cement composites [81]. Nano silica modified cement composites show increased plastic viscosity and the compressive strength [82].

Hui et al. [71] studied the effect of 3, 5 and 10% of nano silica on the mechanical properties of blended mortar samples. They observed that the compressive and flexural strength of the mortars samples containing nano silica was higher than that of the OPC mortar, which increased with the increase in nano silica content. The SEM observations also revealed that the nano silica considerably improved hydration/pozzolanic reaction and the microstructure of the cement paste. Gengying Li [72] investigated the effect of 4% nano silica on the properties of high volume fly ash concrete containing 50% fly ash content. They observed that the addition of nano silica to the fly ash blended concrete improved its compressive strength by 59, 69 and 39% at 3, 7 and 28 days respectively. Hou et al. [83] studied the effect of 0, 0.75, 1.5 and 5% colloidal nano silica on 60% FA blended cement mortar samples. They observed that the compressive strength of the blended mortar samples at 7 and 28 days of curing increased with the increasing amount of CNS. The maximum increase in compressive strength that they observed was achieved with 5% CNS. They found that the addition of 5% CNS increased the 7 and 28 day compressive strengths by approximately 60 and 33% respectively compared the cement fly ash blend not containing nano silica. They attributed the strength gain of a CNS modified fly ash cement paste composite to the acceleration effect of highly amorphous nano silica on cement and fly ash hydration/pozzolanic reaction. Shaikh et al. [84] investigated the effect of 2% nano silica on 68% fly ash blended cement mortars. They observed no difference in strength at 7 days but at 28 days there was 56 % increase in the compressive strength of the nano silica modified cement fly ash blend compared to the mix not containing nano silica.

Said et al. [85] investigated the effect of 0, 3 and 6% of colloidal nano silica on the chloride ion permeability and porposity of the blended concrete containing 30% fly ash. They observed that the rapid chloride ion permeability considerably decreased with the addition of colloidal nano silica and this reduction in chloride ion permeability increased with the increase in colloidal nano silica content. They found that the total porosity and the threshold pore diameter were significantly lower for the mixtures containing nano-silica. This improvement in the porosity increased with the increase in nano silica dosage upto 6%. They also noted that the back scattered electron microcope imagery of the samples containing colloidal nano silica showed a considerably dense cement microstructure at the interfacial transition zone between the aggregates and the cement paste. Supit et al. [86] studied the effect of 2% nano silica on water sorptivity, volume of permeable voids, chloride permeability and porosity tests on cement fly ash blended concrete containing 58% of fly ash content. They found that the addition of 2 % NS reduced the sorptivity of HVFA concretes by 7 and 22% at 28 and 90 days, respectively. They also noticed a considerable reduction in the volume of permeable voids in nano silica modified HVFA concretes compared to that of fly ash cement blend not containing nano silica. They observed a considerable reduction in the chloride ion penetration of HVFA concrete with the addition of 2% nano silica. Their mercury intrusion porosimetry results showed a dense microstructure which they further confirmed with SEM analysis. They found that the addition of nano silica results in a significant reduction in 0.1 and 10μm pores. Moreover, they observed a notable reduction in the cumulative pore volume, concluding that the addition of nano silica significant reduces the total capillary pores and pores diameters of HVFA cement composites.

2.2.2. Nano alumina

There are very few studies conducted on the effect of nano alumina on the properties of plain cement or fly ash blended cement composites. Nazari et al. [87] studied the effect of 0.5, 1, 1.5 and 2% of nano alumina on the properties of plain cement concrete. They observed that all the samples containing nano alumina showed lower workability compared to the control mix not containing nano alumina. The workability of the nano alumina modified concrete decreased with the increase in nano alumina content. They attributed the reduction in the workability to a significant increase in the surface area of the nano alumina modified samples. However the compressive strength of the nano alumina modified samples showed a considerable improvement at 7, 28 and 90 days of curing, upto 1% of nano alumina content

beyond which the strength decreased with the further increase in nano alumina content. They found 1% nano alumina to be the optimum content that provides the maximum improvement in the compressive strength of 16, 15 and 9% at 7, 28 and 90 days respectively. Oltulu et al. [74] studied the effect of 0.5, 1.25 and 2.5% of nano alumina powder on the properties of fly ash cement mortar containing 15% of fly ash. They observed that the addition of NA powder into fly ash cement mortars at a dosage of 0.5% did not yield any discernible results compared to the control mix. With the increase in nano alumina content to 1.25%, they achieved the highest improvement in the compressive strength results of 4, 4 and 5% at 7, 28 and 56 days of curing. When the nano alumina content was increased to 2.5% the results started showing the reduction in compressive strength of the blended mortar. Their nano alumina modified mortar samples showed an increase in the capillary permeability with the increase in nano alumina content with the 2.5% nano alumina content showing 10% increase in the capillary absorption coefficient compared to the control mix.

2.2.3. Nano calcium carbonate

The behaviour of $CaCO_3$ in the hydration of ordinary Portland cement has been intensively studied [88-90] and the use of ground limestone ($CaCO_3$) as a cement replacement material is widely practiced all over the world [91]. The results from the review of past literature show the positive effects of the addition of $CaCO_3$ on the acceleration of hydration reaction and resulting improvement in strength development [88-91]. Sato et al. [75] investigated the effect of 10 and 20% nano $CaCO_3$ as a cement additive on the physicochemical properties of OPC and HVFA cement composites. They observed that the conduction calorimetry showed a significant acceleration in the early hydration reaction of OPC with the addition of nano $CaCO_3$ and the acceleration in hydration reaction increased with the increase in nano $CaCO_3$ content. They found a considerable improvement in the microhardness and modulus of elasticity in the early stage of the hydration. They attributed this improvement in the mechanical properties and the hydration reaction to the seeding effect of the nano $CaCO_3$ particles and the nucleation of C–S–H gel. They found that the addition of nano $CaCO_3$ to HVFA cement composite considerably improved its microhardness, which increased with the increase in nano $CaCO_3$ content. They found that the results were consistent with the observation from the conduction calorimetry curves, which showed the delay in heat development with the addition of fly ash and but showed a considerable acceleration with the addition of nano $CaCO_3$.

Shaikh et al. [76] studied the effect of nano $CaCO_3$ on the mechanical and durability properties of HVFA cement mortar containing 40 and 60% of fly ash content. In the first phase they looked at the effect of 1, 2, 3, and 4% of nano $CaCO_3$ on the OPC concrete and in the second phase they used the optimum content of nano $CaCO_3$, obtained in phase 1, to study its effect on the fly ash blended cement composites. They found that the concrete containing 1% of nano $CaCO_3$ provided the highest compressive strength at all ages. The early age compressive strength of HVFA concretes also showed an improvement compared to that on fly cement concrete samples not containing nano $CaCO_3$. The mix containing 40% fly ash showed 33 and 54% improvement in compressive strength at 7 and 28 days respectively. The one containing 60% fly ash showed no improvement at 7 day and 15% improvement in 28 day compressive strength. In addition, they found that the addition of 1% nano $CaCO_3$ to 40% fly ash blended concrete significantly reduced its water sorptivity showing that nano $CaCO_3$ refining the pore structure of the blended concrete. The volume of the permeable voids also showed a significant decreased compared to the fly ash cement blend containing 40% fly ash. They observed 19% and 12% reduction in chloride ion permeability of HVFA concretes containing 40% and 60% fly ash respectively, with the addition of 1% nano calcium carbonate. They also found that the mercury intrusion porosimetry showed a decreased in the total capillary porosities and pore refinement in HVFA concretes with the addition of nano $CaCO_3$.

2.3. Research gap

The review of the past literature shows that there are very few studies that report the properties of low calcium class F high volume fly ash cement composites replacing cement by 70% or above. Moreover, the mechanical properties of the cement composites at such high replacement levels are not at par with that of ordinary Portland cement concrete [20, 21, 92].

There appears to be very limited study available that investigates the combined effect of hydrated lime and set accelerator on low calcium class F high volume fly ash cement composites replacing cement at 70% and above. Though silica fume, and nano silica have been used to improve the properties of fly ash but there appears to be limited or no research available on their effect on the physicochemical behaviour of low calcium class F high volume fly ash cement composites, when combined with set accelerator and hydrated lime at 70% and above cement replacement levels.

Silica, alumina and calcium oxide form the major component of ordinary Portland cement. Based on the review of past literature, there appears to be limited or no research available on comparative study of these nanomaterials on the properties of low calcium class F high volume fly ash cement composites containing 70% or above of fly ash content. Moreover, the available studies on the effect of various nanomaterials on fly ash cement composites show a significant variation in their respective strength improvements from one researcher to the other. This is most likely because of the variation in the chemical composition, particle size distribution and the amorphous content of the various fly ashes used by the different researchers. Therefore, to look at standardising the effect of nanomaterials on fly ash blended cement composites these factors require due consideration and demand quantitative phase analysis of the raw materials as well as that of the hydration products. Nano materials because of their small particle size and large surface area show high pozzolanic reactivity that holds a great potential for the development of high volume fly ash zero cement composite having mechanical properties at par or better than that of OPC.

Therefore this research was aimed at investigating all these research gaps and to develop an environmental friendly cement composite incorporating high volumes of fly ash and other supplementary cementitious materials.

References

[1] Heidrich C, Feuerborn H-J, Weir A. Coal Combustion Products: a Global Perspective. WOCA; 2013.

[2] Joshi RC, Lohita R. Fly ash in concrete: production, properties and uses: CRC Press; 1997.

[3] ASTM C618-15 : Standard Specification for Coal Fly Ash and Raw or Calcined Natural Pozzolan for Use in Concrete. American society for testing and materials; 2015.

[4] Blissett R, Rowson N. A review of the multi-component utilisation of coal fly ash. Fuel. 2012;97:1-23.

[5] Rangan BV. Fly ash-based geopolymer concrete. Your Building Administrator. 2008;2.

[6] Wang S, Li VC. Engineered cementitious composites with high-volume fly ash. ACI Materials Journal. 2007;104(3).

[7] Moore D. The Roman Pantheon: the triumph of concrete: MARC/CCEOP, University of Guam Station.; 1995.

[8] Davis RE, Carlson RW, JW Kelly HED. Properties of cements and concretes containing fly ash. ACI Journal Proceedings: ACI; 1937.
[9] Nawy EG. Fundamentals of high strength high performance concrete: Addison-Wesley Longman; 1996.
[10] Hansen TC. Long-term strength of high fly ash concretes. Cement and Concrete Research. 1990;20(2):193-6.
[11] Sivasundaram V, Carette G, Malhotra V. Long-term strength development of high-volume fly ash concrete. Cement and Concrete Composites. 1990;12(4):263-70.
[12] Mehta PK. Concrete. Structure, properties and materials. 1986.
[13] Pepper L, Mather B. Effectiveness of mineral admixtures in preventing excessive expansion of concrete due to alkali-aggregate reaction. American Soc Testing & Materials Proc. 1959.
[14] Helmuth R. Water-reducing properties of fly ash in cement pastes, mortars, and concretes: causes and test methods. ACI Special Publication. 1986;91.
[15] Sata V, Jaturapitakkul C, Kiattikomol K. Influence of pozzolan from various by-product materials on mechanical properties of high-strength concrete. Construction and Building Materials. 2007;21(7):1589-98.
[16] Bilodeau A, Malhotra VM. High-volume fly ash system: concrete solution for sustainable development. ACI Materials Journal. 2000;97(1).
[17] Mehta PK. High-performance, high-volume fly ash concrete for sustainable development. Proceedings of the international workshop on sustainable development and concrete technology2004. p. 3-14.
[18] Li G, Wu X. Influence of fly ash and its mean particle size on certain engineering properties of cement composite mortars. Cement and Concrete Research. 2005;35(6):1128-34.
[19] Şahmaran M, Yaman İÖ, Tokyay M. Transport and mechanical properties of self consolidating concrete with high volume fly ash. Cement and concrete composites. 2009;31(2):99-106.
[20] Liu M. Self-compacting concrete with different levels of pulverized fuel ash. Construction and Building Materials. 2010;24(7):1245-52.
[21] Paya J, Monzo J, Peris-Mora E, Borrachero M, Tercero R, Pinillos C. Early-strength development of Portland cement mortars containing air classified fly ashes. Cement and concrete research. 1995;25(2):449-56.

[22] Barbhuiya S, Gbagbo J, Russell M, Basheer P. Properties of fly ash concrete modified with hydrated lime and silica fume. Construction and Building Materials. 2009;23(10):3233-9.
[23] Hill RL. The study of hydration of fly ash in the presence of calcium nitrate and calcium formate, University of North Texas; 1994.
[24] Paillère A-M. Application of admixtures in concrete: CRC Press; 1994.
[25] Cabrera JG, Rivera-Villarreal R. PRO 5: International RILEM Conference on The Role of Admixtures in High Performance Concrete: RILEM; 1999.
[26] Ling X, Setunge S, Patnaikuni I. Effect of different concentrations of lime water on mechanical properties of high volume fly ash concrete. 22nd ACMSM: Materials to Structures: Advancement through Innovation: CRC Press/Balkema; 2012. p. 1135-41.
[27] Branco FA, Mendes P, Mirambell E. Heat of hydration effects in concrete structures. ACI Materials Journal. 1992;89(2).
[28] Turanli L, Uzal B, Bektas F. Effect of large amounts of natural pozzolan addition on properties of blended cements. Cement and concrete research. 2005;35(6):1106-11.
[29] Jiang L, Lin B, Cai Y. A model for predicting carbonation of high-volume fly ash concrete. Cement and Concrete Research. 2000;30(5):699-702.
[30] Papadakis VG, Vayenas CG, Fardis M. A reaction engineering approach to the problem of concrete carbonation. AIChE Journal. 1989;35(10):1639-50.
[31] Atis CD. High-volume fly ash concrete with high strength and low drying shrinkage. Journal of materials in civil engineering. 2003;15(2):153-6.
[32] Nakarai K, Ishida T. Numerical evaluation of influence of pozzolanic materials on shrinkage base on moisture state and pore structure. Creep, Shrinkage and Durability Mechanics of Concrete and Concrete Structures, Two Volume Set: Proceedings of the CONCREEP 8 conference held in Ise-Shima, Japan, 30 September-2 October 2008: CRC Press; 2009. p. 153.
[33] Siddique R, Khan MI. Supplementary cementing materials: Springer; 2011.
[34] Kuroda M, Watanabe T, Terashi N. Increase of bond strength at interfacial transition zone by the use of fly ash. Cement and concrete research. 2000;30(2):253-8.
[35] Mehta PK, Monteiro PJ. Concrete: microstructure, properties, and materials: McGraw-Hill New York; 2006.
[36] Dinakar P, Babu K, Santhanam M. Durability properties of high volume fly ash self compacting concretes. Cement and Concrete Composites. 2008;30(10):880-6.

[37] Skalny J, Brown P. Sulfate attack on concrete: Taylor & Francis; 2002.
[38] Mehta P. Sulfate attack on concrete--a critical review. Mater Sci Concr, IIIpp. 1992;105.
[39] Wong H, Razak HA. Efficiency of calcined kaolin and silica fume as cement replacement material for strength performance. Cement and Concrete Research. 2005;35(4):696-702.
[40] Mazloom M, Ramezanianpour A, Brooks J. Effect of silica fume on mechanical properties of high-strength concrete. Cement and Concrete Composites. 2004;26(4):347-57.
[41] Igarashi S-i, Watanabe A, Kawamura M. Evaluation of capillary pore size characteristics in high-strength concrete at early ages. Cement and Concrete Research. 2005;35(3):513-9.
[42] Khan M. Isoresponses for strength, permeability and porosity of high performance mortar. Building and Environment. 2003;38(8):1051-6.
[43] Rossignolo JA. Interfacial interactions in concretes with silica fume and SBR latex. Construction and Building Materials. 2009;23(2):817-21.
[44] Rao GA. Long-term drying shrinkage of mortar—influence of silica fume and size of fine aggregate. Cement and concrete research. 2001;31(2):171-5.
[45] Buil M, Paillere A, Roussel B. High strength mortars containing condensed silica fume. Cement and Concrete Research. 1984;14(5):693-704.
[46] Hooton R. Influence of silica fume replacement of cement on physical properties and resistance to sulfate attack, freezing and thawing, and alkali-silica reactivity. materials Journal. 1993;90(2):143-51.
[47] Ramezanianpour A, Malhotra V. Effect of curing on the compressive strength, resistance to chloride-ion penetration and porosity of concretes incorporating slag, fly ash or silica fume. Cement and concrete composites. 1995;17(2):125-33.
[48] Skjolsvold O. Carbonation depths of concrete with and without condensed silica fume. Special Publication. 1986;91:1031-48.
[49] Schubert P. Carbonation behavior of mortars and concretes made with fly ash. Special Publication. 1987;100:1945-62.
[50] Mangat P, Khatib J. Influence of fly ash, silica fume, and slag on sulfate resistance of concrete. Materials Journal. 1993;92(5):542-52.
[51] Malhotra VM, Mehta PK. Pozzolanic and cementitious materials: Taylor & Francis; 1996.
[52] Abrams DA. Effect of hydrated lime and other powdered admixtures in concrete: Structural materials research laboratory; 1920.

[53] Stutterheim N. Portland Blast-furnace Cements: A Case for Separate Grinding of Slag: National Building Research Institute; 1968.
[54] Swamy R, Bouikni A. Some engineering properties of slag concrete as influenced by mix proportioning and curing. Materials Journal. 1990;87(3):210-20.
[55] Brooks J, Wainwright P, Boukendakji M. Influence of Slag Type and Replacement Level on Strength Elasticity, Shrinkage and Creep of Concrete. Special Publication. 1992;132:1325-42.
[56] Lim SK, Ling TC, Hussin MW. Strength properties of self-compacting mortar mixed with GGBFS. Proceedings of the Institution of Civil Engineers–Construction Materials. 2012;165(2):87-98.
[57] Özkan Ö, Yüksel I, Muratoğlu Ö. Strength properties of concrete incorporating coal bottom ash and granulated blast furnace slag. Waste management. 2007;27(2):161-7.
[58] Schwiete H, Dolbor F. The effect of cooling conditions and the chemical composition on the hydraulic properties of the haematitic slags. Forschungsber Landes Nordrh-Westfal. 1963:23-9.
[59] Pal S, Mukherjee A, Pathak S. Investigation of hydraulic activity of ground granulated blast furnace slag in concrete. Cement and Concrete Research. 2003;33(9):1481-6.
[60] Oner A, Akyuz S. An experimental study on optimum usage of GGBS for the compressive strength of concrete. Cement and Concrete Composites. 2007;29(6):505-14.
[61] Hogan F, Meusel J. Evaluation for durability and strength development of a ground granulated blast furnace slag. Cement, Concrete and Aggregates. 1981;3(1):40-52.
[62] Binici H, TOKYAY M, KOuml MM. The early heat of hydration of blended cements incorporating GGBFS and ground basaltic pumice (GBP). International Journal of Physical Sciences. 2006;1(3):112-20.
[63] Güneyisi E, Gesoğlu M, Özbay E. Strength and drying shrinkage properties of self-compacting concretes incorporating multi-system blended mineral admixtures. Construction and Building Materials. 2010;24(10):1878-87.

[64] Hester D, McNally C, Richardson M. A study of the influence of slag alkali level on the alkali–silica reactivity of slag concrete. Construction and Building Materials. 2005;19(9):661-5.

[65] Arano N, Kawamura M. Comparative consideration on the mechanisms of ASR suppression due to different mineral admixtures. Proceedings of the 11th international conference on alkali-aggregate reaction in concrete, Quebec2000. p. 553-62.
[66] Osborne G. Durability of Portland blast-furnace slag cement concrete. Cement and Concrete Composites. 1999;21(1):11-21.
[67] Mehta PK. Pozzolanic and cementitious byproducts as mineral admixtures for concrete-a critical review. Special Publication. 1983;79:1-46.
[68] Taylor H. Cement chemistry. 1997.
[69] Osborne G. Carbonation and permeability of blastfurnace slag cement concretes from field structures. Special Publication. 1989;114:1209-38.
[70] Aldea C-M, Young F, Wang K, Shah SP. Effects of curing conditions on properties of concrete using slag replacement. Cement and Concrete Research. 2000;30(3):465-72.
[71] Li H, Xiao H-g, Yuan J, Ou J. Microstructure of cement mortar with nano-particles. Composites Part B: Engineering. 2004;35(2):185-9.
[72] Li G. Properties of high-volume fly ash concrete incorporating nano-SiO_2. Cement and Concrete research. 2004;34(6):1043-9.
[73] Li Z, Wang H, He S, Lu Y, Wang M. Investigations on the preparation and mechanical properties of the nano-alumina reinforced cement composite. Materials Letters. 2006;60(3):356-9.
[74] Oltulu M, Şahin R. Effect of nano SiO_2, nano Al_2O_3 and nano Fe_2O_3 powders on compressive strengths and capillary water absorption of cement mortar containing fly ash: a comparative study. Energy and Buildings. 2013;58:292-301.
[75] Sato T, Beaudoin J. Effect of nano $CaCO_3$ on hydration of cement containing supplementary cementitious materials. Advances in Cement Research. 2011;23(1):33-43.
[76] Shaikh FU, Supit SW. Mechanical and durability properties of high volume fly ash (HVFA) concrete containing calcium carbonate ($CaCO_3$) nanoparticles. Construction and building materials. 2014;70:309-21.
[77] Riahi S, Nazari A. Physical, mechanical and thermal properties of concrete in different curing media containing ZnO_2 nanoparticles. Energy and buildings. 2011;43(8):1977-84.
[78] Shekari A, Razzaghi M. Influence of nano particles on durability and mechanical properties of high performance concrete. Procedia Engineering. 2011;14:3036-41.

[79] Madani H, Bagheri A, Parhizkar T. The pozzolanic reactivity of monodispersed nanosilica hydrosols and their influence on the hydration characteristics of Portland cement. Cement and Concrete Research. 2012;42(12):1563-70.
[80] Quercia G, Hüsken G, Brouwers H. Water demand of amorphous nano silica and its impact on the workability of cement paste. Cement and Concrete Research. 2012;42(2):344-57.
[81] Senff L, Labrincha JA, Ferreira VM, Hotza D, Repette WL. Effect of nano-silica on rheology and fresh properties of cement pastes and mortars. Construction and Building Materials. 2009;23(7):2487-91.
[82] Berra M, Carassiti F, Mangialardi T, Paolini A, Sebastiani M. Effects of nanosilica addition on workability and compressive strength of Portland cement pastes. Construction and Building Materials. 2012;35:666-75.
[83] Hou P, Wang K, Qian J, Kawashima S, Kong D, Shah SP. Effects of colloidal nanoSiO_2 on fly ash hydration. Cement and Concrete Composites. 2012;34(10):1095-103.
[84] Shaikh F, Supit S, Sarker P. A study on the effect of nano silica on compressive strength of high volume fly ash mortars and concretes. Materials & Design. 2014;60:433-42.
[85] Said AM, Zeidan MS, Bassuoni M, Tian Y. Properties of concrete incorporating nano-silica. Construction and Building Materials. 2012;36:838-44.
[86] Supit SWM, Shaikh FUA. Durability properties of high volume fly ash concrete containing nano-silica. Materials and structures. 2015;48(8):2431-45.
[87] Nazari A, Riahi S, Riahi S, Shamekhi SF, Khademno A. Influence of Al2O3 nanoparticles on the compressive strength and workability of blended concrete. Journal of American Science. 2010;6(5):6-9.
[88] Barker A, Cory HP. The early hydration of limestone-filled cements. Blended cements in construction, paper presented at the international conference, University of Sheffield, UK, 9-12 September 1991.
[89] Kakali G, Tsivilis S, Aggeli E, Bati M. Hydration products of C_3A, C_3S and Portland cement in the presence of $CaCO_3$. Cement and Concrete Research. 2000;30(7):1073-7.
[90] Matschei T, Lothenbach B, Glasser FP. The role of calcium carbonate in cement hydration. Cement and Concrete Research. 2007;37(4):551-8.
[91] Neville AM. Properties of concrete1995.

[92] Huang C-H, Lin S-K, Chang C-S, Chen H-J. Mix proportions and mechanical properties of concrete containing very high-volume of Class F fly ash. Construction and Building Materials. 2013;46:71-8.

Chapter 3

Micro and Nano Engineered High Volume Ultrafine Fly Ash Cement Composite with and without additives

This experiment looks at the effect of silica fume, nano silica, set accelerator and hydrated lime on high volume ultrafine fly ash cement composites replacing 80% of ordinary Portland cement. Raw fly ash was micronized using Sturtevant jetmill micronizer to produce ultrafine fly ash.

International Journal of Concrete Structures and Materials
Vol.10, No.1, pp.113–124, March 2016
DOI 10.1007/s40069-015-0122-7
ISSN 1976-0485 / eISSN 2234-1315

Micro and Nano Engineered High Volume Ultrafine Fly Ash Cement Composite with and without Additives

R. Roychand*, S. De Silva, D. Law, and S. Setunge

(Received July 14, 2015, Accepted December 20, 2015, Published online January 11, 2016)

Abstract: This paper presents the effect of silica fume and nano silica, used individually and in combination with the set accelerator and/or hydrated lime, on the properties of class F high volume ultra fine fly ash (HV-UFFA) cement composites, replacing 80 % of cement (OPC). Compressive strength test along with thermogravimetric analysis, X-ray diffraction and scanning electron microscopy were undertaken to study the effect of various elements on the physico-chemical behaviour of the blended composites. The results show that silica fume when used in combination with the set accelerator and hydrated lime in HV-UFFA cement mortar, improves its 7 and 28 day strength by 273 and 413 %, respectively, compared to the binary blended cement fly ash mortar. On the contrary, when nano silica is used in combination with set accelerator and hydrated lime in HV-UFFA cement mortar, the disjoining pressure in conjunction with the self-desiccation effect induces high early age micro cracking, resulting in hindering the development of compressive strength. However, when nano silica is used without the additives, it improves the 7 and 28 day strengths of HV-UFFA cement mortar by 918 and 567 %, respectively and the compressive strengths are comparable to that of OPC.

Keywords: nano silica, silica fume, fly ash, additives, X-ray diffraction, scanning electron microscopy.

1. Introduction

Globally, out of the total fly ash (FA) production of 620–660 Million tons per year, only about 53.5 % is currently being utilized and the remaining forms part of the landfills (Heidrich et al. 2013). FA producers have to spend large amount of money for the safe disposal of this unutilized industrial by product (About Coal Ash—CCP FAQs. American Coal Ash Association 2014). This poses a big challenge to both the fly ash producers and the research community, to bring down this production vs utilization ratio to a minimum possible level.

FA has good pozzolanic properties and it can be used as a supplementary cementitious material (SCM). In addition, the production of cement (OPC) is responsible for 5–7 % of global greenhouse gas emissions (Benhelal et al. 2013). Therefore, using fly ash as a cement replacement material provides dual benefit (i) it helps in increasing the use of this industrial by product and (ii) it assists in cutting down the emissions associated with the cement production. Moreover, it not only enhances the properties of fresh concrete like workability (Sata et al. 2007; Liu 2010) but also improves its mechanical and durability properties such as; greater long term strength (Hansen 1990; Sivasundaram et al. 1990), lower shrinkage (Atis 2003; Nakarai and Ishida 2008), lower water absorption (Malhotra and Mehta 2002; Şahmaran et al. 2009), reduction in chloride permeability (Nagataki and Ohga 1992; Dinakar et al. 2008), increased resistance to sulphate attack (Structure et al. 1986; Turanli et al. 2005), low heat of hydration (Turanli et al. 2005; Kasai et al. 1983) and reduction in alkali aggregate reactivity (Turanli et al. 2005; Pepper and Mather 1959; Islam 2014). Although fly ash has many advantages when used as a cement replacement material, it has one major disadvantage of low reactivity (Liu 2010; Şahmaran et al. 2009). Therefore, it has to be a very judicious decision to choose a percentage of fly ash content as cement replacement material in a mix design. Numerous research studies have been conducted in the past to address its low reactivity and to improve the strength of fly ash blended mixes. Researchers have looked at the effect of particle size (Paya et al. 1995; Chindaprasirt et al. 2005), use of hydrated lime (Şahmaran et al. 2009; Barbhuiya et al. 2009), silica fume (Barbhuiya et al. 2009; Sellevold and Radjy 1983; El-Chabib and Syed 2012; Rashad 2014), metakaolin (Wei et al. 2007; Reis and Camões 2011) to improve the mechanical properties of fly ash blended mixes.

Paya et al. (1995) investigated the effect of reduction in particle size on the reactivity of fly ash blended cement concrete. They found that a linear relation between the particle size and compressive strength exists in fly ash blended concrete. Compressive strength of fly ash concrete increased with the decrease in its particle size (Paya et al.

School of Civil, Environmental and Chemical Engineering, RMIT University, Melbourne, VIC, Australia.
*Corresponding Author;
E-mail: rajeev.roychand@rmit.edu.au

1995; Chindaprasirt et al. 2005; Erdoğdu and Türker 1998; Li and Wu 2005). Hill et al. (1994) studied the effect of calcium nitrate set accelerator (SA) on the hydration reaction of fly ash. They found that calcium nitrate considerably accelerated the hydration reaction of fly ash resulting in the improvement in its setting time and compressive strength. Studies show that hydrated lime (HL) considerably improves the reactivity of fly ash. It accelerates the hydration reaction resulting in a significant improvement of compressive strength of high volume fly ash (HVFA) concrete (Barbhuiya et al. 2009; Jayakumar and Abdullahi 2011). Bharbhuia et al. (Barbhuiya et al. 2009) and Rashad et al. (2014) studied the effect of silica fume (SF) on the mechanical properties of HVFA concrete. They found that addition of silica fume considerably improved the 7 and 28 day strength. Moreover, Silica fume performed considerably better than hydrated lime in improving the early age strength of fly ash concrete (Barbhuiya et al. 2009).

Recently, amorphous nano silica (nS) has been gaining widespread attention of the research community due to its nano sized particles and very high amorphous SiO_2 content (Björnström et al. 2004; Jo et al. 2007; Zhang and Islam 2012; Hou et al. 2012; Singh et al. 2015). It not only takes part in the hydration reaction to provide additional C–S–H but also accelerates the hydration process (Björnström et al. 2004; Zhang and Islam 2012; Hou et al. 2012). Hou et al. (Hou et al. 2012) investigated the effect of 0, 2.25 and 5 % colloidal nano silica (CNS) on 60 % FA blended cement composite. They found that the compressive strength of the mortar samples at 7 and 28 days increased with the increasing amount of CNS but at 3 months no significant difference in their respective strength results was observed. The maximum increase in strength that they observed with 5 % CNS compared to 0 % CNS at 7 and 28 days was approximately 60 and 33 % respectively. Shaikh et al. (Shaikh et al. 2014) studied the effect of 2 % nano silica on 68 % FA blended cement composite and found that there was no difference in strength at 7 days but at 28 days there was 56 % increase in strength as compared to the mix not containing nano silica.

Based on the review of past literature there appears to be limited or no research available on the effect of silica fume and nano silica in combination with hydrated lime and set accelerator on the properties of class F high volume fly ash (HVFA) cement composite. In addition, a significant variation in the effect of nano silica on the percentage of strength improvement of high volume fly ash cement composites has been observed (Zhang and Islam 2012; Hou et al. 2012; Shaikh et al. 2014). Very few studies are available that report the properties of class F high volume fly ash cement composite replacing 80 % of cement (Liu 2010; Huang et al. 2013). With the successful replacement of 80 % cement with supplementary cementitious materials, predominantly containing fly ash, the cement industry could benefit in significantly reducing its CO_2 emissions, and at the same time the production/utilisation rate of fly ash could be reduced. Therefore this study was undertaken to investigate the effect of SF and nS in combination with HL and SA on the physico-chemical behaviour of class F high volume ultrafine fly ash (HV-UFFA) cement composite, replacing 80 % of cement. Compressive strength test has been undertaken to identify the mechanical properties of the blended mortar samples. In addition, thermogravimetric analysis (TGA), X-ray diffraction (XRD) and secondary electron microscopy (SEM) have been undertaken to identify the formation of various hydrates and to understand the morphological changes occuring in the cement matrix due to the addition of various materials under study.

2. Materials and Experimental Procedure

2.1 Materials and Mix Design

The materials used in this study were: Ordinary portland cement, non-chloride calcium nitrate and sodium thiocyanate based set accelerator "Pozzolith NC 534" having water content of 51 % and polycarboxylic ether based superplasticizer "Glenium 79" having water content of 55 %, class F low calcium ultra fine fly ash, hydrated lime, densified silica fume (SF) and powdered nano silica. Raw fly Ash having a mean particle size of 15 μm was ground in a micronizer to produce ultrafine fly ash (UFFA) of mean particle size of 8.1 μm. Chemical composition of OPC, FA, SF, HL and nS is presented in Table 1. Particle size distribution of OPC, UFFA, HL, and SF was obtained by using laser diffraction particle size analyser "Malvern Mastersizer 3000" and is presented in Table 2.

XRD spectra of OPC, HL, FA, SF and nS are shown in Fig. 1. Predominant crystalline content of OPC are calcium silicates (C_2S, C_3S), calcium aluminate (C_3A), calcium alumino ferrite (C_4AF) and gypsum (G). Hydrated lime shows a sharp calcite peak at 29.4° 2-theta in addition to $Ca(OH)_2$ peaks. The crystalline content in FA was mainly from quartz and mullite. SF and nS shows broad peaks centred around 22° and 22.5° 2-theta respectively, which is a typical characteristic of amorphous silica content.

Table 3 summarizes the various mortar mix designs tested. All binding materials used were based on percentage mass of the total binding material. TGA, XRD and SEM samples were prepared with the binder paste only. Amount of superplasticizer was adjusted to get an approximately similar consistency for the self consolidation of the mortar. Water content of SP and SA were included in the total w/b ratio.

2.2 Sample Preparation, Curing & Testing

2.2.1 Compressive Strength of Mortar

All the raw materials were dry mixed at low speed in the mortar mixer for 1 min to obtain a homogenous mix. Then water, SP and SA (as required) were added and mixed for 3 min, followed by a final high speed mixing for another 1 min. Mortar samples were then poured in 50 mm × 50 mm × 50 mm steel moulds. The samples were covered with a plastic sheet, cured in room temperature for 24 h, de-moulded (except CF and S1 which were de-moulded after 48 h and 36 h respectively, because of low early strength) and then further cured in saturated lime water

Table 1 Chemical composition of OPC, HL, FA, SF and nS.

Materials	OPC (%)	HL (%)	FA (%)	SF (%)	NS (%)
SiO_2	22.3	1.5	73.1	88.2	99.9
Al_2O_3	5.2	0.6	22.8	1.2	
Fe_2O_3	0.7	0.3	0.8	2.16	
CaO	63.9	73.7	0.1	1.16	
SO_3	2.7		0.1	1.67	
MgO	1.2	0.5	0.2	1.57	
Na_2O	0.1	0.16	0.01	0.11	
K_2O	0.2	0.07	0.58	0.23	
TiO_2			1.4		
P_2O_5			0.1	1.02	
Mn_2O_3			0.04	0.14	
LOI	3.9	24.1	0.8	2.8	

Table 2 Particle size distribution of OPC, UFFA, RHL, HL, SF and NS.

Material	Mean (μm)	d_{10} (μm)	D_{25} (μm)	D_{50} (μm)	D_{75} (μm)	D_{90} (μm)
OPC	24.6	2.7	6.5	15.4	28.3	44.2
UFFA	8.1	1.2	1.2	4.6	9.2	15.0
HL	8.2	0.9	2.1	4.3	8.6	19.4
SF	3.0	0.3	0.5	1.4	3.9	8.1
NS*	7 nm					

* Particle size of nano silica (nS) is shown in nano meters.

at room temperature as per ASTM C109 until the time of testing. The samples were taken out of lime water, wiped and surface dried after 1, 7 and 28 days of curing. Compressive strength of the mortar samples was measured as per ASTM C109 using a 300kN tecnotest mortar strength testing machine. For every mix at each age, three replicates were tested at a loading rate of 0.36 MPa/s.

2.2.2 TGA, XRD and SEM of Hardened Binder Paste

Mixing procedure and curing method was kept the same for TGA, XRD and SEM binder paste samples. For TGA and XRD, the samples were ground and sieved through 63 μm sieve. To stop hydration and to remove physically bound water the solvent exchange method was adopted using acetone. A 100 mL of acetone was added to 30 g of the sieved sample in a plastic bottle and mixed vigorously by hand for about 3 min. Excess acetone was drained out and the process was repeated. The samples were then dried overnight in an oven at 40 °C temperature. The dried samples were collected and stored in a sealed plastic container till the time of testing.

TGA was conducted using PerkinElmer STA 6000 thermal analyser in a nitrogen environment with a flow rate of 19.8 mL min^{-1}. 10–20 mg of powdered samples were heated from 40 to 550 °C with the heating rate of 10 °C min^{-1}.

XRD was conducted using a Bruker AXS D4 Endeavour system using Cu-Kα radiation operated at 40 kV and 40 mA and a Lynxeye linear strip detector. Samples were tested between 5° and 55° 2-theta (2θ) with a step size of 0.02° and the counting time per step was 5 s.

For SEM, a small thin section of the hardened paste was cut out from the internal part of the specimen. It was then embedded in epoxy, ground, polished, mounted on a steel stub and gold coated. FEI Quanta 200 SEM was used to study the microstructure of the hardened paste samples. The accelerating voltage of the beam was 20 kV and the electron images were acquired at 10 mm working distance and 5000× magnification.

3. Results and Discussion

3.1 Compressive Strength

The effect of silica fume, set accelerator and hydrated lime on HV-UFFA mortar is shown in Fig. 2a. By partially replacing UFFA with SF, there was a 55 % increase in 7 day strength which further increased to 116 % at 28 days in S1 compared to that of CF. This is attributed to the effect of SF on the

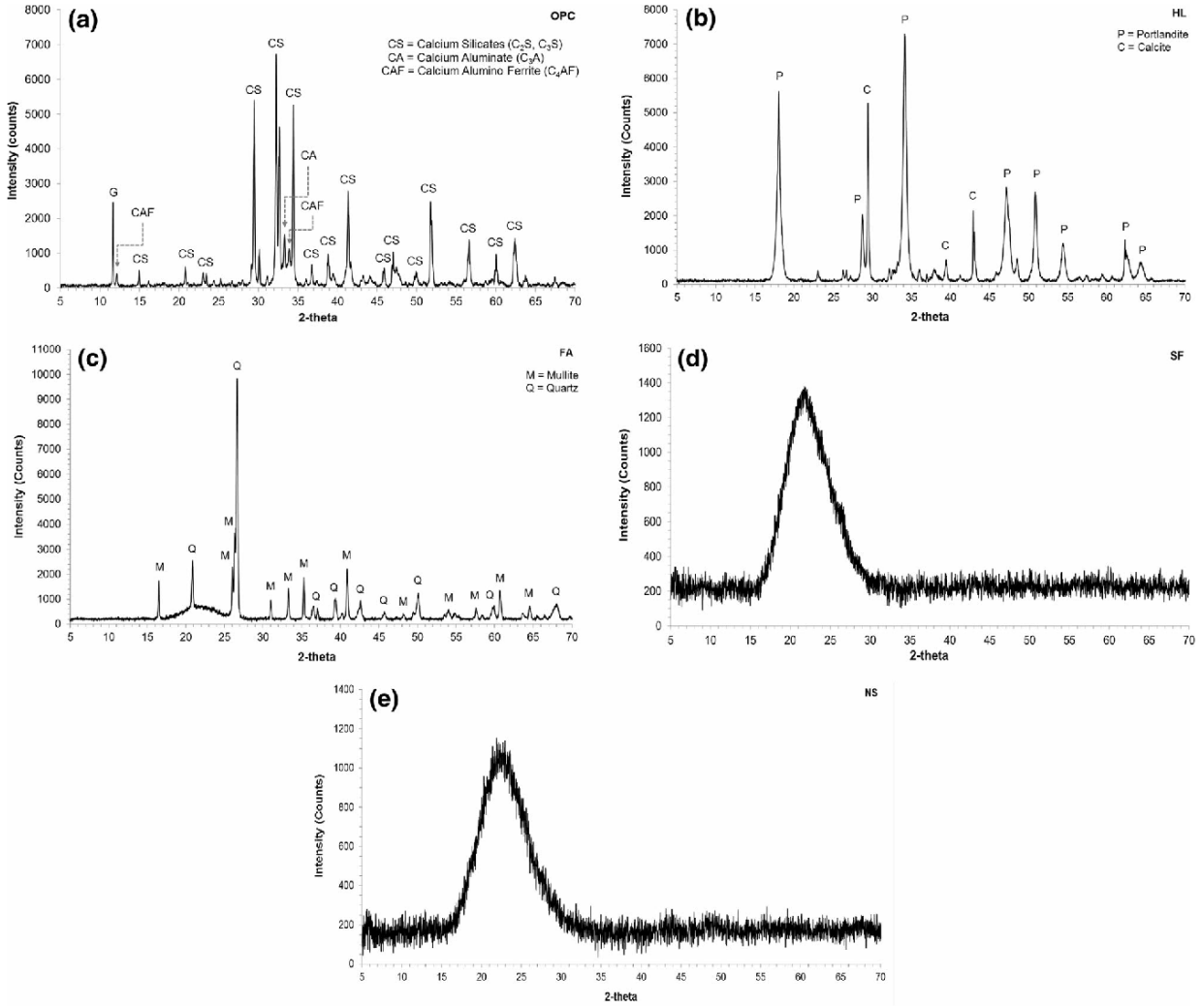

Fig. 1 XRD spectra of **a** OPC, **b** HL, **c** FA, **d** SF and **e** NS.

Table 3 Mortar mix designs.

Mix	Total Binder					S/B	W/B	SP	SA
	OPC (%)	UFFA	HL	SF	NS				
Control	100					2.4	0.3	27.5	
CF	20	80 %				2.4	0.3	11.5	
S1	20	65 %		15 %		2.4	0.3	30.0	
S2	20	65 %		15 %		2.4	0.3	30.0	27.5
S3	20	60 %	5 %	15 %		2.4	0.3	30.0	
S4	20	60 %	5 %	15 %		2.4	0.3	30.0	27.5
N1	20	75 %			5 %	2.4	0.3	60.0	
N2	20	75 %			5 %	2.4	0.3	60.0	27.5
N3	20	70 %	5 %		5 %	2.4	0.3	60.0	
N4	20	70 %	5 %		5 %	2.4	0.3	60.0	27.5

S/B sand/binder ratio, *W/B* water/binder ratio, *SP* superplasticizer = mL kg^{-1} binder, *SA* set Accelerator = mL kg^{-1} binder.

improvement of strength of HVFA cement composite. Silica fume, because of its amorphous character and large surface area, possesses high pozzolanic activity and readily reacts with the available $Ca(OH)_2$ to form additional calcium silicate hydrate, resulting in the improvement of strength. Similar results have been reported by Barbhuiya et al. (Barbhuiya et al. 2009). With

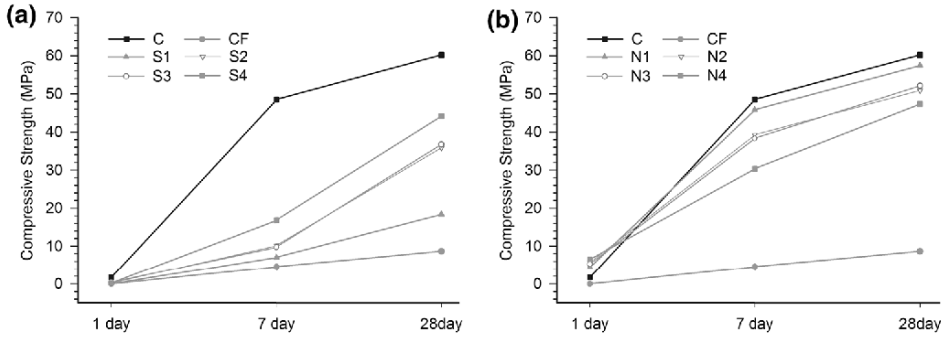

Fig. 2 Compressive strength of mortar samples (a) containing silica fume (b) containing nano silica at 1, 7 & 28 days of curing.

the combination of silica fume and set accelerator in Mix S2, the 7 and 28 day strengths improved by 124 and 316 % respectively, compared to that of Mix CF. This is attributed to the accelerating effect of SA on the pozzolanic reaction of the blended mix, which is discussed in detail in Sect. 3.2. By combining silica fume and hydrated lime in mix S3, the strength improvement was approximately the same as that of S2. The performance of 5 % hydrated lime addition was equivalent to that of set accelerator with 27.5 mL kg^{-1} binder content in improving the compressive strength of silica fume modifed HV-UFFA cement composite. When both SA and HL were added to the silica fume modified HV-UFFA in Mix S4, the 7 and 28 day strengths were improved by 273 and 413 % respectively. The combined acceleration effect imparted by SA and HL significantly improved the compressive strength of S4 compared to that of CF. This shows that the performance of the combined effect of SF, SA and HL is significantly higher than that of their individual additions in improving the compressive strength of HV-UFFA cement composite.

Figure 2b demonstrates the effect of nano silica, set accelerator and hydrated lime on HV-UFFA mortar. By partially replacing UFFA with nS, there was a significant improvement in 1 day strength of mix N1 compared to that of CF and the 7 and 28 day strengths increased by 918 and 567 % respectively. This significant improvement in strength is attributed to the amorphous character and very high surface area of nano silica, which readily reacts with the available $Ca(OH)_2$ to form additional calcium silicate hydrate. Comparing the effect of silica fume in S1 to that of nano silica in N1, nano silica performed significantly better than silica fume in improving the compressive strength. Though, both SF and nS are amorphous in nature but the particle size of nano silica is approximately 425 times smaller than the average particle size of SF. This extremely small particle size of nano silica provides a very high surface area, that accelerates the pozzolanic reaction resulting in much higher compressive strength than that with SF. When set accelerator was combined with nano silica in Mix N2, there was a further 30 % improvement in one day strength, but the 7 and 28 day strengths decreased by approximately 14 and 11 % respectively, compared to N1. This shows that though set accelerator improves the pozzolanic reaction, which results in higher 1 day strength, it has a negative impact at 7 and 28 day strengths. In comparison, the set accelerator had positive impact on silica fume modified HV-UFFA at all ages. By combining nano silica and hydrated lime in mix N3, the strength improvement was approximately the same as that of N2. Similarly, no difference on the treatment of SA and HL was observed on silica fume modified HV-UFFA mixes S2 and S3. When both SA and HL were added to the nano silica modified HV-UFFA in Mix S4, though the 1 day strength improved by 48 %, the 7 and 28 day strengths decreased by 34 and 18 % respectively. The combined effect of SA and HL was positive at 1 day and was higher than that of their individual effects. But at 7 and 28 days the combination of SA and HL proved detrimental to the strength development of HV-UFFA modified with nS and was worse than that of their individual effects.

3.2 TGA, XRD and SEM Analysis

Derivative thermogravimetric (DTG) curves were plotted from the thermogravimetric (TG) data to identify the exact boundaries of the Calcium hydroxide (CH) content at various ages of curing. Figure 3a shows typical TG and DTG curves with identifiable CH endotherm. The onset and the endset point of CH mass loss identified with the help of derivative curve, has been marked with dotted lines. Figure 3b shows a typical TG and DTG curves with no identifiable CH endotherm. The absence of CH endothermic peak shows that the residual CH content, at a particular age of curing was too small (if any) to be detected with the help of TGA.

CH (residual) in Eq. (1) represents the residual CH content at a particular age of curing, expressed in percentage of the mass of dry sample at 500 °C (M_{500}) (De Weerdt et al. 2011). CH (normalised) in Eq. (2) denotes the normalised CH content per g of cement, in which no hydrated lime powder has been added. CH (normalised) in Eq. (3) was modified to suit the addition of hydrated lime powder.

$$\text{CH (residual)} = \frac{M^{S}_{H_2O\ CH} * \frac{74}{18}}{M_{500}} * 100[\%] \quad (1)$$

$$\text{CH (normalised)} = \frac{M^{S}_{H_2O\ CH} * \frac{74}{18}}{M_{500}} * \frac{1}{0.2} * 100[\%] \quad (2)$$

(without additional hydrated lime)

$$\text{CH (normalised)} = \frac{\left[\left\{M^{S}_{H_2O\ CH} * \frac{74}{18}\right\} - \left\{\left(M^{HL}_{H_2O\ CH} * \frac{74}{18}\right) * HL_{\%}\right\}\right]}{M_{500}} * \frac{1}{0.2} * 100[\%] \quad (3)$$

(with additional hydrated lime)

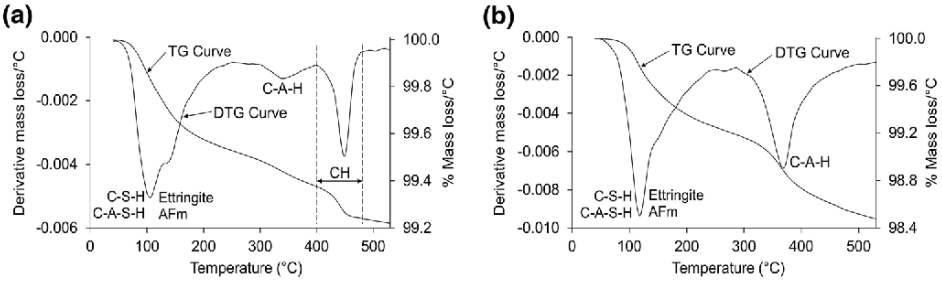

Fig. 3 a Typical TG and DTG curves with identifiable CH endotherm. b Typical TG and DTG curves with no identifiable CH endotherm. *Note* Calcium silicate hydrate (C–S–H), Calcium alumino silicate hydrate (C–A-S–H), Calcium aluminate hydrate (C–A–H), Aluminate ferrite monosulphate (AFm), Calcium hydroxide (CH).

Table 4 (a) Thermogravimetric analysis of silica fume modified samples at 1, 7 and 28 days of curing. (b) Thermogravimetric analysis of nano silica modified samples at 1, 7 and 28 days of curing.

Mix	CH (normalised)			CH (residual)		
	1 day	7 day	28 day	1 day	7 day	28 day
a						
CF	13.7 %	11.1 %	8.3 %	2.8 %	2.2 %	1.7 %
S1	13.7 %	8.8 %	4.7 %	2.8 %	1.8 %	0.9 %
S2	11.5 %	5.2 %	2.5 %	2.3 %	1.0 %	0.5 %
S3	6.1 %	−1.2 %	−13.8 %	5.5 %	4.1 %	1.6 %
S4	−0.1 %	−11.6 %	−18.9 %	4.5 %	2.0 %	0.6 %
b						
CF	13.7 %	11.1 %	8.3 %	2.8 %	2.2 %	1.7 %
N1	4.7 %			0.9 %		
N2						
N3	−13.2 %			1.7 %		
N4	−17.9 %			0.8 %		

$M^{S}_{H_2O\ CH}$ is mass loss due to the dehydroxylation of portlandite present in the hydrated cement paste. The fraction $\frac{74}{18}$ is used to convert CH bound water into CH mass, where 74 is the molar mass of $Ca(OH)_2$ and 18 is the molar mass of H_2O. The fraction $\frac{1}{0.2}$ represents the division of percentage of the OPC content in the sample to normalise the value to per g of OPC. $M^{HL}_{H_2O\ CH}$ is mass loss due to the dehydroxylation of the pure $Ca(OH)_2$ present in the raw hydrated lime, as part of the raw HL was converted to $CaCO_3$ due to its exposure to CO_2 present in the atmosphere. The pure $Ca(OH)_2$ content was 81 % of the raw HL sample. $HL_{\%}$ represnts the percentage of hydrated lime powder added to the sample. TG analysis of silica fume and nano silica modified HV-UFFA pastes cured for 1, 7 and 28 days are shown in Table 4a, b, respectively. Negative CH (normalised) values show that in addition to the CH released by the OPC, a part of the hydrated lime powder added externally, has also been consumed by the pozzolanic reaction.

XRD analysis of silica fume and nano silica modified HV-UFFA pastes cured for 1, 7 and 28 days are shown in Figs. 4a and 5a, respectively. Their SEM images at 28 days of curing are presented in Figs. 4b and 5b, respectively. Though, C–S–H is considered as the main contributor to the compressive strength of mortar/concrete, but because of its near amorphous nature, it is hard to identify through XRD analysis. Since portlandite is considered as a good indicator of the performance of the hydration/pozzolanic reaction, therefore for the clarity in presentation of the important hydration products, the XRD data is presented from 5° 2-theta to 25° 2-theta. Various phases noticed in the XRD patterns were ettringite (E), AFm_{ss} (Aluminate ferrite monosulphate)—most likely a solid solution of hemicarbonate and OH^- substituted monosulphate (Matschei et al. 2007) denoted as (A), hemicarbonate (H_c), calcium aluminium iron oxide carbonate hydroxide hydrate (F_c), monocarbonate (M_c), di-calcium aluminate hydrate (D), mullite (M), portlandite (P), quartz (Q) and calcite (C).

The increase in the pozzolanic reaction, due to the partial replacement of fly ash with silica fume in S1 can be noticed

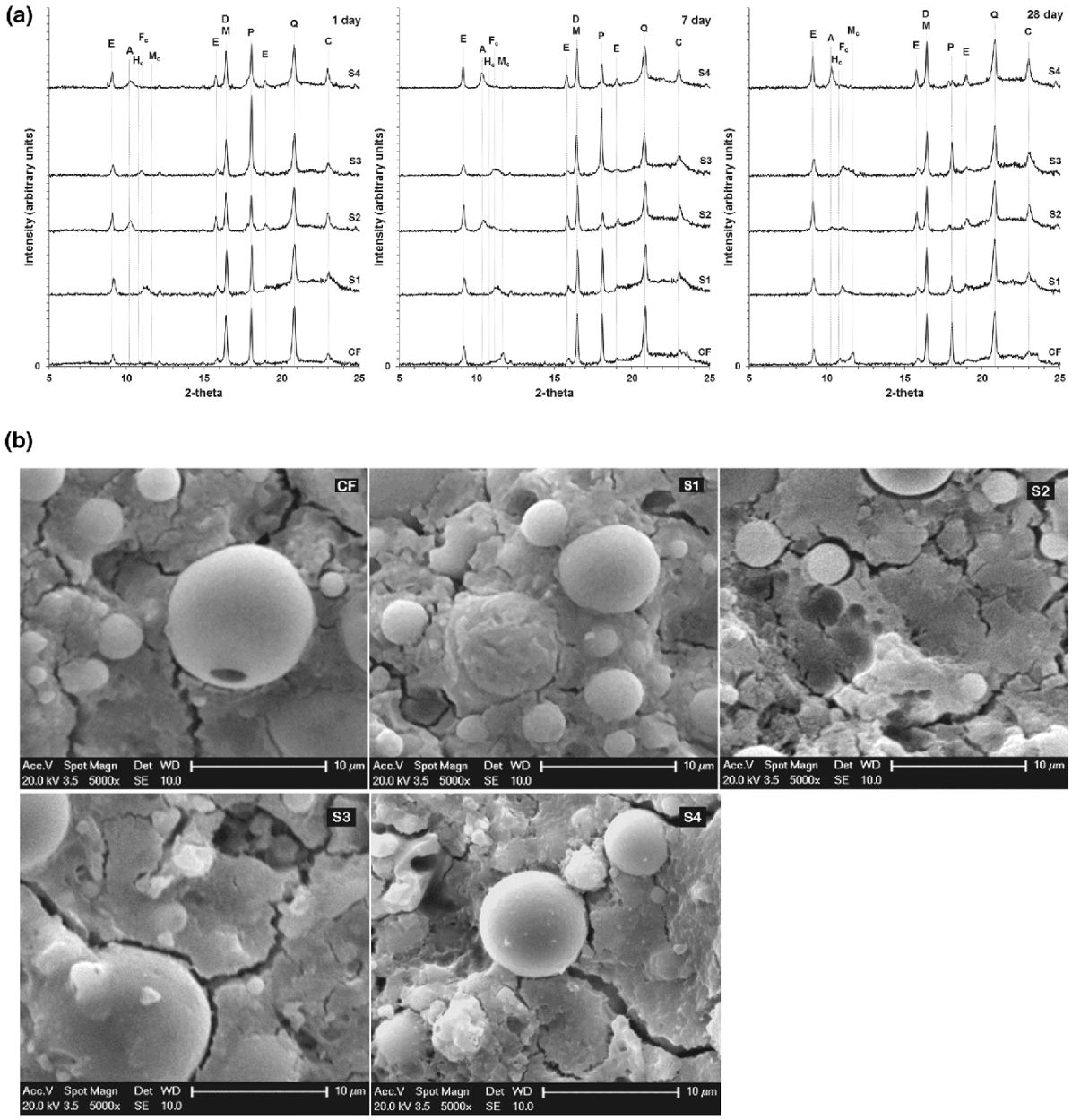

Fig. 4 a XRD spectra of silica fume modified samples at 1, 7 and 28 days of curing. b SEM images of silica fume modified samples at 28 days of curing.

in the reduction of CH (normalised) value in the TGA data and the portlandite peak in the XRD spectra at both 7 and 28 days of curing. This shows that the portlandite consumption was increased due to the presence of SF which is amorphous in nature and has considerably higher surface area than that of FA. The SEM image of S1 shows a denser C–S–H gel with finer cracks, resulting in a stronger cement matrix than that of CF. This was reflected in the corresponding increase in the compressive strength results of S1 compared to CF.

With the addition of SA in mix S2, there was a small reduction in the CH (normalised) value at 1 day, which reduced considerably at 7 and 28 days of curing, compared to S1. Similar observations were seen in the reduction in the portlandite peaks of S2 in the XRD spectra. This increase in the consumption of portlandite is attributed to the accelerating effect of SA on the pozzolanic reaction of the blended mix. The set accelerator used was calcium nitrate and sodium thiocyanate based. Calcium nitrate accelerates the setting time and moderately accelerates hardening whereas sodium thiocyanate accelerates the strength gain (Paillère 1994). As reported by Rettvin and Dalen and cited by Cabrera et al. (Cabrera and Rivera-Villarreal 1999) when calcium nitrate was used in combination with sodium thiocyanate, calcium nitrate started the hydration process earlier which was then hastened by sodium thiocyanate. The SEM image of S2 shows an increase in the density and width of cracks in the cement matrix. The XRD spectra of S2 shows a considerable increase in the intensity of ettringite peaks at 7 and 28 days compared to S1. The growth of ettringite

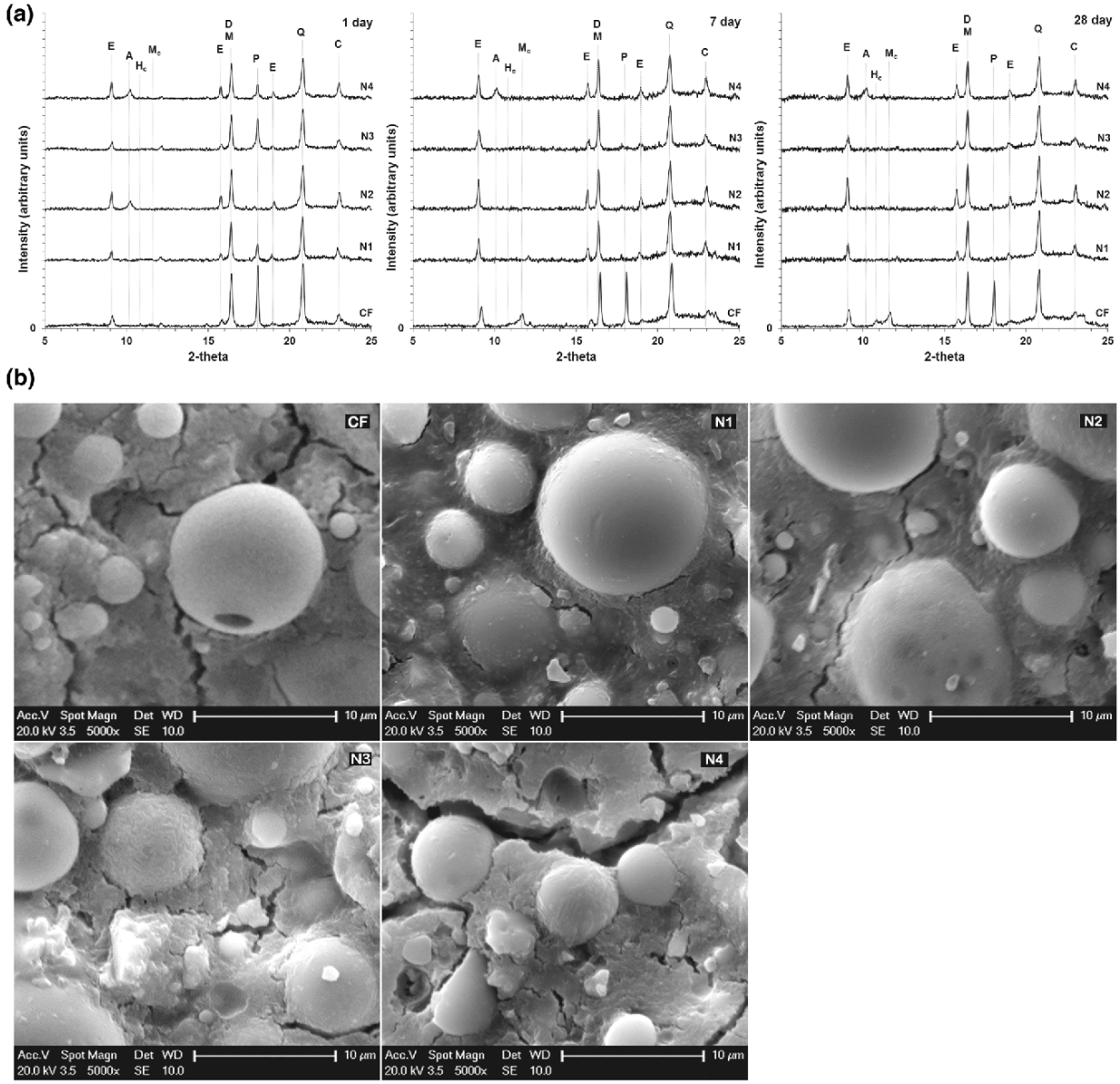

Fig. 5 a XRD spectra of nano silica modified samples at 1, 7 and 28 days of curing. b SEM images of nano silica modified samples at 28 days of curing.

crystals in smaller diameter pores refined by silica fume (Zhang and Gjørv 1991), exerts the highest expansive pressure on the pore walls promoting the development of cracks in the cement matrix (Scherer 1999). Though, based on the increase in ettringite content in S2 and the findings of (Scherer 1999), there is a possibility of ettringite being instrumental in the development of cracks, but no ettringite crystal was found within the cracks, when observed through the electron microscope. The addition of SA significantly increases the pore solution concentration of calcium ions (Ca^{+}, $CaOH^{+}$) which induces a high degree of super saturation of portlandite (Nonat 2000) that leads to the increase in disjoining pressure resulting in the development of micro cracks (Beltzung et al. 2001). Beltzung et al. (Beltzung et al. 2001) in their research on the influence of $Ca(OH)_2$ on shrinkage stresses observed that the samples containing high residual portlandite content (portlandite available in pore water after pozzolanic reaction and ettringite formation) showed higher shrinkage stresses resulting from high disjoining pressure, compared to the one having low residual portlandite. They also found that the specimens in which the portlandite produced in the system was progressively consumed during secondary pozzolanic and ettringite reactions, showed very low shrinkage stresses. They concluded that with the use of low alkali cements a significant reduction in the shrinkage stresses originating from the disjoining pressure can be achieved. Tazawa et al. (Tazawa and Miyazawa 1993) and Persson (Persson 1997) studied the relationship of self desiccation effect with the autogenous shrinkage. They reported that the self desiccation (reduction in internal relative humidity) at a particular age of curing increased with the decrease in w/c ratio, resulting in the increase in

autogenous shrinkage. Tazawa et al. (Tazawa and Miyazawa 1993) also reported that the resultant increase in autogenous shrinkage leads to early age cracking. Therefore, the increase in the development of micro cracks in S2 could be attributed to the combined effect of disjoining pressure and the self desiccation effect.

By combining silica fume and hydrated lime in mix S3, there was a considerable reduction in the CH (normalised) values at 1 and 7 days of curing, compared to S1. This shows that the addition of hydrated lime powder significantly increased the pozzolanic reaction of the blended mix. The TGA data and the XRD spectra of S3 show a significant increase in CH (residual) content and portlandite peak intensity, respectively, at all curing ages, compared to S1. This could be associated with the fact that the additional hydrated lime increased the portlandite content more than that was required to react with the amorphous silica present in SF and FA at 1 and 7 days of curing. At 7 days there was a considerable reduction in the portlandite peak of S3, which further reduced significantly by 28 days, compared to that of S1, showing an increase in the pozzolanic reaction. Comparing the consumption of the portlandite by S3 with that of S2, at 1, 7 and 28 days of curing, S3 showed a higher pozzolanic activity than S2. But the compressive strength results show no difference between S3 and S2 at all curing ages. The SEM image of S3 shows wider cracks than that of S2. This again shows that with the increases in pore solution concentration of Ca^{+} ions, and the decrease in relative internal humidity there is a corresponding increase in the development of micro cracks. The wider the cracks, the deeper they are, indicating that the higher volume of the strength forming C–S–H gel was weakened in S3, thereby, counterbalancing in reducing the strength that was improved by the increase in C–S–H gel.

When both SA and HL were added to the silica fume modified HV-UFFA in Mix S4, there was a significant improvement in the consumption of portlandite at all curing ages as seen from both the TGA data and the XRD spectra. Comparing the TGA data and the XRD spectra of S4 with that of S3, the consumption of portlandite was significantly higher in S4 at all curing ages, due to the combined accelarating effect of the SA and the HL. This increase in the pozzolanic activity was reflected in the compressive strength results of S4 which had the highest strength among all SF modified mixes. This shows that the combined effect of SA and HL provides the best performance in improving the pozzolanic reaction of SF modified HV-UFFA compared to their respective individual effects. The SEM image of S4 shows a further increase in crack width compared to that of S3. This reinforces our finding that there is a strong correlation of the combined effect of increase in portlandite content and the reduction in relative internal humidity with the resulting increase in crack formation. In-spite of the increase in micro cracking in S4, the increase in the production of C–S–H gel from the accelerated pozzolanic reaction resulted in counterbalancing the effect of increased cracking, thereby, improving its strength compared to that of S1, S2 and S3. It is to be noted, that the internal humidity can be increased without altering the w/c ratio and negatively hampering the compressive strength results, with the help of internal curing method as reported by Bentz et al. (2010), though it is not the scope of the present work.

The increase in the pozzolanic reaction, due to the partial replacement of fly ash with silica fume in S1 can be noticed in the reduction of CH (normalised) value in the TGA data and the portlandite peak in the XRD spectra at both 7 and 28 days of curing.

When the fly ash was partially replaced with nS in mix N1, there was a significant reduction in the CH (normalised) value and the corresponding intensity of the portlandite peak at 1 day, compared to CF. At 7 and 28 days of curing no identifiable portlandite content was observed in both the TGA and the XRD data of N1. This shows that with the addition of nS, the consumption of the portlandite content in pozzolanic reaction increased significantly, because of its highly amorphous nature and significantly higher surface area than that of FA. The SEM image of N1 shows a very dense C–S–H gel with a significant reduction in micro cracking, compared to that of CF, resulting in a stronger cement matrix. Since a significant amount of portlandite produced by the OPC was consumed at day 1, and its production at later ages was progressively being consumed due to the accelerated pozzolanic reaction, the resulting micro-cracking due to the disjoining pressure (Beltzung et al. 2001) were considerably reduced. Moreover, the self desiccation effect of the cement matrix alone had a minimal impact on the propagation of micro-cracking, resulting in a significant reduction in crack formation. The combination effect of increased pozzolanic reaction and highly dense cement matrix, was reflected in the corresponding increase in the compressive strength of N1 compared to CF, at all curing ages. Comparing the effect of silica fume in S1 to that of nano silica in N1, nano silica performed considerably better than SF in improving the pozzolanic reaction and densifiying the cement matrix. Though both SF and nS are amorphous in nature, the significantly higher surface area of nS was the main driving force in accelerating the pozzolanic reaction and densifying the cement matrix.

With the addition of SA in mix N2, though the pore solution concentration of Ca^{+} ions from the portlandite increases (Nonat 2000), a considerable reduction in the portlandite content was observed in both the TGA and the XRD data, compared to that of N1. There was no identifiable CH (residual) content and any noticeable intensity of the portlandite peak in N2 at all curing ages. This increase in portlandite consumption at 1 day shows that the pozzolanic reaction of N2 improved considerably with the addition of SA and the further release of portlandite from OPC at later ages, was progressively being consumed. This considerable improvement in the pozzolanic reaction of N2 resulted in 30 % increase in its compressive strength, compared to that of N1 at 1 day of curing. But, the 7 and 28 day strengths decreased by 14 and 11 % respectively. The SEM image of N2 shows increased micro-cracking than that in N1. Though, the SA considerably increases the pore solution concentration of portlandite, but it was progressively being consumed.

Therefore, the occurrence of micro cracks was most likely due to the self desiccation effect which increases with the increase in hydration/pozzolanic reaction (Persson 1997). Since, the contribution of fly ash in the production of C–S–H gel is minimal at early age i.e. before 7 days of curing, the skeleton structure of the cement matrix produced primarily from the pozzolanic reaction of nano silica is probably not strong enough to resist internal stresses, resulting in the early devlopment of micro cracks. This weakening of the cement matrix at early age, inspite of the increased pozzolanic reaction results in the reduction of 7 and 28 day compressive strength results of N2 compared to that of N1.

By adding HL to nS modified HV-UFFA in mix N3, the intensity of the portlandite peak and the CH (residual) content, increased considerably compared to that of N1 at 1 day of curing. But when compared with S3, the intensity of its portlandite peak and its CH (normalised) content was significantly lower. This shows that though the addition of HL significantly increased the portlandite content, the nano silica present in N3 consumed a large amount of it due to the accelerated pozzolanic reaction at 1 day of curing. There was no identifiable portlandite content observed in both the TGA and the XRD data of N3 at later ages of curing, showing that the remaining portlandite was consumed by the 7th day and any further release of portlandite from OPC was progessively being consumed. Though the increase in pozzolanic activity resulted in 20 % increase in 1 day strength of N3 compared to N1, the 7 and 28 days showed a strength reduction of 16 and 9 % respectively. The SEM image of N3 showed an increase in crack formation compared to that of N1. Therefore the decrease in 7 and 28 day strengths, inspite of the increase in pozzolanic reaction could be attributed to the the combined effect of high disjoing pressure because of the high portlandite content at 1 day and the self desiccation effect due to the decrease in relative humidity.The strucutral weakness so introduced in the skeleton of the cement matrix at early age negatively impacted its strength development.

When both SA and HL were added together to the nano silica modified HV-UFFA in Mix N4, the consumption of portlandite increased further, as can be seen in the considerable reduction in the CH (normalised) content and the intensity of the portlandite peak at 1 day of curing, compared to that of N3. This shows that the combined effect of nS, SA and HL provided the highest acceleration in the pozzolanic reaction of HV-UFFA cement composite compared to that of their individual effects. The compressive strength results show a further 23 % increase in 1 day strength of N4 compared to that of N3. But the 7 and 28 day strengths show a further decrease of 21 and 9 % respectively. The SEM image of N4 shows a further increase in crack width compared to that of N2 and N3. This increase in crack width could be attributed to the combined effect of increased disjoining pressure and decreased internal relative humidity at early age of curing. Since the intensity of the portlandite peak was lower than that of N1 at 1 day of curing, possibly the effect of disjoining pressure was small. But with the increase in the pozzolanic reaction, the self desiccation effect coupled with the increase in disjoining pressure could probably have aggravated the development of micro cracks. The decrease in 7 and 28 day strength of N4 inspite of a significant increase in its pozzolanic reaction, compared to that of N1, N2 and N3 shows that the formation of micro cracks at early age is a major deteriorating factor affecting the development of its compressive strength.

4. Conclusions

Based on the findings of this research, the following conclusions can be drawn:

(i) Silica fume, when used in conjunction with SA or HL considerably improves the pozzolanic reaction of HV-UFFA cement composite resulting in the improvement of its compressive strength. But, when both SA and HL are used in conjunction with the SF, the combined effect provides the best performance in accelerating the pozzolanic reaction resulting in a significant improvement in its compressive strength.

(ii) Use of silica fume considerably reduces the the development of micro cracks but when it is combined with the SA or HL increases the formation of micro cracks due to the combined effect of disjoining pressure and self desiccation effect. The highest stresses are induced when both the SA and the HL are combined with SF resulting in a significant increase in crack formation. However, this mix presented the best compressive strength because the increase in the production of C–S–H gel from the accelerated pozzolanic reaction resulted in counterbalancing the effect of increased cracking, thereby, improving its compressive strength.

(iii) Nano silica, when used in conjunction with the SA or the HL considerably improves the pozzolanic reaction of HV-UFFA cement composite resulting in the improvement of its 1 day compressive strength. But the formation of micro cracks due the disjoining pressure and self desiccation effect hinders the development of its later age strengths inspite of the increase in pozzolanic reaction. When both SA and HL are used in conjunction with the nS, the combined effect further accelerates the pozzolanic reaction, resulting in considerably improving its 1 day strength. But at later ages their combined effect significantly increases the formation of early age micro cracks resulting in considerably hindering the development of 7 and 28 day strengths, inspite of the increase in pozzolanic reaction.

(iv) Ultra-fine fly ash when combined with nano silica can help in achieving 80 % replacement of cement, having comparable mechanical properties to that of OPC.

However, the limitation of this work is that It does not address the issue of control of micro cracking induced by the self-desiccation effect and disjoining pressure, and will form part of future studies. If the formation of micro cracks are controlled in SA and HL blended HV-UFFA cement

composites modified with SF and nS, there is a great potential of tapping the benefits of their accelerated pozzolanic reaction, to further improve their compressive strength results.

Though nano silica presents a great potential in the production of highly environmental friendly cementitious material, its high cost limits its immediate application in the construction industry. But, the recent advances in the research of the production of amorphous nano silica (Lazaro et al. 2012; Lazaro Garcia AA 2014), has paved a way for its cost effective mass production method, which makes its application in construction industry within reach (Quercia and Brouwers 2010).

5. Acknowledgements

The authors greatly appreciate the scientific and technical support provided by the RMIT Microscopy & Microanalysis Facility (RMMF), at RMIT University. The authors would like to thank Cement Australia for providing the material support to carry out this research.

Open Access

References

About Coal Ash-CCP FAQs (2014). American Coal Ash Association; p. Coal Combustion Products-Frequently Asked Questions.

Atis, C. D. (2003). High-volume fly ash concrete with high strength and low drying shrinkage. *Journal of Materials in Civil Engineering, 15*(2), 153–156.

Barbhuiya, S., Gbagbo, J., Russell, M., & Basheer, P. (2009). Properties of fly ash concrete modified with hydrated lime and silica fume. *Construction and Building Materials, 23*(10), 3233–3239.

Beltzung, F., Wittmann, F., & Holzer, L. (2001). Influence of composition of pore solution on drying shrinkage. Creep, Shrinkage and Durability Mechanics of Concrete and other Quasi-Brittle Materials, edited by Ulm, F-J, Bazant, ZP and Wittmann, FH, Elsevier Science Ltd.

Benhelal, E., Zahedi, G., Shamsaei, E., & Bahadori, A. (2013). Global strategies and potentials to curb CO_2 emissions in cement industry. *Journal of Cleaner Production, 51*, 142–161.

Bentz D. P., & Weiss, W. J. (2011). Internal curing: a 2010 state-of-the-art review: US Department of Commerce, National Institute of Standards and Technology.

Björnström, J., Martinelli, A., Matic, A., Börjesson, L., & Panas, I. (2004). Accelerating effects of colloidal nano-silica for beneficial calcium–silicate–hydrate formation in cement. *Chemical Physics Letters, 392*(1), 242–248.

Cabrera, J. G., Rivera-Villarreal, R. (1999). PRO 5: International RILEM Conference on the Role of Admixtures in High Performance Concrete: RILEM.

Chindaprasirt, P., Jaturapitakkul, C., & Sinsiri, T. (2005). Effect of fly ash fineness on compressive strength and pore size of blended cement paste. *Cement & Concrete Composites, 27*(4), 425–428.

De Weerdt, K., Haha, M. B., Le Saout, G., Kjellsen, K. O., Justnes, H., & Lothenbach, B. (2011). Hydration mechanisms of ternary Portland cements containing limestone powder and fly ash. *Cement and Concrete Research, 41*(3), 279–291.

Dinakar, P., Babu, K., & Santhanam, M. (2008). Durability properties of high volume fly ash self compacting concretes. *Cement & Concrete Composites, 30*(10), 880–886.

El-Chabib, H., & Syed, A. (2012). Properties of self-consolidating concrete made with high volumes of supplementary cementitious materials. *Journal of Materials in Civil Engineering, 25*(11), 1579–1586.

Erdoğdu, K., & Türker, P. (1998). Effects of fly ash particle size on strength of Portland cement fly ash mortars. *Cement and Concrete Research, 28*(9), 1217–1222.

Hansen, T. C. (1990). Long-term strength of high fly ash concretes. *Cement and Concrete Research, 20*(2), 193–196.

Heidrich C., Feuerborn H. -J., & Weir A. (2013). Coal Combustion Products: a Global Perspective. WOCA.

Hill, R. L. (1994). The study of hydration of fly ash in the presence of calcium nitrate and calcium formate, University of North Texas, Denton, TX.

Hou, P., Wang, K., Qian, J., Kawashima, S., Kong, D., & Shah, S. P. (2012). Effects of colloidal nanoSiO_2 on fly ash hydration. *Cement & Concrete Composites, 34*(10), 1095–1103.

Huang, C.-H., Lin, S.-K., Chang, C.-S., & Chen, H.-J. (2013). Mix proportions and mechanical properties of concrete containing very high-volume of Class F fly ash. *Construction and Building Materials, 46*, 71–78.

Islam, M. S. (2014). Comparison of ASR mitigation methodologies. *International Journal of Concrete Structures and Materials, 8*(4), 315–326.

Jayakumar, M., & Abdullahi, M. S. (2011). Experimental study on sustainable concrete with the mixture of low calcium fly ash and lime as a partial replacement of cement. *Advanced Materials Research, 250*, 307–312.

Jo, B.-W., Kim, C.-H., Tae, G.-H., & Park, J.-B. (2007). Characteristics of cement mortar with nano-SiO_2 particles. *Construction and Building Materials, 21*(6), 1351–1355.

Kasai, Y., Matsui, I., Fukushima, Y., & Kamohara, H. (1983). Air permeability and carbonation of blended cement mortars. ACI Special Publication, p. 79.

Lazaro, A., Brouwers, H., Quercia, G., & Geus, J. (2012). The properties of amorphous nano-silica synthesized by the dissolution of olivine. *Chemical Engineering Journal, 211*, 112–121.

Lazaro Garcia, A. A., Quercia, G. G., & Brouwers, H. (2014). Synthesis of nano-silica at low temperatures and its application in concrete. In *Proceedings of the International Conference Non-Traditional Cement & Concrete V*, June 16–19, 2014, Brno, Czech Republic.

Li, G., & Wu, X. (2005). Influence of fly ash and its mean particle size on certain engineering properties of cement composite mortars. *Cement and Concrete Research, 35*(6), 1128–1134.

Liu, M. (2010). Self-compacting concrete with different levels of pulverized fuel ash. *Construction and Building Materials, 24*(7), 1245–1252.

Malhotra, V. M., Mehta, P. K., & Development SCMfS. (2002). High-performance, high-volume fly ash concrete: materials, mixture proportioning, properties, construction practice, and case histories: Suppementary Cementing Materials for Sustainable Development.

Matschei, T., Lothenbach, B., & Glasser, F. (2007). The AFm phase in Portland cement. *Cement and Concrete Research, 37*(2), 118–130.

Mehta, P. K. (1986). Concrete. Structure, properties and materials

Nagataki, S., & Ohga, H. (1992). Combined effect of carbonation and chloride on corrosion of reinforcement in fly ash concrete. ACI Special Publication.

Nakarai, K., & Ishida, T. (2009). Numerical evaluation of influence of pozzolanic materials on shrinkage base on moisture state and pore structure. In *Creep, Shrinkage and Durability Mechanics of Concrete and Concrete Structures, Two Volume Set: Proceedings of the CONCREEP 8 conference*, Ise-Shima, Japan. CRC Press.

Nonat, A. (2000). *PRO 13: 2nd International RILEM Symposium on Hydration and Setting-Why Does Cement Set?* An interdisciplinary approach: RILEM Publications.

Paillère, A. M. (1994). Application of admixtures in concrete: CRC Press.

Paya, J., Monzo, J., Peris-Mora, E., Borrachero, M., Tercero, R., & Pinillos, C. (1995). Early-strength development of Portland cement mortars containing air classified fly ashes. *Cement and Concrete Research, 25*(2), 449–456.

Pepper, L., & Mather, B. (1959). Effectiveness of mineral admixtures in preventing excessive expansion of concrete due to alkali-aggregate reaction. American Soc Testing & Materials Proc.

Persson, B. (1997). Self-desiccation and its importance in concrete technology. *Materials and Structures, 30*(5), 293–305.

Quercia, G., & Brouwers, H. (2010). Application of nano-silica (nS) in concrete mixtures. In *8th fib PhD symposium in Kgs Lyngby, Denmark, 2010* (pp. 431–436).

Rashad, A. M. (2014). Seleem HE-DH, Shaheen AF. Effect of silica fume and slag on compressive strength and abrasion resistance of HVFA concrete. International Journal of Concrete. *Structures and Materials, 8*(1), 69–81.

Reis, R., & Camões, A. (2011). Eco-efficient ternary mixtures incorporating fly ash and metakaolin. In *International Conference on Sustainability of Constructions – Towards a Better Built Environment. Proceedings of the Final Conference of COST Action C25*, Feb 3–5, 2011, University of Innsbruck, Austria.

Şahmaran, M., Yaman, İ. Ö., & Tokyay, M. (2009). Transport and mechanical properties of self consolidating concrete with high volume fly ash. *Cement & Concrete Composites, 31*(2), 99–106.

Sata, V., Jaturapitakkul, C., & Kiattikomol, K. (2007). Influence of pozzolan from various by-product materials on mechanical properties of high-strength concrete. *Construction and Building Materials, 21*(7), 1589–1598.

Scherer, G. W. (1999). Crystallization in pores. *Cement and Concrete Research, 29*(8), 1347–1358.

Sellevold E, Radjy F (1983). Condensed silica fume (microsilica) in concrete: water demand and strength development. ACI Special Publication, p. 79.

Shaikh, F., Supit, S., & Sarker, P. (2014). A study on the effect of nano silica on compressive strength of high volume fly ash mortars and concretes. *Materials and Design, 60*, 433–442.

Singh, L. P., Goel, A., Bhattachharyya, S. K., Ahalawat, S., Sharma, U., & Mishra, G. (2015). Effect of Morphology and Dispersibility of Silica Nanoparticles on the Mechanical Behaviour of Cement Mortar. *International Journal of Concrete Structures and Materials, 9*, 1–11.

Sivasundaram, V., Carette, G., & Malhotra, V. (1990). Long-term strength development of high-volume fly ash concrete. *Cement & Concrete Composites, 12*(4), 263–270.

Tazawa, E., & Miyazawa, S. (1993). Autogenous shrinkage of concrete and its importance in concrete technology. In *RILEM Proceedings* (p. 159). Chapman & Hall.

Turanli, L., Uzal, B., & Bektas, F. (2005). Effect of large amounts of natural pozzolan addition on properties of blended cements. *Cement and Concrete Research, 35*(6), 1106–1111.

Wei, X., Zhu, H., Li, G., Zhang, C., & Xiao, L. (2007). Properties of high volume fly ash concrete compensated by metakaolin or silica fume. *Journal of Wuhan University of Technology-Mater Science, 22*(4), 728–732.

Zhang, M.-H., & Gjørv, O. E. (1991). Effect of silica fume on pore structure and chloride diffusivity of low parosity cement pastes. *Cement and Concrete Research, 21*(6), 1006–1014.

Zhang, M.-H., & Islam, J. (2012). Use of nano-silica to reduce setting time and increase early strength of concretes with high volumes of fly ash or slag. *Construction and Building Materials, 29*, 573–580.

Chapter 4

High volume fly ash cement composite modified with nano silica, hydrated lime and set accelerator

This experiment looks at the effect of different concentrations of nano silica on high volume fly ash cement composites with and without the use of set accelerator and hydrated lime. The cement replacement level in this experiment was 70% and the fly ash used was raw fly ash.

Materials and Structures (2016) 49:1997–2008
DOI 10.1617/s11527-015-0629-z

ORIGINAL ARTICLE

High volume fly ash cement composite modified with nano silica, hydrated lime and set accelerator

Rajeev Roychand · Saman De Silva · David Law · Sujeeva Setunge

Received: 19 March 2015 / Accepted: 4 May 2015 / Published online: 10 May 2015

Abstract This paper presents the effect of nano silica, used individually and in combination with set accelerator or hydrated lime, on the properties of high volume fly ash (HVFA) cement composites, replacing 70 % of cement. Compressive strength test along with X-ray diffraction and thermogravimetric analysis were undertaken to study the effect of various elements on the physico-chemical behaviour and the pozzolanic activity of the blended samples. The addition of 5 % nano silica improved the 7 day strength of the blended sample by 76 % and by further increasing the nano silica content to 7.5 %, the 7 day strength increased by 94 %. However, at 28 days both 5 and 7.5 % nano silica modified samples showed approximately the similar improvement in strength i.e. 54 and 50 % respectively. With the addition of set accelerator to nano silica modified HVFA cement blend, there was a considerable reduction in both 7 and 28 day strengths. Addition of 5 % hydrated lime to HVFA blend, modified with 5 % nano silica showed no effect on the further improvement of strength. However, when 5 % hydrated lime was added to the 7.5 % nano silica modified HVFA blend, there was a considerable reduction in both 7 and 28 day strengths. This demonstrates that nano silica is highly effective in improving the strength of high volume fly ash cement blends when used alone, but when it is used in combination with either hydrated lime or set accelerator, shows no or negative effect on the development of strength.

Keywords Nano silica · Fly ash · Hydrated lime · Set accelerator · X-ray diffraction · Thermo-gravimetric analysis

Electronic supplementary material The online version of this article (doi:10.1617/s11527-015-0629-z) contains supplementary material, which is available to authorized users.

R. Roychand (✉) · S. De Silva · D. Law · S. Setunge
School of Civil, Environmental and Chemical Engineering, RMIT University, Melbourne, VIC, Australia
e-mail: rajeev.roychand@rmit.edu.au

S. De Silva
e-mail: saman.desilva@rmit.edu.au

D. Law
e-mail: david.law@rmit.edu.au

S. Setunge
e-mail: sujeeva.setunge@rmit.edu.au

1 Introduction

The cement industry is estimated to be responsible for 5–7 % of the global anthropogenic CO_2 emissions [1]. Extensive research has been going on to cut down these emissions by making the maximum use of industrial by products such as fly ash, slag, silica fume etc. as cement replacement materials [2–4]. Of these various supplementary cementitious materials, fly ash (FA) is the most abundantly available and least utilised

material worldwide [5, 6]. Therefore a major focus has been given to increasing the use of fly ash as a cement replacement material. The majority of global fly ash production falls into the low calcium class F category [7] which has low reactivity [8]. Several studies have been conducted in the past to address its low reactivity and to improve the mechanical properties of high volume fly ash (HVFA) blended cementitious composites by making use of various materials such as hydrated lime [2], set accelerator [9], silica fume [2], and metakaoline [10]. All of them have proved to improve the properties of high volume fly ash cement composites in their own capacity, each having a different effect in its contribution towards improvement in hydration reaction and subsequent strength formation.

Recently, there has been a strong inclination towards the use of nano silica (nS) in improving the properties of plain cement and high volume fly ash blended mixes because of its highly amorphous nature and nano sized particles. Nano silica readily reacts with the free lime available in mix to produce additional calcium silicate hydrate (C–S–H) gel, thereby significantly contributing towards early strength development [11]. In addition, it helps in refining the pore structure [12] which is highly beneficial for the enhancement of the durability properties of mortar/concrete. Though, its high surface area produces a strong positive effect on the mechanical and durability properties, it significantly reduces the workability, thereby increasing the superplasticizer requirement [13]. Zhang et al. [14] found that by replacing fly ash with 1 % nano silica in 50 % ordinary portland cement (OPC) and 50 % FA blended mix there was 17 % increase in 7 day strength which reduced to a 7 % increase at 28 days. They also observed that the superplasticizer (SP) requirement increased by 171 % in the case of powdered nano silica and by 238 % in the case of colloidal nano silica in comparison to a mix not containing nano silica. Shaikh et al. [15] investigated the effect of 1, 2, 4 and 6 % nano silica on OPC and found that 2 % was the optimum content which gave the maximum improvement in 7 and 28 day strength of 13 % and 14 % respectively. They further investigated the effect of 2 % nano silica on OPC and fly ash blended mix containing 68 % FA and found that there was no difference in strength at 7 days but at 28 days there was 56 % increase in strength as compared to the mix not containing nano silica. Hou et al. [16] studied the effect of 0, 2.25 and 5 % colloidal nano silica in high volume fly ash cement composite containing 60 % FA. They found that with the increasing amount of nano silica no difference was noticed at 1 day, at 3 and 7 days the strength increased with the increasing amount of nano silica but at 3 months samples containing colloidal nano silica (CNS) had lower strength than the one not containing CNS, indicating that it has negative effect at later ages. The maximum increase that they observed with 5 % nano silica at 3 and 7 days was approximately 60 % higher than the one containing 0 % CNS.

Based on the past research it can be observed that there is a significant variation in the effect of nano silica on the percentage of strength improvement of high volume fly ash cement composites. Moreover, though hydrated lime (HL) and set accelerator (SA) have been shown to improve the mechanical properties of HVFA cement composites, there appears to be no research that investigates their effect in combination with nano silica. Therefore this study was undertaken to investigate the effect of 0, 5 and 7.5 % nano silica on the compressive strength of HVFA cement mortar with and without SA and HL. In this study the cement was replaced with 70 % of varying proportions of FA, nS and HL. X-ray diffraction (XRD) and thermogravimetric analysis (TGA) have been undertaken to identify the formation of various hydrates and their variation over time.

2 Materials and experimental procedure

2.1 Materials and mix design

The materials used in this study were: Ordinary portland cement, non-chloride set accelerator "Pozzolith NC 534" having water content of 51 % and polycarboxylic ether based superplasticizer "Glenium 79" having water content of 55 %, class F low calcium fly ash, hydrated lime and nano silica. Chemical composition of OPC, FA, HL and nS is presented in Table 1. Particle size distribution of OPC, FA and HL was obtained by using laser diffraction particle size analyser "Malvern Mastersizer 3000" and is presented in Table 2.

XRD spectra of OPC, FA, HL and nS are shown in Fig. 1. The predominant crystalline content of OPC is

Table 1 Chemical composition of OPC, HL, FA and nS

Materials	OPC (%)	HL (%)	FA (%)	nS (%)
SiO_2	22.3	1.5	73.1	99.9
Al_2O_3	5.2	0.6	22.8	–
Fe_2O_3	0.7	0.3	0.8	–
CaO	63.9	73.7	0.1	–
SO_3	2.7	–	0.1	–
MgO	1.2	0.5	0.2	–
Na_2O	0.1	0.16	0.01	–
K_2O	0.2	0.07	0.58	–
TiO_2	–	–	1.4	–
P_2O_5	–	–	0.1	–
Mn_2O_3	–	–	0.04	–
LOI	3.9	24.1	0.8	–

calcium silicate (CS) and gypsum (G). Hydrated lime shows a sharp calcite peak at 29.4° 2-theta in addition to $Ca(OH)_2$ peaks, indicating that a part of hydrated lime was converted to Calcite, due to its exposure to the atmospheric CO_2. The crystalline content in FA was mainly from quartz and mullite. Nano silica shows a broad peak centred around 22.5° 2-theta, which is a typical characteristic of amorphous silica content.

Table 3 summarizes the various mortar mix designs tested. All binding materials were used based on the percentage mass of the total binding material. XRD and TGA samples were prepared with the binder paste only. Amount of superplasticizer was adjusted in the mix designs to get approximately similar consistency for the self consolidation of the mortar into the steel moulds. Mixes containing nano silica required the

Table 2 Particle size distribution of OPC, FA, HL and nS

Material	Mean (μm)	D_{10} (μm)	D_{25} (μm)	D_{50} (μm)	D_{75} (μm)	D_{90} (μm)
OPC	24.6	2.7	6.5	15.4	28.3	44.2
FA	28.7	2.3	5.8	14.0	33.1	75.2
HL	8.2	0.9	2.1	4.3	8.6	19.4
nS*	7 nm	–	–	–	–	–

* Particle size of nS is shown in nano meters

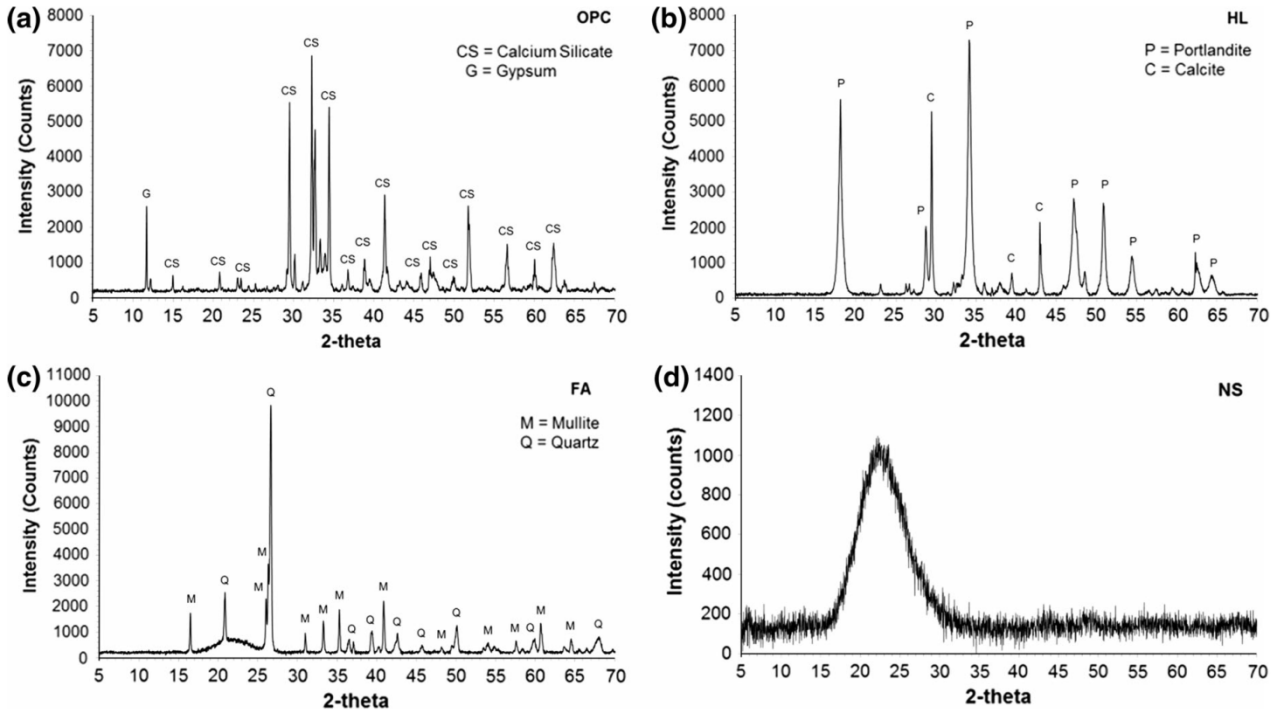

Fig. 1 XRD spectra of **a** OPC, **b** HL, **c** FA and **d** NS

Table 3 Mortar mix designs

Mix	Total binder				S/B[a]	W/B[b]	SP[c]	SA[d]
	OPC (%)	FA (%)	HL (%)	nS (%)				
Control	100	–	–	–	2.4	0.3	27.5	–
M1	30	70	–	–	2.4	0.3	11.5	–
M2	30	70	–	–	2.4	0.3	11.5	27.5
M3	30	65	5	–	2.4	0.3	11.5	–
M4	30	65	–	5	2.4	0.3	50.0	–
M5	30	65	–	5	2.4	0.3	50.0	27.5
M6	30	60	5	5	2.4	0.3	50.0	–
M7	30	62.5	–	7.5	2.4	0.3	60.0	–
M8	30	62.5	–	7.5	2.4	0.3	60.0	27.5
M9	30	57.5	5	7.5	2.4	0.3	60.0	–

[a] Sand/binder ratio

[b] Water/binder ratio

[c] Superplasticizer = mL kg^{-1} binder

[d] Set accelerator = mL kg^{-1} binder

highest amount of superplasticizer because of its very high surface area as compared to OPC and other supplementary cementitious materials. Water content of SP and SA was included in the total *w/b* ratio.

2.2 Sample preparation, curing and testing

2.2.1 Compressive strength

All the raw materials were dry mixed at low speed in a mortar mixer for 1 min to obtain a homogenous mix. Then 65 % of water was added and mixed for 2 min followed by 1 min mixing after the addition of remaining water, SP and SA (as required), followed by a final high speed mixing for another 1 min. Mortar samples were then poured in 50 mm × 50 mm × 50 mm steel moulds. The samples were covered with a plastic sheet, cured in room temperature for 24 h, de-moulded and then further cured in lime water at room temperature until the time of testing. The samples were taken out of lime water, wiped and surface dried after 7 and 28 days of curing. Then compressive strength of the mortar samples was measured as per ASTM C109 using a 300 kN tecnotest mortar strength testing machine. For every mix at each age, three replicates were tested at a loading rate of 0.36 MPa s^{-1}.

2.2.2 XRD and TGA of binder paste

All binding materials were dry mixed at low speed in a mortar mixer for 1 min to obtain a homogeneous mixture. Then 65 % of water was added and mixed for 2 min followed by 1 min mixing after the addition of remaining water, SP and SA (as required), followed by a final high speed mixing for another 1 min. Paste samples were then poured in sealed plastic vials and cured in room temperature for 24 h, de-moulded and then further cured in lime water at room temperature until the time of testing. At the end of required curing period, the samples were ground and sieved through a 63 μm sieve. To stop hydration and to remove physically bound water the solvent exchange method was adopted using acetone. A 100 mL of acetone was added to 30 g of the sieved sample in a plastic bottle and mixed vigorously by hand for about 3 min. Excess acetone was drained out and the process was repeated. The samples were then dried overnight in an oven at 40 °C temperature. The dried samples were collected and stored in a sealed plastic container till the time of testing.

XRD was conducted using a Bruker AXS D4 Endeavour system using Cu-Kα radiation operated at 40 kV and 40 mA and a Lynxeye linear strip detector.

Samples were tested between 5° and 55° 2-theta (2θ) with a step size of 0.02° and the counting time per step was 5 s.

TGA was conducted using PerkinElmer STA 6000 thermal analyser in a nitrogen environment with a flow rate of 19.8 mL min^{-1}. 10–20 mg of powdered samples were heated from 40 to 600 °C with the heating rate of 10 °C min^{-1}.

3 Results and discussion

3.1 Compressive strength analysis

The compressive strength results along with the standard deviation between the replicates, of all the samples at 7 and 28 days are shown in Fig. 2.

It was found that the SA improved the strength of C–F–S sample at 28 days, though no difference was noticed at 7 days in comparison to the corresponding C–F sample, without SA. This delay in the improvement of strength could be due to the low reactivity of fly ash. The presence of SA in C–F–N–S samples showed a negative effect on the strength of 5 and 7.5 % nS blended HVFA samples at both 7 and 28 days. It can be noticed in XRD spectra of both C–F–N–S samples that there was a significant increase in their ettringite content. Nano silica has been shown to decrease the pore size and the total porosity of the blended samples [17] and the growth of ettringite crystals in smaller diameter pores exert highest expansive pressure on the pore walls, thereby promoting the development of cracks [18]. This combination of smaller pore size and higher ettringite content in C–F–N–S samples could be attributed to its lower compressive strength as compared to the C–F–N samples. However, fly ash blended C–F–S samples, despite having high delayed ettringite content, showed an increase in 28 day strength. This could be due to the fact that addition of high volume of fly ash, increases the pore size and the total porosity of the blended sample [17]. This provides enough space for the growth of ettringite crystals without having any detrimental effect on the compressive strength.

Addition of HL, did not show any difference in the 7 day strength of C–F–L sample, but at 28 days there was a 14 % increase in strength as compared to the C–F. This is attributed to the low reactivity of FA, due to which the addition of HL had a delayed effect on the strength development of C–F–L sample. In the case of C–F–N–L samples the presence of HL showed no effect on the one containing 5 % nS and negative effect on the other containing 7.5 % nS at both 7 and 28 days in comparison to their corresponding C–F–N samples. This shows that the excess of portlandite is detrimental to the strength development of blended samples containing nano silica. This effect increases with an increase in nS content. In the C–F–N samples, where the portlandite content is significantly lower than the C–F–N–L samples, there is a significant improvement in the compressive strength as compared to the C–F sample. Moreover, the strength increases with an increase in nS content. This shows that nano silica is more effective in improving the strength of FA blended samples when there is a limited release of portlandite content. Excess of portlandite, in combination with high nano silica content, is detrimental to the development of compressive strength.

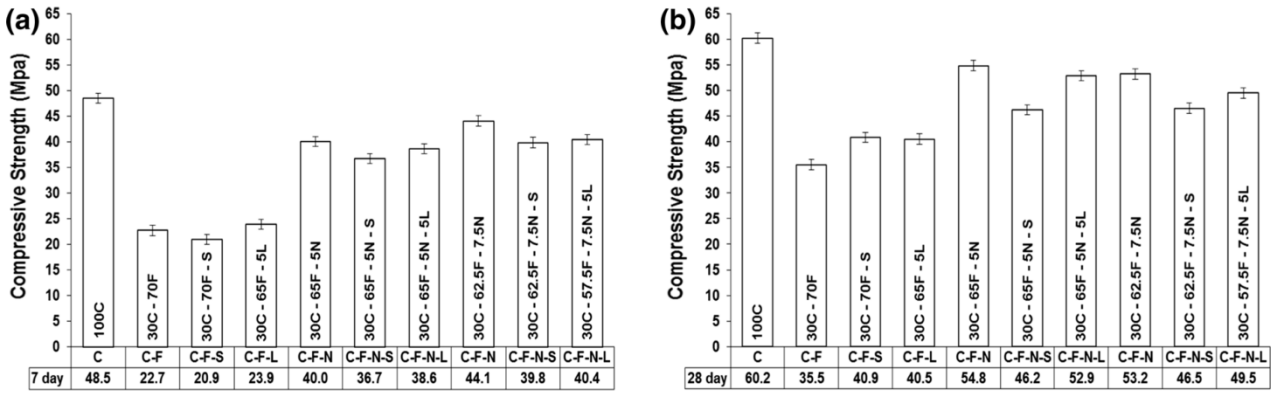

Fig. 2 Compressive strength of the mortar samples **a** 7 day and **b** 28 day (*Note C* cement, *F* fly ash, *S* set accelerator, *L* hydrated lime, *N* nano silica)

3.2 X-ray diffraction (XRD) analysis

Figure 3, presents the XRD patterns of OPC and blended cement pastes at 7 and 28 days. The various phases identified in the XRD patterns were ettringite, AFm_{ss} (most likely a solid solution of hemicarbonate and $O\bar{H}$ substituted monosulphate) [19], mono-carbonate, di-calcium aluminate hydrate, mullite, portlandite, quartz, calcite, calcium silicate, calcium silicate hydrate and tri-calcium aluminate hydrate. The di-calcium alumino hydrate peak had an overlap with the mullite peak at the same 16.4° 2θ. Another peak overlap effect was noticed around 29.5° 2θ from calcite, calcium cilicate and calcium silicate hydrate peaks. The primary quartz peak located at 26.7° 2θ had a very high intensity and was overshadowing the low intensity hydrated phases in the stacked XRD spectra of all the samples. Therefore, for the clarity in the presentation of all the hydration products, the XRD data for 25°–27° 2θ is not shown in Fig. 3.

It was found that the effect of SA was predominantly visible on the ettringite and portlandite peaks. The intensity of the ettringite peak of C–F–S was 78 % higher than that of C–F at 28 days, but in both C–F–N–S samples, the intensity almost doubled at 7 days with no further change at 28 days, as compared to C–F–N samples. This shows that the SA promotes the formation of ettringite content but its formation also depends upon the rate of hydration. Calcium nitrate, which is the dominant constituent of the SA used in this study, induces a high degree of super saturation of portlandite [20]. This high degree of supersaturation acts as a driving force for the growth of ettringite crystals resulting in the development of the highest expansive pressure on smaller diameter pores [18], resulting from pore refinement by pozzolanic reaction

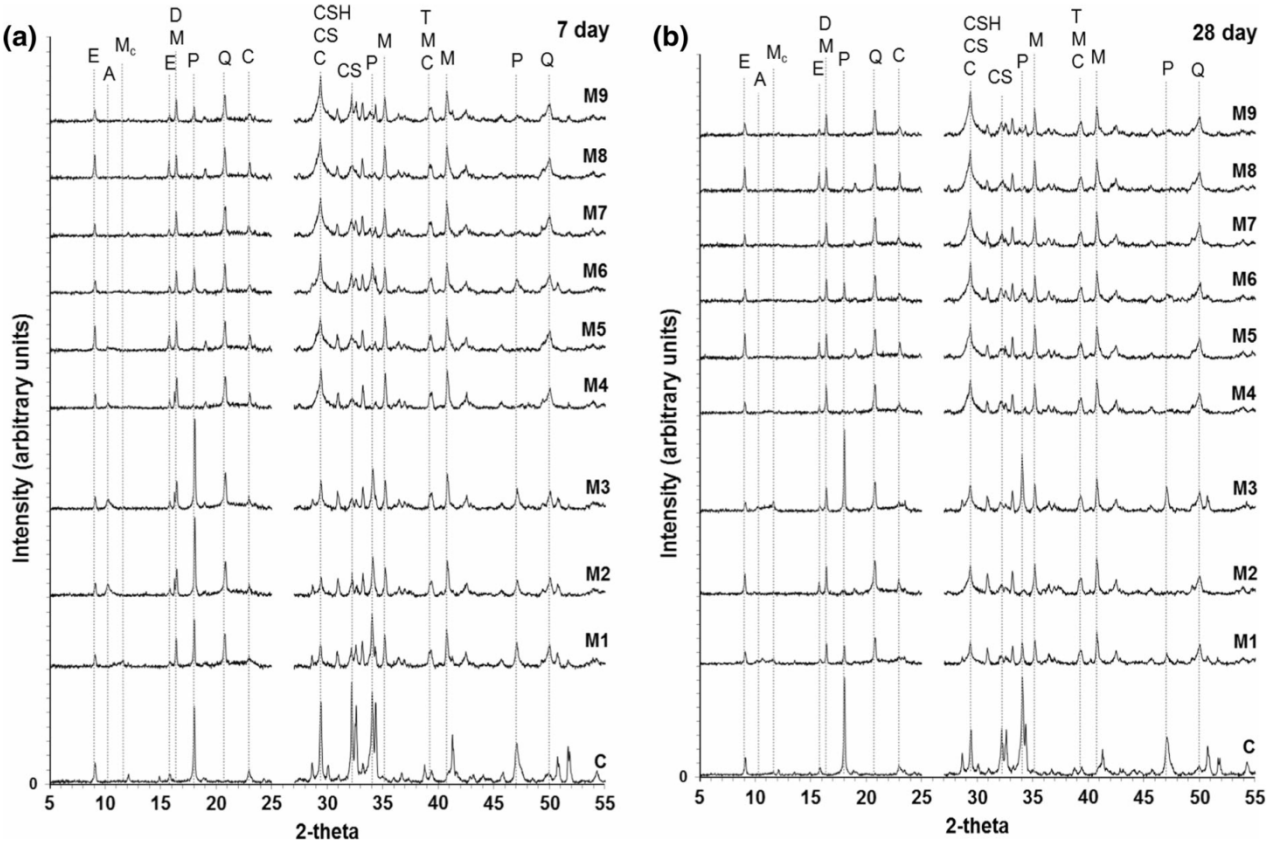

Fig. 3 X-ray diffraction patterns at 7 and 28 days of hydration. The peaks are labelled as: *E* ettringite, *A* AFm_{ss} (solid solution of hemicarbonate and OH^- substituted monosulphate), *Mc* mono-carbonate, *D* di-calcium aluminate hydrate (C_2AH_8), *M* mullite, *P* portlandite, *Q* quartz, *C* calcite, *CS* calcium silicate, *CSH* calcium silicate hydrate, *T* tri-calcium aluminate hydrate (C_3AH_6)

of nano silica [17, 21]. This combination is detrimental and promotes the development of cracks due to the crystallisation pressure [18]. The negative effect induced by the significant increase in the ettringite content on nano silica modified C–F–N–S samples was evident from the corresponding reduction in their compressive strength results at both 7 and 28 days. This shows that the addition of SA to nS modified HVFA composites, produces an adverse effect on strength gain. However, the C–F–S sample showed an improvement in its 28 day strength. This could be due to the super saturation of portlandite which is highly effective in increasing the reactivity of FA, in addition to the larger pore size available in HVFA blended mix [17], which are least affected by the crystallisation pressure of ettringite [18].

Though, C–S–H is considered as the main contributor to the compressive strength of mortar/concrete but because of its near amorphous nature [22] it is hard to identify through XRD analysis. Therefore, portlandite content is used as another indicator for the comparison of strength. Portlandite, which is a product of cement hydration, reacts with amorphous silica present in various SCM's to produce additional C–S–H gel, thereby improving its strength. As such, portlandite is considered as a good indicator of the performance of the hydration reaction. The major peaks of portlandite were present at 18.05° and 34.1° 2-theta. The 18.05° 2-theta peak was used for comparison as it had the highest intensity and was isolated from any overlapping peaks.

It was observed that the addition of SA, increased the intensity of the portlandite peak by 60 % in C–F–S at 7 days. This is attributed to the SA significantly increasing the pore solution concentration of calcium ions (Ca^{+}, $CaOH^{+}$) which induces a high degree of super saturation of portlandite [20]. In contrast, no increase in portlandite intensity was noticed in C–F–N–S samples at 7 day hydration. This difference can be attributed to the presence of nano silica in C–F–N–S samples, which because of its amorphous nature and very small particle size consumed the additional portlandite to produce more C–S–H gel. In comparison, FA has very low reactivity as the reactive silica present in it is accumulated in the interior part of its particles, which are very slowly corroded in the presence of portlandite. Interestingly, it can be noticed that C–F–S sample took 28 days to consume this additional portlandite which was already consumed by C–F–N–S at 7 days. This difference was also reflected in the corresponding difference in the compressive strength of C–F–S in comparison with C–F–N–S samples.

With the addition of hydrated lime, there was a significant increase in the intensity of portlandite peaks of C–F–L and C–F–N–L as compared to C–F and C–F–N samples respectively. This could be associated with the fact that the additional hydrated lime increased the portlandite content more than that was required to react with the amorphous silica present in FA and nS. But, for the same amount of hydrated lime addition, there was a significant difference in the portlandite content of C–F–N–L samples as compared to C–F–L which can be attributed to the presence of nano silica in the former. Moreover, C–F–N–L having 7.5 % nS content had a lower portlandite content as compared to the one containing 5 % nS. This again shows that with the increase in the proportion of amorphous and nano size content, there is a corresponding increase in the pozzolanic reaction. However, this increase in pozzolanic reaction was not reflected by a corresponding increase in compressive strengths. The C–F–L sample did show an increase in 28 days strength as compared to the C–F sample, but the C–F–N–L sample containing 5 % nS showed no difference both at 7 and 28 days as compared to its corresponding C–F–N sample. The C–F–N–L sample containing 7.5 % nS showed a small reduction in strength at both ages, as compared to their respective C–F–N samples. To further identify the reasons behind no or negative effect of HL on the compressive strength of C–F–N–L samples, thermogravimetric analysis was undertaken

The presence of nS in C–F–N samples, significantly reduced the intensity of portlandite peaks, as compared to that of C–F, at both 7 and 28 days. This shows a significant increase in the pozzolanic reaction due to the addition of nS. This was reflected in the substantial improvement in their corresponding compressive strengths. Although the C–F–N samples containing 7.5 % nS had higher compressive strength at 7 days as compared to the one containing 5 % nS, the intensities of their respective portlandite peaks were not strong enough to be differentiated. Both these samples had their portlandite peaks lying within the noise level. Therefore, thermogravimetric analysis was undertaken to further identify the possible reasons behind this effect.

3.3 Thermogravimetric analysis

Thermogravimetric (TG) curves of hydrated cement paste samples at 7 and 28 days of curing are shown in Fig. 4. Derivative thermogravimetric (DTG) curves were plotted from the TG data to identify the exact boundaries of various phases or group of phases present in the hydrated samples. DTG curves of the hydrated cement paste samples are shown in Fig. 5. The observed endotherms and their corresponding mass losses are ascribed to:

- ~60–250 °C: C–S–H, C_2ASH_8, Ettringite, AFm_{ss}, mono-carbonate (Mc)
- ~250–450 °C: C_2AH_8, C_3AH_6
- ~400–500 °C: CH

Typically the breakdown of C–A–H phases ranged between ~250 and 400 °C, but in some of the samples the C–A–H phases were extended to ~450 °C. The exact boundary of the C–A–H phases was identified from the DTG curves.

The breakdown of the phases or group of phases for both 7 and 28 day hydration are shown in Table 4. It was noticed that for the samples containing nS at 28 days, the distinct boundaries between C–A–H and CH phases were not found in DTG curves. Therefore, only 7 day strength results of C–A–H and CH content were chosen for the comparison purposes, as their respective individual proportions has an effect on the understanding of the mechanism of the hydration reaction and its subsequent effect on the compressive strength results.

CH (normalised) represents the normalised CH content per g of cement and corrections were made for the hydrated lime added to some of the samples. The analysed bound water of various hydrated phases (H) and the $Ca(OH)_2$ content (CH) are expressed as percentage of the dry sample weight at 500 °C (M_{500}) [23]. Equations (4) and (5) were modified to suit the addition of hydrated lime to reflect the normalised CH content to per g of OPC and to suit the addition of hydrated lime:

$$H_{PG1} = \frac{M_{60} - M_{250}}{M_{500}} * 100\,(\%) \quad (H_{PG1}\text{: bound water in phase group 1}) \tag{1}$$

$$H_{PG2} = \frac{M_{250} - M_{450}}{M_{500}} * 100\,(\%) \quad (H_{PG2}\text{: bound water in phase group 2}) \tag{2}$$

$$\text{CH (residual)} = \frac{M^{S}_{H2OCH} * \frac{74}{18}}{M_{500}} * 100\,(\%) \tag{3}$$

$$\text{CH (normalised)} = \frac{M^{S}_{H2OCH} * \frac{74}{18}}{M_{500}} * \frac{1}{0.3} * 100\,(\%) \quad \text{(without additional hydrated lime)} \tag{4}$$

$$\text{CH (normalised)} = \frac{\left[\left\{M^{S}_{H2OCH} * \frac{74}{18}\right\} - \left\{\left(M^{HL}_{H2OCH} * \frac{74}{18}\right) * HL_{\%}\right\}\right]}{M_{500}} * \frac{1}{0.3} * 100\,(\%) \quad \text{(with additional hydrated lime)}, \tag{5}$$

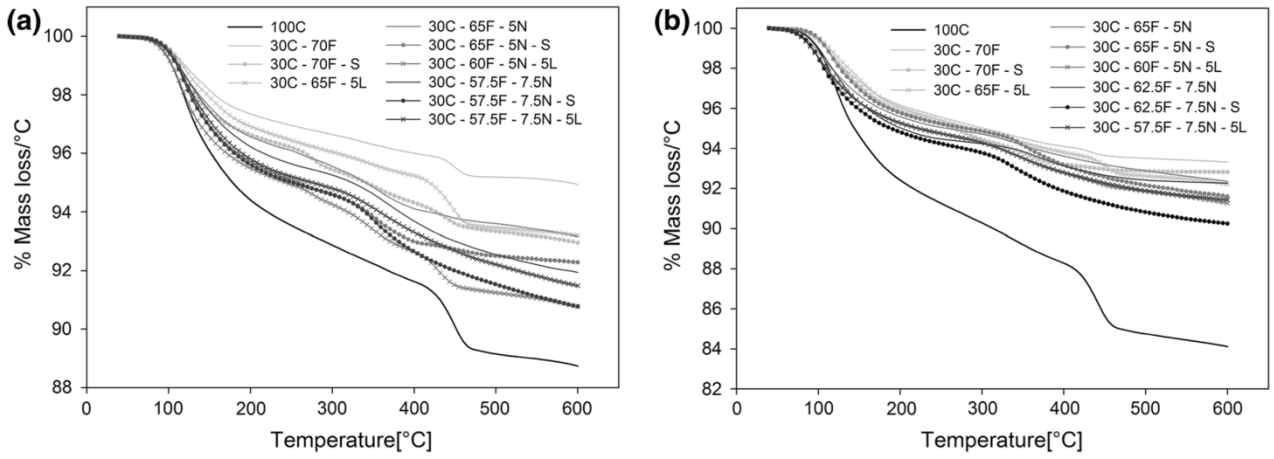

Fig. 4 TG curves of hydrated cement paste samples at **a** 7 day, **b** 28 day

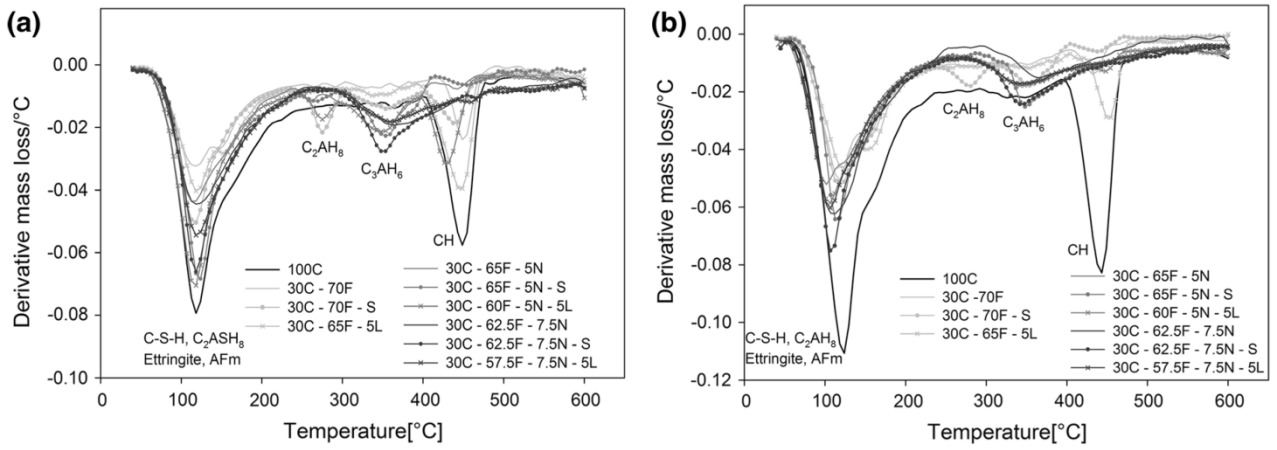

Fig. 5 DTG curves of hydrated cement paste samples at **a** 7 day, **b** 28 day

Table 4 Mass loss of blended cement pastes, expressed as percentage of dry weight at 500 °C

Mix	C–S–H + C_2ASH_8 + Ettringite + AFm_{ss} + Mc (H_{PG1})		C–A–H (C_2AH_8 + C_3AH_6) (H_{PG2})		CH (residual)		CH (normalised)	
	7	28	7	28	7	28	7	28
100C	7.2	10.3	2.1	2.4	11.4	16.6	11.4	16.6
30C–70F	3.2	4.6	1.0	1.6	3.2	2.0	10.6	6.6
30C–70F–S	3.9	5.0	2.2	2.3	3.8	1.3	12.5	4.3
30C–65F–5L	3.6	5.0	1.2	1.7	7.7	4.8	11.0	1.4
30C–65F–5N	4.1	5.1	2.2	–	1.6	–	5.3	–
30C–65F–5N–S	5.2	5.3	2.3	–	1.8	–	6.1	–
30C–60F-5N–5L	5.4	5.7	2.4	–	6.0	–	5.0	–
30C–62.5F–7.5N	4.7	6.0	2.9	–	1.0	–	3.2	–
30C–62.5F–7.5N-S	5.4	6.3	3.3	–	1.2	–	4.1	–
30C–57.5F–7.5N-5L	5.2	5.7	2.6	–	2.4	–	−6.7	–

where M_{60}, M_{250}, M_{450} and M_{500} represents the mass of sample at 60, 250, 450, 500 °C temperatures respectively. M^{S}_{H2OCH} mass loss due to the dehydroxylation of portlandite present in the hydrated cement paste. The fraction 74/18 is used to convert the CH bound water into the CH mass, where 74 is the molar mass of $Ca(OH)_2$ and 18 is the molar mass of H_2O. The fraction 1/0.3 represents the division of percentage of the OPC content in the sample to normalise the value to per g of OPC. M^{HL}_{H2OCH} mass loss due to the dehydroxylation of the pure $Ca(OH)_2$ present in the raw hydrated lime, as part of the raw HL was converted to $CaCO_3$ due to its exposure to CO_2 present in the atmosphere. The pure $Ca(OH)_2$ content was 81 % of the raw HL sample. $HL_{\%}$ represents the percentage of hydrated lime added to the sample.

It was observed that the presence of set accelerator in C–F–S and C–F–N–S samples showed an increase in mass loss in H_{PG1}, compared to the corresponding C–F and C–F–N samples at 7 days, but at 28 days, this increase was considerably reduced. The XRD spectra of the C–F–S sample shows AFm_{ss} phase in addition to ettringite at 7 days and an increase in ettringite content at 28 days as compared to the C–F sample, which is responsible for the higher mass loss in C–F–S. The C–F–N–S samples show higher quantities of ettringite compared to C–F–N at 7 days, but no further increase in ettringite was noted at 28 days. Ettringite binds

significantly higher amount of water as compared to C–S–H and C_2ASH_8 phases. The high amount of ettringite content, is identified as being responsible for the higher mass loss observed in H_{PG1} in C–F–N–S samples at 7 days. Between 7 and 28 days, C–F–N samples showed a significant increase in mass loss in H_{PG1} compared to the C–F–N–S samples. Since there was no change in the respective ettringite peaks of both C–F–N and C–F–N–S samples, the increase in mass loss could be attributed to the production of higher C–S–H/C_2ASH_8 gel.

The C–F–N–S sample containing 5 % nS had a higher mass loss in H_{PG1} at 7 days as compared to the C–F–S, but at 28 days no significant difference was observed. Though, the intensity of ettringite peak of C–F–N–S sample is 85 % higher than that of C–F–S at 7 days but C–F–S shows an additional broad peak of Afm_{ss}. Therefore the higher mass loss at 7 days can be attributed to the nS producing a higher quantity of C–S–H/C_2ASH_8 gel in C–F–N–S sample as compared to the C–F–S. At 28 days the intensity of ettringite peak is approximately the same in both C–F–N–S and C–F–S samples but C–F–S has an additional broad peak of AFm_{ss}. The presence of AFm_{ss} phase considerably contributed to H_{PG1} mass loss in C–F–S sample, but in the case of C–F–N–S, AFm_{ss} phase was not present, therefore the higher compressive strength in C–F–N–S is likely due to the presence of higher C–S–H/C_2ASH_8 gel. Moreover, nano silica refines the pore size and lowers the total porosity [17], which also helps in improving the strength properties.

The bound water H_{PG2} associated with the C–A–H content of the SA modified C–F–S sample was considerably higher than its corresponding C–F sample at 7 days, but no significant difference in C–A–H content was noticed between C–F–N–S and C–F–N samples containing 5 % nS at the same age. Moreover, the C–A–H content of C–F–N and C–F–N–S samples containing 5 % nS had approximately the same H_{PG2} value as that of C–F–S. In addition the C–A–H content of the C–F–N and C–F–N–S samples containing 7.5 % nS was higher than the C–F–S sample at 7 days. This shows that the accelerating effect of SA on the formation of C–A–H in the samples containing nS had little or no difference but on the other hand nS was more dominant in accelerating the hydration reaction of C_3A content as comapred to the SA.

The normalised CH content of the C–F–S and C–F–N–S samples was higher than their corresponding C–F and C–F–N samples. This is because SA significantly increases the pore solution concentration of calcium ions (Ca^+, $CaOH^+$) which induces a high degree of dissolution of portlandite [20]. The normalised CH content of C–F–S sample was significantly higher than the C–F–N–S sample containing 5 % nS, which further had higher value than the one containing 7.5 % nS. This shows that, though the addition of the SA resulted in the production of more portlandite, the increased portlandite was largely consumed by the amorphous nS to produce additional C–S–H gel. This is supported by the compressive strength results.

It was found that the presence of HL in C–F–L sample considerably improved its 28 day strength. But, the hydrated lime modified C–F–N–L sample containing 5 % nS showed no improvement in strength, and the one containing 7.5 % nS showed a considerable reduction in 7 and 28 day compressive strength results, compared to the C–F–N samples. The C–F–L showed slightly less consumption of portlandite at 7 days compared to C–F, but at 28 days there was a significant reduction in the portlandite content as can be seen in CH (normalised). This indicates that the reactivity of FA increased with the addition of HL, resulting in the increase in compressive strength. This is in agreement with other authors [2, 3]. In regards to the mass loss in H_{PG1}, C–F–L had a higher mass loss at both 7 and 28 days compared to C–F. The XRD spectra showed no variation in the ettringite content between the C–F–L and C–F samples. However, AFm_{ss} phase was noted in C–F–sL, in addition to the ettringite, at 7 days. This additional AFm_{ss} resulted in an increase in the bound water in H_{PG1}. At 28 days there was a considerable reduction in ettringite and AFm_{ss} content followed by increase in Mc content, this would indicates that the ettringite and AFm_{ss} phases were converted to Mc. Since both AFm_{ss} and Mc bind considerably lower amounts of water, compared to ettringite, this indicates that the contribution of C–S–H/C_2ASH_8 increased in the total mass loss. This is reflected in the increase in compressive strength of C–F–L sample in comparison to C–F.

The C–F–N–L sample containing 5 % nS showed slightly higher consumption of portlandite and significantly higher mass loss in H_{PG1} at 7 day in comparison to the corresponding C–F–N sample. In the case of 7.5 % nS specimen the consumption of portlandite was significantly increased. Though, its mass loss in H_{PG1} was higher than the corresponding

C–F–N sample, the increase was less significant than the 5 % nS specimens. Moreover, both C–F–N samples showed significant increase in their respective mass loss in H_{PG1} between 7 and 28 days, whereas both C–F–N–L samples showed a small increase. This indicates that the addition of HL, although accelerates the early pozzolanic reaction in the presence of nS to produce additional C–S–H gel, this gel, once formed, acts as a barrier for the further progress of the hydration reaction. Moreover, since fly ash has very low reactivity, this additional C–S–H gel is possibly blocking the portlandite access to the fly ash particles, thereby restricting its pozzolanic reaction. On the contrary, the relative low release of portlandite from OPC alone in the case of C–F–N samples, slows down the pozzolanic reaction thereby allowing enough time for the fly ash to react with the available portlandite to produce additional C–S–H gel.

The compressive strength results of C–F–N–L sample, containing 5 % nS was similar to that of the corresponding C–F–N sample at both 7 and 28 days. The 7.5 % nS C–F–N–L sample demonstrated a small reduction in strength compared to its corresponding C–F–N sample at both 7 and 28 days. But, both C–F–N–L samples showed higher C–S–H content compared to their corresponding C–F–N samples. This indicates that the compressive strength of cementitious material is a highly complex phenomenon and does not solely depend upon the amount of C–S–H gel but its distribution also plays an important role in strength development. Since the net volume of fly ash as compared to nano silica is very large, the fly ash that stays unreacted provides a weak cellular zone and higher the proportion of the unreacted fly ash the lower is its strength.

4 Conclusions

Based on the findings of this research, the following conclusions can be drawn:

1. The addition of nano silica significantly improved the pozzolanic reaction of HVFA cement blends, which increased with the increase in nano silica content. This increase in pozzolanic activity, which is directly proportional to the increase in nano silica content, was only effective at 7 days. By 28 days the percentage increase in nano silica content had no additional benefit in improving the compressive strength.
2. Partial replacement of fly ash with 5 % nano silica in HVFA blended mix, improved the 7 day strength by 76 % and by increasing the nano silica content to 7.5 %, there was 94 % increase in its 7 day strength. At 28 days, the mix containing 5 % nano silica showed 54 % increase in strength but the further increase in nano silica showed no additional improvement in the development of compressive strength.
3. Addition of set accelerator, considerably increased the amount of delayed ettringite content. This increase in delayed ettringite content had a detrimental impact on the compressive strength of nano silica modified HVFA blends. The effect of ettringite content at 7 days was inversely proportional to the the percentage of nano silica content. Since, higher nano silica content results in higher early strength, the detrimental effect of the expansive forces of delayed ettringite was reduced, thereby resulting in higher strength in 7.5 % nS blended mix as compared to the one containing 5 % nano silica.
4. Addition of 5 % hydrated lime to nano silica modified HVFA cement blends significantly improved the pozzolanic reaction but this increased pozzolanic activity did not result in the improvement of compressive strength. Since amorphous nano silica is highly reactive and fly ash has very low reactivity, this demonstrates that the addition of hydrated lime to nano silica modified HVFA blend accelerated the pozzolanic reaction of nano silica but it hindered the reaction of fly ash thereby resulting in no or negative improvement in the development of its compressive strength. Higher the nano silica content, higher is the C–S–H gel formation that acts as a barrier to the pozzolanic reaction of fly ash, thereby resulting in its lower compressive strength.
5. Amount of available portlandite content in a nano silica modified HVFA blended mix has a considerable impact on its strength development. The higher the portlandite content, the quicker is its consumption by highly reactive nano silica to form C–S–H gel, which further hinders the pozzolanic reaction of fly ash that is low in reactivity.

References

1. Benhelal E et al (2013) Global strategies and potentials to curb CO_2 emissions in cement industry. J Clean Prod 51:142–161
2. Barbhuiya S et al (2009) Properties of fly ash concrete modified with hydrated lime and silica fume. Constr Build Mater 23(10):3233–3239
3. Şahmaran M, Yaman İÖ, Tokyay M (2009) Transport and mechanical properties of self consolidating concrete with high volume fly ash. Cem Concr Compos 31(2):99–106
4. Hannesson G et al (2012) The influence of high volume of fly ash and slag on the compressive strength of self-consolidating concrete. Constr Build Mater 30:161–168
5. Heidrich C, Feuerborn H-J, Weir A (2013) Coal combustion products: a global perspective. In: WOCA
6. Joshi RC, Lohita R (1997) Fly ash in concrete: production, properties and uses. CRC Press, Boca Rocton
7. Rangan BV (2008) Fly ash-based geopolymer concrete, vol 2. Your Building Administrator
8. Wang S, Li VC (2007) Engineered cementitious composites with high-volume fly ash. ACI Mater J 104(3):233–241
9. Thomas MD (2010) Optimizing fly ash content for sustainability, durability, and constructability. In: Proceedings of Coventry University and The University of Wisconsin, Milwaukee Centre for by-products utilization second international conference on sustainable construction materials and technologies, Universita Politecnica Delle Marche, Ancona
10. Güneyisi E, Gesoğlu M (2008) Properties of self-compacting mortars with binary and ternary cementitious blends of fly ash and metakaolin. Mater Struct 41(9):1519–1531
11. Li H et al (2004) Microstructure of cement mortar with nano-particles. Compos B 35(2):185–189
12. Zhang M-H, Li H (2011) Pore structure and chloride permeability of concrete containing nano-particles for pavement. Constr Build Mater 25(2):608–616
13. Senff L et al (2009) Effect of nano-silica on rheology and fresh properties of cement pastes and mortars. Constr Build Mater 23(7):2487–2491
14. Zhang M-H, Islam J (2012) Use of nano-silica to reduce setting time and increase early strength of concretes with high volumes of fly ash or slag. Constr Build Mater 29:573–580
15. Shaikh F, Supit S, Sarker P (2014) A study on the effect of nano silica on compressive strength of high volume fly ash mortars and concretes. Mater Des 60:433–442
16. Hou P-K et al (2013) Effects of colloidal nanosilica on rheological and mechanical properties of fly ash–cement mortar. Cement Concr Compos 35(1):12–22
17. Li G (2004) Properties of high-volume fly ash concrete incorporating nano-SiO_2. Cem Concr Res 34(6):1043–1049
18. Scherer GW (1999) Crystallization in pores. Cem Concr Res 29(8):1347–1358
19. Matschei T, Lothenbach B, Glasser F (2007) The AFm phase in Portland cement. Cem Concr Res 37(2):118–130
20. Nonat A (2000) In: PRO 13: 2nd international RILEM symposium on hydration and setting-why does cement set? An interdisciplinary approach, vol 13, RILEM Publications, Quebec
21. Nazari A, Riahi S (2011) Splitting tensile strength of concrete using ground granulated blast furnace slag and SiO_2 nanoparticles as binder. Energy Build 43(4):864–872
22. Medvešček S et al (2006) Hydration products in water suspension of Portland cement containing carbonates of various solubility. Acta Chim Slov 53(2):172–179
23. De Weerdt K et al (2011) Hydration mechanisms of ternary Portland cements containing limestone powder and fly ash. Cem Concr Res 41(3):279–291

Chapter 5

A quantitative comparative study on the effect of nano SiO_2, nano Al_2O_3 and nano $CaCO_3$ on the physicochemical properties of very high volume fly ash cement composite

This experiment looks at the effect of various nano materials on the physicochemical properties of high volume fly ash cement composites, replacing 80% of OPC. The various nano materials used were nano silica, nano alumina and nano calcium carbonate. A quantitative comparative phase analysis was undertaken on various high volume fly ash nano composites using thermogravimetric analysis in conjunction with XRD quantitative rietveld analysis (external standard method). In addition, nitrogen adsorption/desorption analysis was undertaken to study the effect of different nano materials on the porosity of the cement matrix of various mix designs.

A quantitative comparative study on the effect of nano SiO_2, nano Al_2O_3 and nano $CaCO_3$ on the physicochemical properties of very high volume fly ash cement composite

Rajeev Roychand [a,*], Saman De Silva [a,**], Sujeeva Setunge [a,**] and David Law [a,**]

[a] *School of Civil, Environmental and Chemical Engineering, RMIT University, Melbourne, Victoria, Australia*

** Corresponding author's Email: rajeev.roychand@rmit.edu.au*

*** Other authors' Email: saman.desilva@rmit.edu.au; sujeeva.setunge@rmit.edu.au; david.law@rmit.edu.au*

Abstract

This paper presents a quantitative comparative study of the effect of 5% and 7.5% of nano silica (nS), 2.5% and 5% of nano alumina (nA) and 2.5% and 5% of nano calcium carbonate (nCC), on the properties of low calcium class F very high volume fly ash (VHVFA) cement composites, replacing 80% of cement. Compressive strength test along with thermogravimetric analysis, quantitative x-ray diffraction analysis, and scanning electron microscopy were undertaken to study the effect of various nanomaterials on the physicochemical behaviour of VHVFA cement blends. The results show that the addition of nS significantly improves the compressive strength of VHVFA cement composites and considerably increases the formation and thermal stability of silica-rich hydrogarnet phase [$Ca_3(Al_xFe_{1-x})_2(SiO_4)_y(OH)_{4(3-y)}$], which increases with the increase in nS content. The addition of nCC to VHVFA cement composite does not show any effect on the pozzolanic reaction at 7 days of curing but at 28 days considerably improves its pozzolanic reaction, which increases with the increase in nCC content. The performance of nCC in improving the mechanical properties is less pronounced than that of nS. The addition of nA though improves the hydration/pozzolanic reaction of VHVFA cement composite, resulting in the improvement in compressive strength, but only if added in small quantities (2.5% or less). If it is added in higher amounts, it promotes the formation of $Al(OH)_3$ gel that severely inhibits the hydration/pozzolanic reaction within the cement matrix. nA shows inferior performance compared to that of nS and nCC.

Keywords: nano silica, nano alumina, nano calcium carbonate, fly ash, x-ray diffraction, thermogravimetric analysis, scanning electron microscopy, rietveld analysis

1. Introduction

As the concern for environmental sustainability grows, the cement industry is focussing more and more on the increased use of supplementary cementitious materials (SCM) to cut down its carbon footprint. Fly ash (FA) is the most abundantly available and least utilised SCM in the world, and therefore the majority of the research on SCM's focusses on the increased use of FA as a cement replacement material. The major characteristic of fly ash that is hindering its use in high quantities is its low reactivity [1] which has an adverse impact on its early strength properties. Therefore the majority of research on the use of FA as a cement replacement material concentrates on the improvement of early strength properties of the blended cement composites. To improve the early strength properties of cement blends containing FA, researchers have investigated various options, such as; fly ash particle size reduction [2], use of hydrated lime [3], set accelerator [4], silica fume [4, 5] and metakaolin [6]. As the quest for the increased use of FA in cement replacement is growing, the research focus is shifting towards the use of nanomaterials, because of their high reactivity and large surface area. Some researchers have studied the effect of nano silica [4, 7], nano iron oxide [8], nano titanium oxide [9], nano alumina [9] and nano calcium carbonate [10] on the properties of FA blended cement composites. Shaikh et al. [7] investigated the effect of 2% nano silica on HVFA cement blend containing 68% fly ash. Their research finding showed that there was no difference in strength at 7 days, but at 28 days there was a 56% increase in compressive strength, compared to that of the mix not containing nano silica. They found that the 28day strength of nS modified fly ash blend achieved 40% relative strength compared to that of the control mix containing 100% Ordinary Portland cement (OPC). Roychand et al. [4] studied the effect of partially replacing 70% fly ash with 5% and 7.5% nano silica on HVFA cement composites. They found that by replacing fly ash with 5% nano silica, the 7 day strength of the mortar samples increased by 76% and with the further increase of nano silica to 7.5%, there was a 94% improvement in its compressive strength results. However, they found that at 28 days both 5% and 7.5% nS blended mixes showed a similar increase in strength i.e. 54% and 50% respectively. Moreover, the 28 day strength of 5% nS modified fly ash blend achieved 91% relative strength compared to that of OPC. They did a further study [11] on the effect of 5% nano silica on HVFA cement composite containing 75% of micronised fly ash, which was ground to approximately half of its original mean particle size. They found that 7 and 28 day strengths of 5% nS modified HV-UFFA cement mortar increased by 918% and 567% respectively. They also observed that the 28 day strength of

5% nS modified UFFA cement blend achieved 95% relative strength compared to that of OPC.

Meral Oltulu et al. [8] studied the effect of 0.5, 1.25 and 2.5% of nA on 15% FA blended cement composites. They found that the optimum content of nA for their mix design was 1.25%, but the improvement in the compressive strength achieved was very small i.e. approximately 4% at both 7 and 28 days, compared to the FA blended mix not containing nA. The maximum 28 day strength they achieved with 1.25% nA and 15% FA was approximately 48 MPa. Ehsan et al. [9] investigated the effect of 1, 3 and 5% of nA on 25% FA blended cement composites. They found that the addition of 1% nA improved the 7 and 28 day strengths by approximately 17 and 19% respectively, compared to the fly ash blended mix not containing nA. But with the further increase in the percentage of nA the strength decreased with the increase in nA content.

Kawashima et al. [12] studied the effect of 5% nCC in blended and sonicated forms on cement paste samples containing 30% FA. They found that the 7 day compressive strength of 5% nCC that was sonicated before mixing performed considerably better than the one that was blended in the dry mix. Moreover, the addition of 5% sonicated nCC to a blended paste containing 30% FA improved its 3 and 7 day strengths by 25% and 42% respectively. Supit et al. [13] studied the effect of 1% nCC on 60% FA blended cement mortars. They found that the addition of 1% nCC to the blended mortar containing 60% FA, improved the 7 and 28 day strengths by approximately 100 and 106% respectively.

Based on the review of past literature, there appears to be limited or no research available on the comparative study of various nanomaterials on the properties of low calcium class F very high volume fly ash cement composites containing 70% or above of fly ash content. Moreover, the available studies on the effect of various nanomaterials on fly ash cement composites show a significant variation in their respective strength improvements from one researcher to the other. This is most likely because of the variation in the chemical composition, particle size distribution and the amorphous content of the various fly ashes used by the different researchers. Therefore, to look at standardising the effect of nanomaterials on fly ash blended cement composites these factors require due consideration and demand quantitative phase analysis of the raw materials as well as that of the hydration products. To fill up the gap, this study was undertaken to investigate the effect of nano silica, nano alumina and nano calcium carbonate on the physicochemical behaviour of VHVFA

cement composites, replacing 80% of cement. The dosage of various nanomaterials used in this study was; 5% and 7.5% of nano silica (nS), 2.5% and 5% of nano alumina (nA) and 2.5% and 5% of nano calcium carbonate (nCC). Nano silica was used in higher quantity based on the results obtained from the previous study [4] undertaken by the authors. Compressive strength tests were undertaken to identify the mechanical properties of the blended mortar samples. In addition, to identify and quantify the physicochemical changes taking place in the hydrated pastes, thermogravimetric analysis (TGA), secondary electron microscopy (SEM) and X-ray diffraction (XRD) techniques were used. Quantitative phase analysis was undertaken using XRD rietveld refinement method in combination with the TGA data.

2. Materials and Experimental Procedure

2.1 Materials and mix design

The materials used in this study were: OPC, low calcium class F fly ash, nano silica, nano alumina, nano calcium carbonate and polycarboxylic ether based superplasticizer (SP) “Glenium 79” having a water content of 55%. The chemical composition of OPC, FA, nS, nA and nCC is shown in Table 1. Tables 2 and 3 show the crystalline and amorphous composition of OPC and fly ash respectively, as determined by XRD rietveld refinement method. To calculate the amount of amorphous silica, quartz and the crystalline component of silica present in mullite were deducted from the total silica present in FA as shown in table 1. Similarly, the crystalline component of alumina present in mullite was deducted from the total alumina present in the FA to calculate the amount of amorphous alumina. Particle size distribution of OPC and FA obtained with the help of laser diffraction particle size analyser “Malvern Mastersizer 3000” is presented in Table 4 in addition to the mean particle size of nanomaterials provided by the chemical supplier.

Table 1: Chemical composition of OPC, FA, nS, nA and nCC

Oxides	OPC (%)	FA (%)	nS (%)	nA (%)	nCC (%)
SiO_2	19.9	72.9	99.9	99.9	98.5
CaO	62.9	0.3	-	-	-
Al_2O_3	4.6	22.3	-	-	-
Fe_3O_4	3.2	1.1	-	-	-
SO_3	2.8	0.2	-	-	-
MgO	2.1	0.3	-	-	0.5
Na_2O	0.2	0.2	-	-	-
K_2O	0.4	0.3	-	-	-
TiO_2	-	1.2	-	-	-
LOI	2.8	1.2	-	-	-

Table 2: Mineral composition of OPC, determined by XRD rietveld analysis

Alite	Larnite	Calcium Aluminate	Calcium Aluminoferrite	Portlandite	Calcite	Gypsum	Bassanite	Quartz	Periclase
62.1%	6.2%	7.7%	7.2%	1.8%	7.5%	3.9%	1.1%	0.5%	2.0%

Rietveld refinement factors: GOF = 2.12, Rexp = 1.60, Rwp = 3.22, Rp = 2.35

Table 3: Crystalline and amorphous mineral composition of FA, determined by XRD rietveld analysis

Phases	Quartz	Mullite	Magnetite	Rutile	Amorphous Silica	Amorphous Alumina
	22.8%	29.9%	1.4%	1.0%	42.9%	0.5%

Rietveld refinement factors: GOF = 2.01, Rexp = 1.52, Rwp = 3.05, Rp = 2.23

Table 4: Particle size distribution of OPC and FA (expressed in µm), and the mean particle size of nS, nA and nCC (expressed in nm)

Material	Mean	d_{10}	D_{25}	D_{50}	D_{75}	D_{90}
OPC	24.6 µm	2.7 µm	6.5 µm	15.4 µm	28.3 µm	44.2 µm
FA	28.7 µm	2.3 µm	5.8 µm	14.0 µm	33.1 µm	75.2 µm
nS	7 nm	-	-	-	-	-
nA	50 nm	-	-	-	-	-
nCC	15 - 40 nm	-	-	-	-	-

Figure 1(a-e) shows XRD diffractograms of OPC, FA, nS, nA and nCC along with their respective identified crystalline phases. Figure 2 shows the thermogravimetric (TG) mass loss data of OPC and its derivative curve. TG analysis of OPC was undertaken to help in identifying the calcite content, which has a very close peak overlap with Alite and Larnite in XRD data. In addition, it also helps in identifying other phases containing chemically bound water like portlandite, gypsum, and bassanite. TG and XRD analysis of OPC shows the presence of 1.8% free lime in the form of $Ca(OH)_2$ which is not detrimental compared to if it were present in the form of CaO, that causes expansion and cracking at the time of cement hydration [14]. Rather, the presence of free lime in OPC is beneficial in improving the setting time and the compressive strength of fly ash blended mix [15]. However, the content of OPC being just 20% in the blended cement composites, the reduced proportion of free lime would have negligible effect on the properties of hydrated cement composites.

The predominant crystalline peaks identified in FA were that of quartz and mullite in addition to the minor peaks of rutile and magnetite. Nano silica showed a broad hump centred around 22° 2-theta, which is a typical characteristic of amorphous silica content.

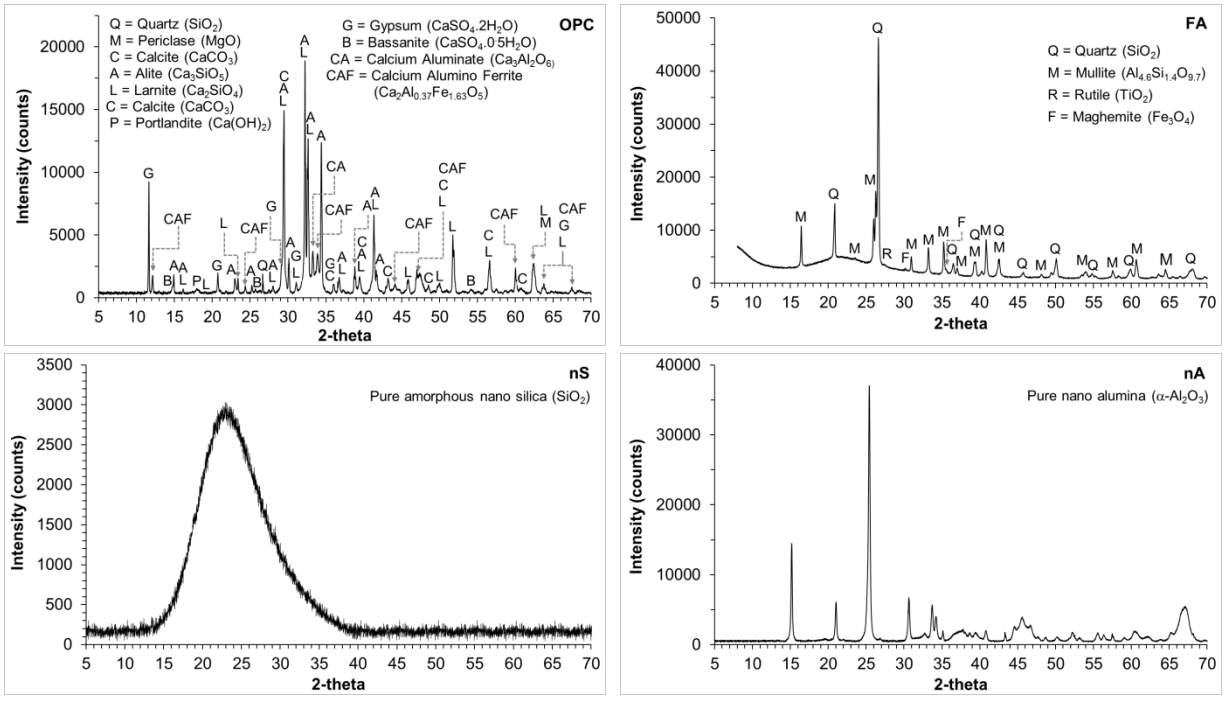

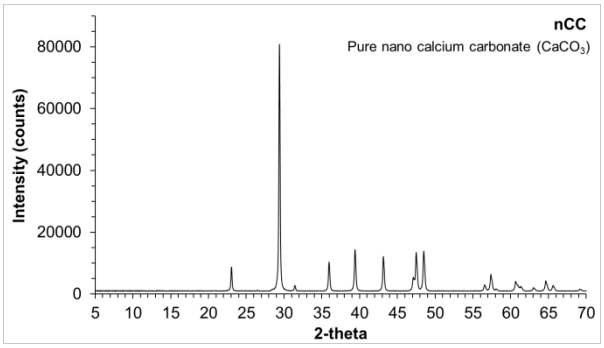

Figure 1: XRD diffractograms of OPC, FA, nS, nA and nCC

Table 5 summarizes the various mortar mix designs tested. All binding materials used were based on percentage mass of the total binding material. TGA, XRD, and SEM were conducted on hydrated binder paste only. The amount of superplasticizer requirement for each mix design was calculated in the trial work, to get an approximate similar consistency for the self-consolidation of the mortar samples. The water content of SP was adjusted in the total w/b ratio.

Table 5: Mortar Mix Designs

Mix	Total binder (B)		Nano materials as additives			S/(B+A)	W/(B+A)	SP
	OPC	FA (%)	nS (%)	nA (%)	nCC			
M1	20	80	-	-	-	2.4	0.3	7.5
M2	20	80	5.0	-	-	2.4	0.3	65.0
M3	20	80	7.5	-	-	2.4	0.3	
M4	20	80	-	2.5	-	2.4	0.3	10.0
M5	20	80	-	5.0	-	2.4	0.3	12.5
M6	20	80	-	-	2.5	2.4	0.3	25.0
M7	20	80	-	-	5.0	2.4	0.3	32.5

S = Sand; W = Water; SP = Superplasticizer (mL kg^{-1} binder)

2.2 Sample preparation, curing & testing

2.2.1 TGA and XRD of binder material and nano additives

TGA was conducted on OPC powder sample to ascertain the presence of $CaCO_3$ since it has XRD peak overlap with Alite and Larnite. TGA also helped in identifying the presence of $Ca(OH)_2$ in OPC. Thermogravimetric analysis was conducted using PerkinElmer STA 6000 thermal analyser in a nitrogen environment with a flow rate of 19.8 mL min^{-1}. 20 - 30 mg of

powdered samples were initially heated at 40^0C for 5 minutes to expel any moisture caught by the samples while handling. Then the samples were heated from 40 – 850 ^{0}C with the heating rate of 20 ^{0}C min^{-1}.

XRD was conducted on all the raw materials using a Bruker AXS D4 Endeavour system with a Cu-Kα radiation source, operated at 40 kV and 40 mA and a Lynxeye linear strip detector. Samples were tested between 5° and 90° 2-theta (2θ) with a step size of 0.01° and counting time of 1s per step.

2.2.2 Compressive strength of mortar samples

All the raw materials were dry mixed at low speed in the mortar mixer for 1 min to obtain a homogenous mix. Then water and superplasticiser were added and mixed for another 3 min, followed by a final high speed mixing for 1 min. The wet samples were then poured in 50 mm x 50 mm x 50 mm steel moulds, cured at room temperature for 24 hrs, de-moulded and then further cured in water at room temperature until the time of testing. The samples were taken out of the water, wiped and surface dried after 7 and 28 days of curing. The compressive strength of the mortar samples was measured as per ASTM C109 with a loading rate of 0.36 MPa/s. For every mix design, three replicates were tested for each curing age.

2.2.3 TGA, XRD, SEM and Nitrogen adsorption/desorption analysis of hydrated paste samples

Mixing procedure and curing method were kept the same for hydrated paste samples for TGA, XRD, and SEM. For TGA and XRD, the samples at a particular curing age were taken out of the curing tank, surface dried, ground and sieved through 45 μm sieve. To remove the physically bound water and to stop hydration the solvent exchange method using acetone was adopted. A 100 mL of pure acetone was added to 25 g of the powdered sieved sample in a plastic bottle, mixed vigorously by hand for about 3 mins and then kept on the table for about 5 minutes. Part of the excess acetone was carefully taken out from the top using a syringe, making sure that no material settled down at the bottom gets into it. This process was repeated, and the samples were then kept in the oven at 40 °C temperature for 24 hrs drying. The dried powder samples were collected and stored in a sealed plastic container till the time of testing. TGA and XRD were conducted on all the hydrated paste samples at 7 and 28 days of curing, using method described in section 2.3.1

For SEM analysis, a small section of the hardened paste sample was cut out from the internal part of the specimen, embedded in epoxy, ground, polished, mounted on a steel stub and was gold coated. The microstructure of the hardened paste samples was study using FEI Quanta 200 SEM. The accelerating voltage of the beam was 20 kV, and the electron images were acquired at 10mm working distance and 5000x magnification. Five images of each sample were taken to check the consistency in the observations. Four images were taken on four sides i.e. top left, top right, bottom left and bottom right regions and one image was taken in the middle region. The SEM images largely reflected the consistency in the observations.

For nitrogen adsorption analysis, the hardened paste samples were sliced into small pieces of 1-2 g. To stop hydration and to remove the water present in the pore structure, solvent exchange method using isopropanol was adopted. Few pieces of each specimen were immersed in 500 mL of isopropanol for 2 days. The samples were then taken out and surface dried. Approximately 1.5 g of dried sample of each specimen was weighed and degassed under vacuum at 105 °C temperature to remove isopropanol and any left-over pore water (if any) present in the pores, using Micromeritic ASAP 2400 surface area analyser for 24 hrs. N2 adsorption/desorption for pore size analysis was then undertaken on the degassed specimens. N2 adsorption/desorption data analysis shows a sharp peak in the incremental pore size distribution of all the samples in ~15 to ~40 Å pore diameter range and the remaining pore size distribution spreads over pore size greater than 40 Å to ~1500 Å. Figure 7 (a) and (b) presents the incremental pore size distribution and the cumulative pore volume of all the samples at 7 and 28 days of curing.

3. Results and Discussion

Hydrates of calcium silicate and calcium aluminium silicate, which are the main phases responsible for the strength development are difficult to identify from the XRD and TGA data individually. In X-ray diffraction data, these phases don't show sharp crystalline peaks because of their amorphous nature [16]. The large amorphous hump present in XRD diffraction data of hydrated samples containing SCM can be a number of combinations of un-hydrated amorphous content, C-S-H and C-A-S-H phases. XRD data of VHVFA cement composite pastes at 7 and 28 days of curing are shown in Figure 2. The primary quartz peak located at ~26.7° 2**θ** had a very high intensity and was overshadowing the low intensity hydrated phases used in the analysis. Therefore, for the clarity in the presentation of the crystalline phases used in the analysis, the XRD data is presented from 8° 2-theta to 25° 2-

theta. Table 6 presents the chemically bound water and CO_2 content of various phases used in the combined TGA and XRD analysis, expressed as a percentage of original dried mass of hydrated samples at 50 °C.

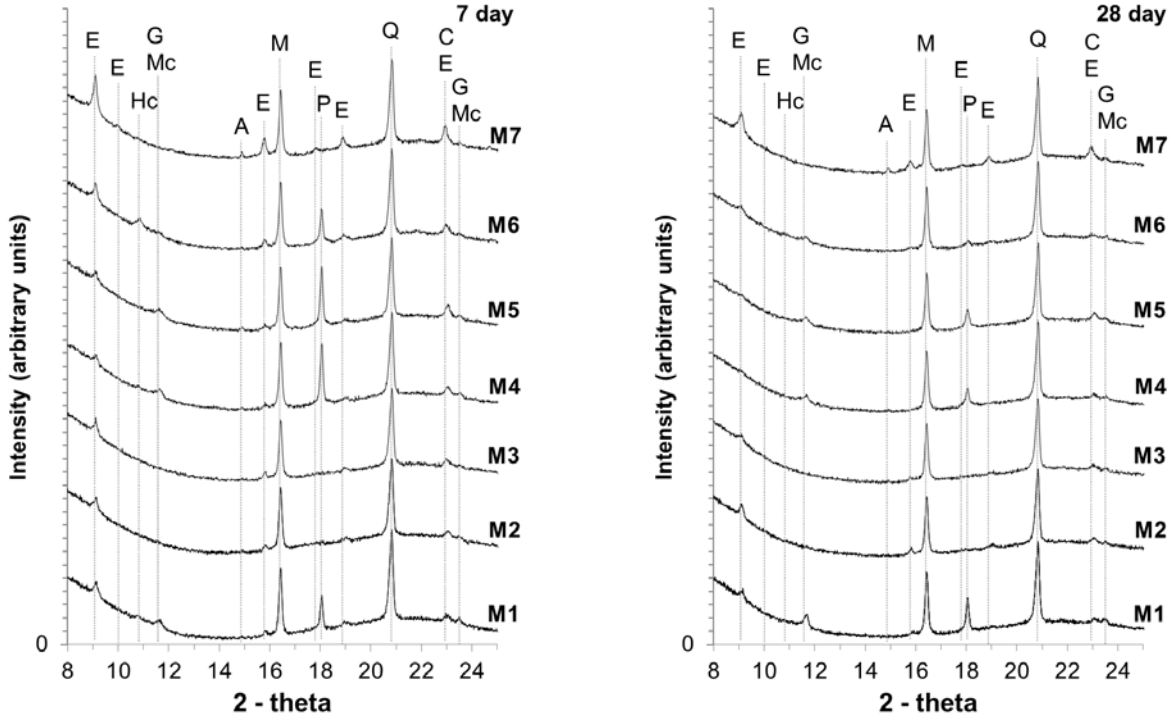

Figure 2: Xray diffraction data at 7 and 28 days of curing

E = ettringite ($Ca_6Al_2(SO_4)_3(OH)_{12}(H_2O)_{26}$), G = gypsum ($CaSO_4 \cdot 2H_2O$), Hc = hemi-carboaluminate ($Ca_4Al_2(OH)_{12})(OH(CO_3)_{0.5}(H_2O)_4$), Mc = mono-carboaluminate ($Ca_4\ Al_2(OH)_{12}(CO_3)(H_2O)_5$), Alite ($Ca_3SiO_5$), M = mullite ($Al_{4.6}Si_{1.4}O_{9.7}$), P = portlandite ($Ca(OH)_2$), Q = quartz ($SiO_2$) and C = calcite ($CaCO_3$).

Table 6: Chemically bound water and CO_2 contents of mineral phases of hydrated cement paste samples

Mineral	Chemical formula	Bound water (Wt. %)	CO_2 content (Wt. %)
Ettringite	$Ca_6Al_2(SO_4)_3(OH)_{12} \cdot 26H_2O$	52.64	-
Hemicarboaluminate	$Ca_4Al_2(CO_3)_{0.5}(OH)_{13} \cdot 5.5H_2O$	38.30	3.9
Monocarboaluminate	$Ca_4Al_2(CO_3)(OH)_{12} \cdot 5H_2O$	34.86	7.7
Gypsum	$CaSO_4 \cdot 2H_2O$	20.93	-
Calcite	$CaCO_3$	-	44.0

In TGA, the thermal breakdown temperature of chemically bound water of ettringite, C-S-H, C-A-S-H, gypsum, mono-carbonate, hemi-carbonate and mono-sulphate phases have an

endothermic peak overlap between 50 and ~300 °C temperature range as described in [17]. Therefore, to identify the proportion of the main strength forming gel in cement i.e. C-S-H / C-A-S-H, TGA was combined with XRD quantitative phase analysis. The quantitative phase analysis on XRD data was undertaken using the rietveld refinement external standard method as described in [17]. The external standard used was 99.9% pure quartz powder having particle size less than 45µm. Chemically bound water was calculated from the percentage proportion of the identified ettringite, gypsum, mono-carbonate and hemi-carbonate phases using table 6. The chemically bound water, so obtained from the XRD data, was deducted from the total mass loss between 50 to ~300 °C from TGA data, to calculate the mass loss from C-S-H and C-A-S-H phases. The exact boundaries of the mass loss due to various phases or group of phases were identified with the help of TG derivative curve (DTG) as shown in the figures 3(a) and (b).

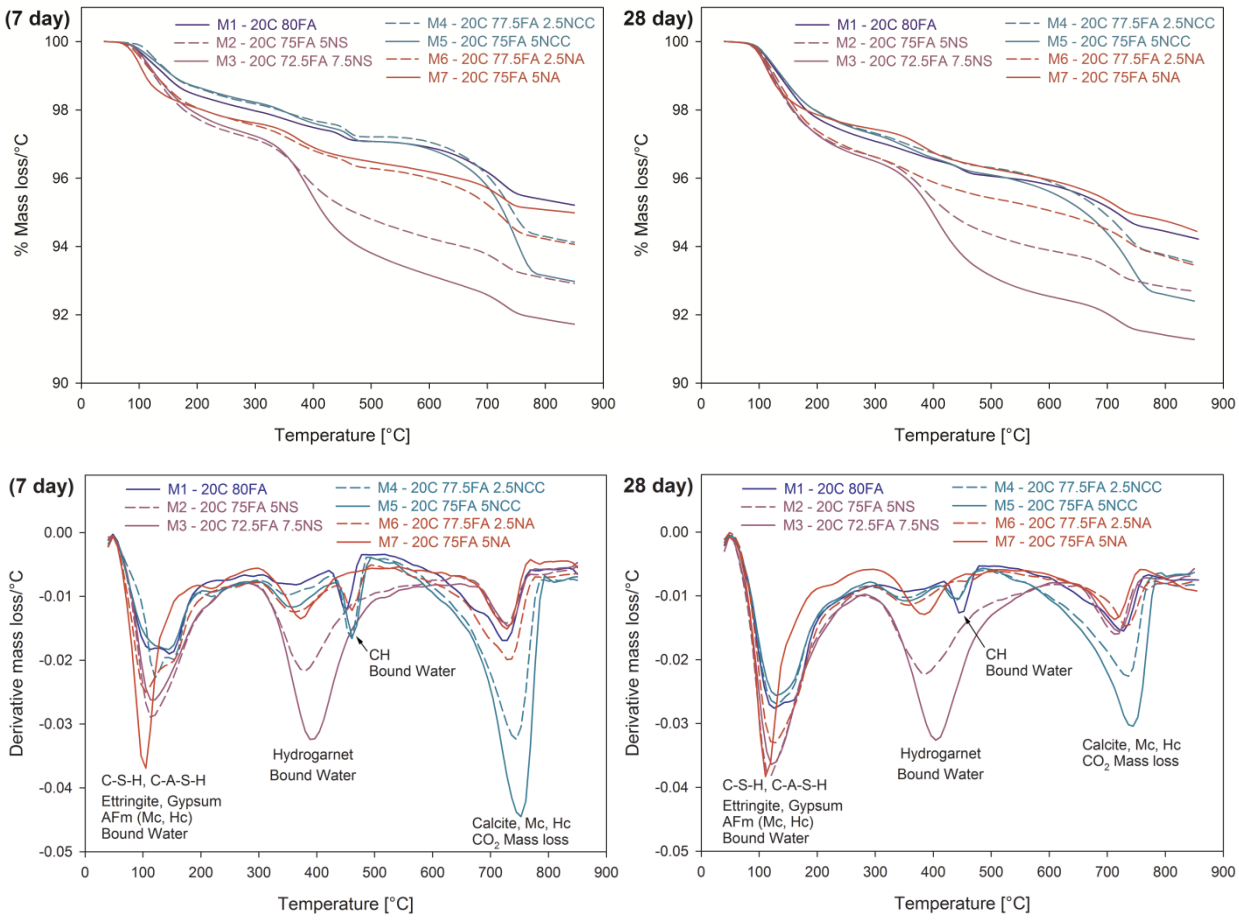

Figure 3(a): TG and DTG curves at 7 days Figure 3(b): TG and DTG curves at 28days

Note: C-S-H= calcium silicate hydrate, C-A-S-H = calcium alumino silicate hydrate, AFm = mono-carbonate, hemi-carbonate, mono-sulphate, CH = calcium hydroxide

The second endothermic peak is associated with a hydrogarnet phase which shows an endothermic peak varying between ~310 to ~450 °C temperature [17-21]. The various phases that come under hydrogarnet family are: non siliceous $Ca_3(Al_xFe_{1-x})_2(OH)_{12}$ and silica rich $Ca_3(Al_xFe_{1-x})_2(SiO_4)_y(OH)_{4(3-y)}$ [21-24]. Previous studies show that some siliceous hydrogarnets show very poor crystallinity [25-27]. Carlson, E.T. (1956) in his study on the formation of hydrogarnets found that the hydrogarnets containing increasing amounts of silica underwent decomposition at progressively higher temperatures [25].

Figure 4 presents the chemically bound water of ettringite, gypsum, Hc, Mc and C-S-H/C-A-S-H phases at 7 and 28 days of curing, expressed as a percentage of dried mass of powder sample at 50 °C. The value shown at the top of each bar represents the total mass loss of the chemically bound water in 50 to ~300 °C temperature range as calculated with the TGA derivative curves. The legend in the bottom of the graph shows the chemically bound water of individual phases calculated with the help of combined TGA and XRD quantitative analysis.

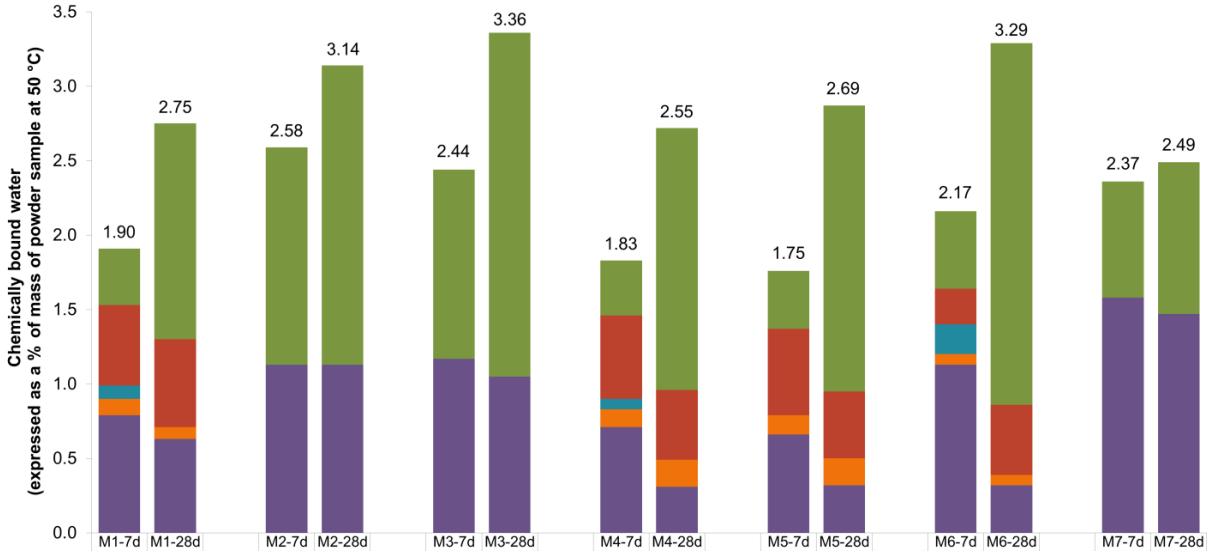

	M1-7d	M1-28d	M2-7d	M2-28d	M3-7d	M3-28d	M4-7d	M4-28d	M5-7d	M5-28d	M6-7d	M6-28d	M7-7d	M7-28d
C-S-H	0.38	1.45	1.46	2.01	1.27	2.31	0.37	1.76	0.39	1.92	0.52	2.43	0.78	1.02
Mc	0.54	0.59	0.00	0.00	0.00	0.00	0.56	0.47	0.58	0.45	0.24	0.47	0.00	0
Hc	0.09	0.00	0.00	0.00	0.00	0.00	0.07	0.00	0.00	0.00	0.20	0.00	0.00	0
Gypsum	0.11	0.08	0.00	0.00	0.00	0.00	0.12	0.18	0.13	0.18	0.07	0.07	0.00	0
Ettringite	0.79	0.63	1.13	1.13	1.17	1.05	0.71	0.31	0.66	0.32	1.13	0.32	1.58	1.47

Figure 4: Chemically bound water of ettringite, gypsum, Hc, Mc and C-S-H/C-A-S-H phases at 7 and 28 days of curing, expressed as a percentage of dried mass of the sample at 50 °C

Table 7 shows the chemically bound water of hydrogarnet phase, portlandite and the calcite content of all the samples. The CH and the CC content was calculated using the equations (1),

(2) and (3). CH and CC in equations (1) and (2) are expressed in percentage of the initial mass of dry sample at 40 °C (M_{40}). CC in equation (3) was modified to suit the addition of nCC.

$$CH = \frac{M^{S}_{H2O\ CH} * \frac{74}{18}}{M_{40}} * 100\ [\%] \quad (1)$$

$$CC = \frac{M^{S}_{CO2\ CC} * \frac{100}{44}}{M_{40}} * 100\ [\%] \quad (2)$$

(without additional nano calcium carbonate)

$$CC = \frac{\left[\left\{M^{S}_{CO2\ CC} * \frac{100}{44}\right\} - nCC_{\%}\right]}{M_{40}} * 100\ [\%] \quad (3)$$

(with additional nano calcium carbonate)

$M^{S}_{H2O\ CH}$ is the mass loss associated with the dehydroxylation of portlandite present in the hydrated cement paste. The fraction $\frac{74}{18}$ is used to convert CH bound water to CH mass, where 74 is the molar mass of $Ca(OH)_2$ and 18 is that of H_2O. $M^{S}_{CO2\ CC}$ is mass loss due to the de-carbonation of the calcite phase. The fraction $\frac{100}{44}$ is used to convert mass loss due to CO_2 to Calcium carbonate mass, where 100 is the molar mass of $CaCO_3$ and 44 is the molar mass of CO_2. $nCC_{\%}$ represents the percentage of nano calcium carbonate powder added to the sample.

Also, the mono-carbonate and hemi-carbonate phases have CO_2 mass loss overlap with the calcite phase at 550 – 800 °C temperature range. To calculate, the calcite content, CO_2 mass loss due to mono-carbonate and hemi-carbonate phases were deducted from the total mass loss between 550 – 800 °C temperature range. The difference in the quantification of CH and CC phases between the XRD and TG analysis techniques varied between ±0.2% to 0.7% in various mix designs. This difference in quantification results between different techniques has also been reported by Scrivener et al. [28]. For consistency, the quantification results of CH and CC presented in table 8 are reported from TGA data.

Table 7: Chemically bound water of hydrogarnet, portlandite and calcite content expressed as % of initial dried mass at 50 °C

Mix	Hydrogarnet bound water (%) $Ca_3(Al_xFe_{1-x})_2(SiO_4)_y(OH)_{4(3-}$		Portlandite (%) CH		Calcite (%) CC	
	7d	28d	7d	28d	7d	28d
M1	0.66	0.60	1.45	1.50	4.02	4.00
M2	2.36	2.40	0.00	0.00	2.56	2.50
M3	3.58	3.61	0.00	0.00	2.58	2.50
M4	0.68	0.72	1.60	1.51	4.06	3.48
M5	0.72	0.75	1.60	1.48	4.10	3.00
M6	0.93	1.00	1.28	0.90	4.20	4.00
M7	0.94	1.00	0.00	0.00	2.84	2.56

Table 7 shows the C-S-H bound water of the control mix M1 was 0.38% which increased to 1.45% at 28 days. The increase in the formation of C-S-H gel also improved the pore structure of the cement matrix. The 28 day N2 adsorption/desorption results (Figure 7) show a considerable decrease in the total pore volume and a marked reduction in the pore size great than 40 Å followed by an increase in pore size smaller than 40 Å indicating the refinement of pore structure, compared to that at 7 days of curing. This increase in the C-S-H content and the reduction/refinement of pore structure of M1 was also reflected in the considerable improvement in its 28 day compressive strength. The increase in C-S-H doesn't show the corresponding reduction in CH content from 7 to 28 days; this is because the increase in the degree of hydration of calcium silicate phases releases more CH content into the system, thereby making it available for further reaction with the amorphous silica present in FA. Unhydrated OPC contained 7.5% calcite, but the 7 and 28 day hydrated M1 samples containing 20% OPC, showed approximately 3.8% CC content. This indicates that part of the CH produced during hydration was converted to CC due to the exposure to CO_2 present in the atmosphere. In addition, the XRD analysis shows there was 0.5% gypsum, 1.55% of Mc and 0.35% of Hc at 7 days of curing. At 28 days the Mc content showed a slight increase followed by the extinction of Hc. This is probably due to the conversion of Hc to Mc phase by 28 days of curing.

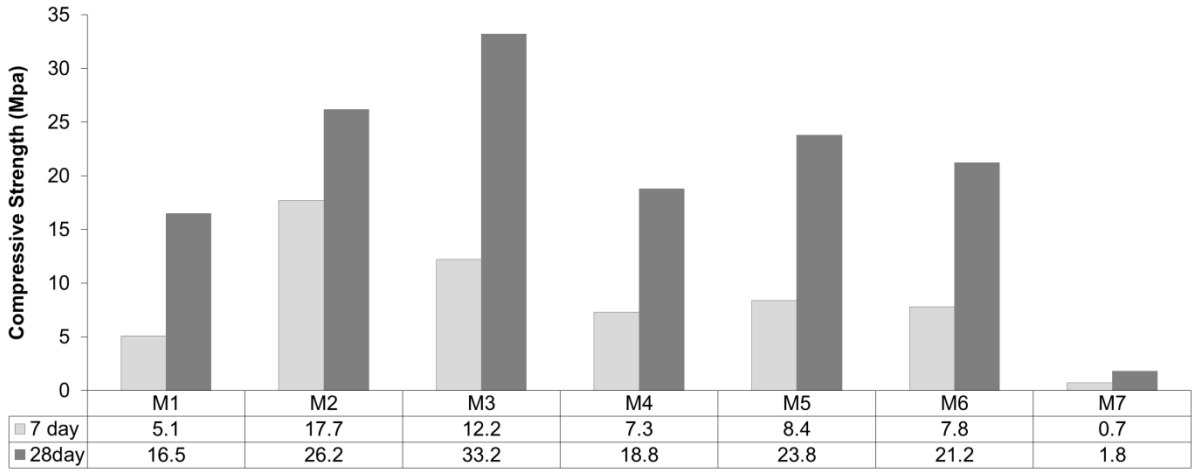

	M1	M2	M3	M4	M5	M6	M7
7 day	5.1	17.7	12.2	7.3	8.4	7.8	0.7
28day	16.5	26.2	33.2	18.8	23.8	21.2	1.8

Figure 5: Compressive strength of mortar samples at 7 and 28 days of curing

With the replacement of FA by 5% nS in M2, the XRD, and TGA data show the total consumption of CH content followed by a considerable increase in the C-S-H gel, both at 7 and 28 days of curing. A significant reduction in the total pore volume of M2 was observed at both 7 and 28 days, compared to that of M1, indicating the formation of dense microstructure from the pozzolanic reaction of nano sized amorphous nano silica and the micro sized FA particles. This increase in C-S-H gel followed by a significant reduction and the refinement of the pore structure of M2 is also evident in the SEM image (figure 5) and is reflected in the corresponding improvement in 7 and 28 day strengths (figure 4), compared to that of M1. A considerable increase in the formation of hydrogarnet was also observed. The increase in hydrogarnet content with the addition of amorphous nano silica indicates that it is most likely a siliceous hydrogarnet. Moreover, the endothermic peak of the siliceous hydrogarnet so formed shifted from 350 °C in M1 to 390 °C in M2. Interestingly, the increase in C-S-H gel between 7 and 28 days in M2 was considerably less than that of M1 but both the mixes showed a similar increase in strength between these curing ages. This could be attributed to the increase in the density of C-S-H gel due to the pozzolanic reaction of nano-silica in M2 that resulted in a stronger strength forming gel, compared to that of M1. No XRD peak reflection of silica rich hydrogarnet phase was noticed in the x-ray diffraction data of M2, indicating that it is very poorly crystalline or in an amorphous form. Similar observations of the formation of very poorly crystalline siliceous hydrogarnet were made by E. T. Carlson [25]. A small increase in the formation of Ettringite was observed at 7 days, which didn't show any further increase at 28 days. The Mc and Hc phases that were formed in M1 were also not present in M2. The calcite content showed a considerable reduction compared to M1,

but it was still higher than 1.5% introduced into the mix from raw OPC. This indicates that though the majority of the portlandite was consumed by nano silica to produce C-S-H, but a part of it also got converted into CC due to its exposure to the atmospheric CO_2. When nS content was increased to 7.5% in M3, C-S-H content of M3 showed a small decrease at 7 days, but a significant increase in siliceous hydrogarnet content was observed compared to that of M2. This indicates that the increase in amorphous nano silica shows a higher affinity towards the reaction with the C-A-H phase(s) to form silica-rich hydrogarnet in initial days of curing, compared to the reaction with portlandite to form C-S-H gel. M3 showed a considerable decrease in pore size greater than 40 Å and an increase in pore size less than 40 Å, with an overall increase in total pore volume at 7 days, compared to that of M2. The refinement in the pore structure (i.e. the reduction in larger size pores and the increase in smaller size pores) is most likely due to the total increase in the pozzolanic reaction products due to the increase in amorphous nano silica content. The increase in total porosity could be because of the possible formation and conversion of metastable CAH_{10}, C_2AH_8 phases to a stable and denser C_3AH_6 hydrogarnet phase [29, 30]. Since no crystalline peak of C_3AH_6 phase was visible in the XRD diffractogram, this hydrogarnet phase so formed in the presence of amorphous nano silica is most likely a siliceous hydrogarnet having very poor crystallinity [25-27]. The reduction in 7 day strength of M3 could be attributed to the decrease in the formation of C-S-H gel and the increase in the total porosity of the cement matrix, compared to that of M2. After 28 days of curing a significant increase in the C-S-H gel was observed but no further increase in the hydrogarnet phase was noticed. This shows that reaction of hydrogarnet phase was exhausted in the initial 7 days allowing the available nano silica and the amorphous silica present in the fly ash to react with the available portlandite content to produce an additional C-S-H gel, which was considerably higher than that of M2. This increase in the formation C-S-H gel resulted in a considerable reduction in the total pore volume of M3 compared to that of M2, at 28 days of curing. The combined effect of the increase in the C-S-H gel and a considerable reduction in the total pore volume resulted in a significant improvement in compressive strength of M3 compared to that of M2. The SEM image of M3 showed a reduction in micro-cracking compared to that of M2 at 28 days of curing. This possibly could be attributed to the combined effect of the increase in the C-S-H gel and the hydrogarnet phase and the reduction in the total porosity, that densified the cement matrix. The endothermic peak associated with the formation of siliceous hydrogarnet phase in the DTG curve of M3 was observed to be shifted further to a higher temperature of

410 °C. This shows that the presence of nano silica not only favours the formation of silica-rich hydrogarnet phase but also improves its thermal stability which increases with the increase in nano silica content.

With the replacement of FA by 2.5% nCC in M4, there was no change in the C-S-H, CH and CC contents at 7 day compared to that of M1. In spite of having no difference in the C-S-H content between M1 and M4, there was a small increase in 7 day M4 strength. This could possibly be attributed to the dense particle packing effect provided by the addition of nCC to the cement matrix which was reflected in a considerable reduction in the total pore volume of M4 compared to that of M1. At 28 days of curing a small increase in the C-S-H content followed by a corresponding decrease in calcite and no change in the CH content was observed in M4 compared to that of M1. This shows that a part of calcite was converted to portlandite beyond 7 days which was further consumed by the amorphous silica present in fly ash to produce additional C-S-H gel, resulting in the reduction and refinement of the pore structure at 28 days of curing. This increase in the C-S-H gel in addition to the reduction and refinement of the pore structure resulted in a small increase in 28 day strength of M4 compared to that of M1.

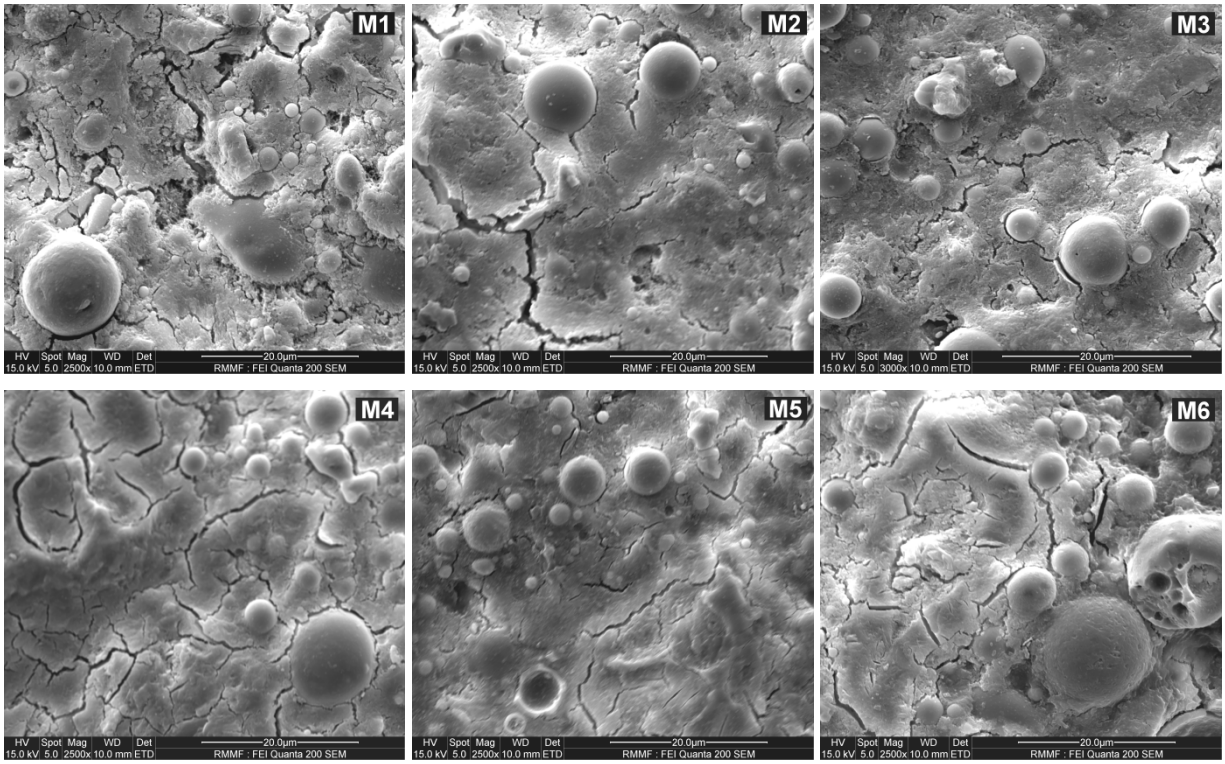

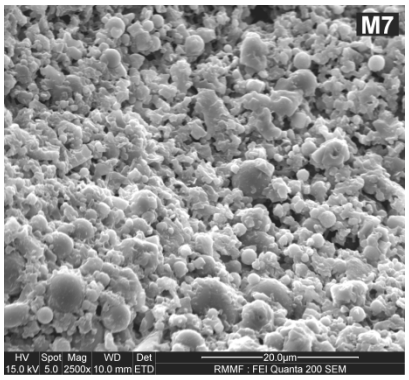

Figure 6: Scanning electron microscopy images of hydrated samples at 28 days of curing

With a further increase in nCC to 5% in M5, no considerable change in the C-S-H content was observed at 7 days but a further small increase in 7 day strength was observed, compared to that of M4. Figure 7 (a) shows a reduction and refinement of the pore structure of M5 compared to that of M4. This shows that at early age of curing nCC has no visible effect on the reactivity of fly ash but it provides a small improvement in strength possible because of the reduction and refinement of the pore structure. At 28 days M5 showed a considerable increase in the C-S-H gel and a marked decrease in the total pore volume, which was reflected in a considerable increase in its compressive strength results, compared to that of M4. Portlandite content of M5 showed no change compared to that of M4, but the calcite content showed a considerable decrease. This indicates that part of the added nCC got converted to portlandite which further reacted with the amorphous silica present in the fly ash to produce additional C-S-H gel resulting in the increase in compressive strength results.

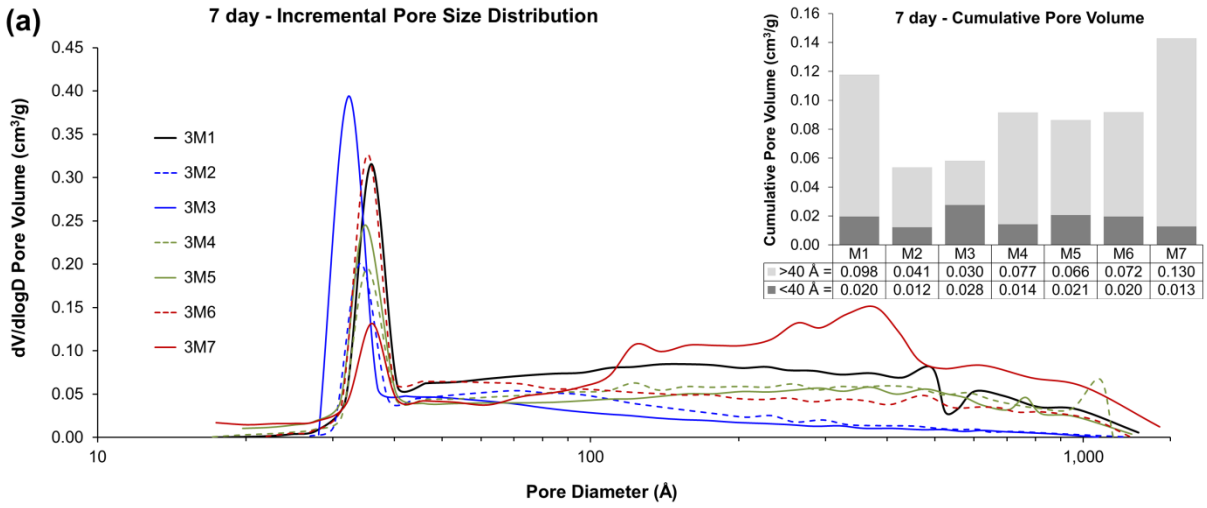

Figure 7(a): Incremental pore size distribution and Cumulative pore volume at 7 days of curing

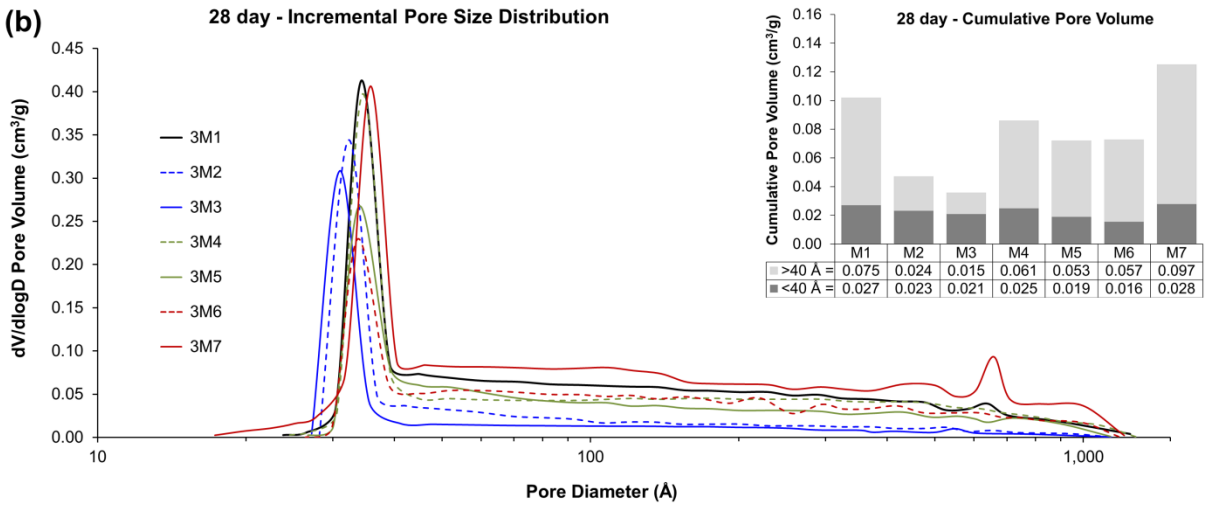

Figure 7(b): Incremental pore size distribution and Cumulative pore volume at 28 days of curing

When the FA in M1 was partially replaced with 2.5% nA in M6, there was a small increase in 7 day strength but the mass loss due to C-S-H/C-A-S-H was considerably higher than that of M4 and M5 having similar strength. This considerable difference in mass loss could possibly be because of formation of $Al(OH)_3$ gel in addition to the formation of C-S-H/C-A-S-H phases. A considerable reduction in the total pore volume of M6 was observed at 7 days compared to that of M1. This could be attributed to the formation of a dense microstructure produced due to the pozzolanic reaction of nano sized particles of nA. The mass loss associated with C-S-H/C-A-S-H gel at 28 days was significantly higher than that of M1, coupled with a considerable reduction in the portlandite content, which is a good indicator of a pozzolanic reaction. Moreover, a significant reduction and a considerable refinement of the pore structure of M6 was observed at 28 days compared to that of M1. This increase in the C-S-H/C-A-S-H gel in addition to the reduction and refinement of pore structure was also reflected in the corresponding increase in the compressive strength of M6 at 28 days of curing, compared to that of M1. A considerable increase in the formation of Ettringite and Hc phases in addition to a marked decrease in the Mc phase was observed in M6 at 7 days compared to that of M1. However, by 28 days a considerable reduction in the Ettringite content along with the total elimination of Hc phase was observed. This indicates that the Ettringite and Hc phases were unstable, resulting in the partial conversion of Ettringite and the complete conversion of Hc into Mc phase via a reaction with the available $CaCO_3$. This was also evident in the decrease in the calcite content at 28 days compared to that at 7 days of curing. With a further increase in nA to 5% in M7, a considerable reduction in the portlandite and calcite contents were observed, but no difference in the hydrogarnet phase was noted,

compared to that of M6. There was a significant increase in the ettringite content of M7 at 7 days but Mc and Hc phases were not observed. This indicates that the presence of nA in high concentration, demonstrates strong affinity towards the sulphate bearing phase in the hydration/pozzolanic reaction, which increases with an increase in nA content, thereby resulting in the increase in the ettringite formation and total elimination of Mc and Hc phases observed. The phases that were present (as visible in XRD data) and have the possibility of formation due to the addition of nA in 50 to 300 °C temperature range are ettringite, C-S-H/C-A-S-H and aluminium hydroxide. After deducting the mass loss due to chemically bound water of ettringite, M7 showed a considerably higher amount of chemically bound water associated with the C-S-H/C-A-S-H and aluminium hydroxide phases. However, there was a significant reduction in the 7 day strength of M7 compared to that of M6. Moreover, the SEM image of M7 didn't show any sign of C-S-H/C-A-S-H gel as was visible in M6, though a significant amount of needle shape Ettringite crystals were clearly visible in M7. This indicates that the remaining mass loss associated with C-S-H/C-A-S-H and aluminium hydroxide phases contains a negligible amount of strength forming C-S-H/C-A-S-H gel (if any) that also resulted in a considerable increase in the total pore volume of M7, thereby resulting in a significant reduction in its 7 day strength, compared to that of M6. At 28 days, there was a small increase in the mass loss of chemically bound water associated with C-S-H/C-A-S-H and aluminium hydroxide phases in M7 followed by a considerable reduction and refinement of the pore structure. Also a minor increase in compressive strength was observed at 28 days compared to that at 7 days of curing. This difference in physicochemical changes and the mechanical properties are not sufficient to indicate any significant change within the cement matrix. Moreover, this indicates that the improvement in the pore size distribution and the total pore volume in the presence of very low amount of strength forming C-S-H/C-A-S-H gel has little or no significance in the improvement of compressive strength of a cement matrix. The results obtained from the addition of 2.5% and 5% nA in HVFA cement composite suggest that the addition of nA is only beneficial in the improvement of mechanical properties if added in small quantities i.e. 2.5% or possibly lower. The addition of nA higher than 2.5% is highly detrimental in strength development due to the formation of large amount of $Al(OH)_3$ gel which inhibits the hydration/pozzolanic reaction within the cement matrix.

4. Conclusions

Based on the observations made in this sudy, the following conclusions can be drawn:

i) The addition of nano silica totally consumes the available portlandite and significantly increases the formation of C-S-H gel, resulting in a considerable increase in its compressive strength. The formation of C-S-H gel and the corresponding improvement in strength at 28 days increases with an increase in nano silica content. At early age of curing i.e. at 7 days, the increase in nano silica favours the reaction with C-A-H phase resulting in the increase in silica-rich hydrogarnet phase and a drop in C-S-H gel leading to the reduction in early strength results.

ii) The addition of nano silica to class F low calcium HVFA cement composite considerably increases the formation and thermal stability of silica-rich hydrogarnet phase, which increases with the increase in nano silica content.

iii) The addition of both 2.5% and 5% nCC content show no increase in the pozzolanic reaction at 7 days of curing, but shows a small increase in compressive strength, which increases with the increase in nCC content. This could possibly be attributed to dense particle packing effect provided by nCC to the cement matrix. The improvement in the reactivity of fly ash due to the addition of nCC is evident at 28 days of curing from the increase in C-S-H gel and corresponding increase in compressive strength. This increase in the formation of C-S-H gel and the commensurate increase in 28 day strength increases with the increase in nCC content.

iv) The addition of nano alumina helps in improving the mechanical properties of VHVFA cement composite, only if added in small quantity i.e. 2.5% or possibly lower. At higher concentration the hydration/pozzolanic reaction is severely inhibited due to the formation of large amounts of $Al(OH)_3$ gel resulting in negligible formation of C-S-H/C-A-S-H gel (if any), leading to a significant reduction in the compressive strength results, compared to that of M6 having lower nA content.

5. Acknowledgement

The authors fully acknowledge the scientific and technical support provided by the Microscopy & microanalysis facility, Rheology and material characterisation facility and the X-ray facility at RMIT University. The authors would like to thank Cement Australia for providing the material support to carry out this research.

References

[1] Kumar S, Kumar R, Mehrotra S. Influence of granulated blast furnace slag on the reaction, structure and properties of fly ash based geopolymer. Journal of Materials Science. 2010;45(3):607-15.

[2] Paya J, Monzo J, Peris-Mora E, Borrachero M, Tercero R, Pinillos C. Early-strength development of Portland cement mortars containing air classified fly ashes. Cement and concrete research. 1995;25(2):449-56.

[3] Barbhuiya S, Gbagbo J, Russell M, Basheer P. Properties of fly ash concrete modified with hydrated lime and silica fume. Construction and Building Materials. 2009;23(10):3233-9.

[4] Roychand R, De Silva S, Law D, Setunge S. High volume fly ash cement composite modified with nano silica, hydrated lime and set accelerator. Materials and Structures. 2016;49(5):1997-2008.

[5] El-Chabib H, Syed A. Properties of self-consolidating concrete made with high volumes of supplementary cementitious materials. Journal of Materials in Civil Engineering. 2012;25(11):1579-86.

[6] Wei X, Zhu H, Li G, Zhang C, Xiao L. Properties of high volume fly ash concrete compensated by metakaolin or silica fume. Journal of Wuhan University of Technology-Mater Sci Ed. 2007;22(4):728-32.

[7] Shaikh F, Supit S, Sarker P. A study on the effect of nano silica on compressive strength of high volume fly ash mortars and concretes. Materials & Design. 2014;60:433-42.

[8] Oltulu M, Şahin R. Effect of nano-SiO_2, nano-Al_2O_3 and nano-Fe_2O_3 powders on compressive strengths and capillary water absorption of cement mortar containing fly ash: a comparative study. Energy and Buildings. 2013;58:292-301.

[9] Mohseni E, Miyandehi BM, Yang J, Yazdi MA. Single and combined effects of nano-SiO_2, nano-Al_2O_3 and nano-TiO_2 on the mechanical, rheological and durability properties of self-compacting mortar containing fly ash. Construction and Building Materials. 2015;84:331-40.

[10] Shaikh FU, Supit SW. Mechanical and durability properties of high volume fly ash (HVFA) concrete containing calcium carbonate ($CaCO_3$) nanoparticles. Construction and Building Materials. 2014;70:309-21.

[11] Roychand R, De Silva S, Law D, Setunge S. Micro and nano engineered high volume ultrafine fly ash cement composite with and without additives. International Journal of Concrete Structures and Materials. 2016;10(1):113-24.

[12] Kawashima S, Hou P, Corr DJ, Shah SP. Modification of cement-based materials with nanoparticles. Cement and Concrete Composites. 2013;36:8-15.

[13] WM Supit S, UA Shaikh F. Effect of nano-$CaCO_3$ on compressive strength development of high volume fly ash mortars and concretes. Journal of Advanced Concrete Technology. 2014;12(6):178-86.

[14] Bye GC. Portland cement: composition, production and properties: Thomas Telford; 1999.

[15] Kaewmanee K, Krammart P, Sumranwanich T, Choktaweekarn P, Tangtermsirikul S. Effect of free lime content on properties of cement–fly ash mixtures. Construction and Building Materials. 2013;38:829-36.

[16] HUNNICUTT WA. Characterization of Calcium-silicate-hydrate and Calcium-alumino-silicate-hydrate, University of Illinois at Urbana-Champaign; 2013.

[17] Scrivener K, Snellings R, Lothenbach B. A Practical Guide to Microstructural Analysis of Cementitious Materials: Crc Press; 2016.

[18] Madej D, Szczerba J, Pięta A, Śnieżek E, Prorok R. Reactions in the system CaO-Al_2O_3-H_2O. Selected Aspects of Modern Engineering: Wydawnictwa AGH; 2013. p. 113-25.

[19] Cardoso FA, Innocentini MD, Akiyoshi MM, Pandolfelli VC. Effect of curing time on the properties of CAC bonded refractory castables. Journal of the European Ceramic Society. 2004;24(7):2073-8.

[20] Schmitt N, Hernandez J-F, Lamour V, Berthaud Y, Meunier P, Poirier J. Coupling between kinetics of dehydration, physical and mechanical behaviour for high alumina castable. Cement and concrete research. 2000;30(10):1597-607.

[21] Dilnesa BZ, Lothenbach B, Renaudin G, Wichser A, Kulik D. Synthesis and characterization of hydrogarnet $Ca_3(Al_xFe_{1-x})_2$ $(SiO_4)_y$ $(OH)_{4(3-y)}$. Cement and Concrete Research. 2014;59:96-111.

[22] Passaglia E, Rinaldi R. Katoite, a new member of the Ca_3Al_2 $(SiO_4)_3$-Ca_3Al_2 $(OH)_{12}$ series and a new nomenclature for the hydrogrossular group of minerals. Bull Mineral. 1984;107:605-18.

[23] De Jong J, Stein H, Stevels J. Influence of amorphous silica on the hydration of tricalcium aluminate. Journal of Applied Chemistry. 1969;19(1):25-8.

[24] Dilnesa BZ. Fe-containing hydrates and their fate during cement hydration: thermodynamic data and experimental study, ÉCOLE POLYTECHNIQUE FÉDÉRALE DE LAUSANNE; 2011.

[25] Carlson ET. Hydrogarnet Formation in the System Lime-AI flumina-Silica-Water. Journal of Research of the National Bureau of Standards. 1956;56(6).

[26] Dilnesa B, Wieland E, Lothenbach B, Dähn R, Scrivener K. Fe-containing phases in hydrated cements. Cement and Concrete Research. 2014;58:45-55.

[27] Vespa M, Wieland E, Dähn R, Lothenbach B. Identification of the Thermodynamically Stable Fe-Containing Phase in Aged Cement Pastes. Journal of the American Ceramic Society. 2015;98(7):2286-94.

[28] Scrivener K, Füllmann T, Gallucci E, Walenta G, Bermejo E. Quantitative study of Portland cement hydration by X-ray diffraction/Rietveld analysis and independent methods. Cement and Concrete Research. 2004;34(9):1541-7.

[29] Odler I. Hydration, setting and hardening of Portland cement. LEA’s Chemistry of Cement and Concrete. 1998;4:241-97.

[30] K.L. Scrivener AC. Calcium Aluminate Cements. Lea's Chemistry of Cement and Concrete (fourth ed): Elsevier Butterworth-Heinmann; 2004. p. 714–82.

Chapter 6

Nano engineered zero cement composite

This experiment was designed to replace 100% of ordinary Portland cement. Based on the previous experiments, nano silica proved to be the most effective in improving the properties of high volume fly ash cement composites, therefore nano silica was used in different concentrations in this experiment. The other materials used were high volume raw fly ash, ground granulated blast furnace slag and hydrated lime. Various material characterisation techniques used were (i) SEM for the microstructure studies and (ii) thermogravimetric analysis in conjunction with XRD analysis using rietveld refinement external standard method to study the quantitative phase analysis of the various phases formed within the cement matrix of various mix designs.

Nano engineered zero cement composite

Rajeev Roychand [a,*], Saman De Silva [a,**] and Sujeeva Setunge [a,**]

[a] *School of Civil, Environmental and Chemical Engineering, RMIT University, Melbourne, Victoria, Australia*

** Corresponding author's Email: rajeev.roychand@rmit.edu.au*

*** Other authors' Email: saman.desilva@rmit.edu.au; sujeeva.setunge@rmit.edu.au*

Abstract

In quest of developing a green cement composite with the lowest possible carbon footprint and the highest possible use of industrial by-products, an experimental investigation was undertaken replacing 100% of cement. This paper presents the results of an experimental program to develop a nano-engineered zero cement composite, incorporating nano silica, class f low calcium fly ash, slag and hydrated lime. The proportion of various supplementary cementitious materials (SCM) used were; nano silica 2.5%, 5% and 7.5%, fly ash 72.5%, 70% and 67.5%, slag 25% and hydrated lime used as a cement additive at 10% and 15% of the total SCM. Compressive strength tests were undertaken to identify the mechanical properties of the blended mortar samples. In addition, scanning electron microscopy, thermogravimetric and x-ray diffraction analysis in conjunction with quantitative phase analysis were undertaken to investigate the various physicochemical changes taking place within the cement matrix and to formulate strategies for its further development.

The results show that both slag and fly ash require portlandite as an external alkaline activator to initiate a pozzolanic reaction within the cement matrix. The portlandite added externally in the form of $Ca(OH)_2$ powder, to the nS modified SCM blend, activates the pozzolanic reaction which increases with the increase in portlandite content. The addition of nano silica and hydrated lime to a fly ash and slag blend can help in achieving an environmental friendly zero cement composite without the need of any heat treatment. The optimum content of nano silica was found to be 5%. With the further increase in nano silica content, although the pozzolanic reaction and the resulting C-S-H/C-A-S-H gel formation increases, it also increases the micro-cracking within the cement matrix, resulting in the reduction in compressive strength at both 7 and 28 days of curing. The siliceous hydrogarnet formed due to the pozzolanic reaction of amorphous silica (FA, slag, nS) with the calcium aluminate present in the slag, shows very poor crystallinity with no visible peak reflection in x-ray diffraction data. The formation of siliceous hydrogarnet increases with the increase in amorphous nano silica but decreases with the increase in hydrated lime content.

Keywords: nano silica, fly ash, slag, hydrated lime, zero cement, x-ray diffraction, thermogravimetric analysis, scanning electron microscopy, rietveld analysis

1. Introduction

The research and development of an environmental friendly green cementitious materials have been getting an extensive and sustained focus for their potential to bring about a significant transformation into the carbon footprint of the cement industry. The majority of the research focus is given to the increase in the use of supplementary cementitious materials like; slag, fly ash and silica fume in quest of a sustainable and green alternative to the conventional ordinary portland cement. Fly ash being the most abundantly available and least utilised material worldwide with an average utilisation rate of 53.5% [1] attracts the maximum attention of the research community [2-4]. The second most widely studied SCM for its application in cement replacement is ground granulated blast furnace slag [5, 6]. The worldwide demand of slag by cement industry exceeds its supply [7]. Therefore, the research on fly ash attracts more attention of the research community to increase its use as a cement replacement material and reduce its production vs utilisation ratio. The majority of global fly ash production falls under low calcium class F category [8] which has low reactivity [9] that considerably hinders the early strength development [10, 11]. Over time a significant progress has been made in addressing the low reactivity and the slow rate of strength development of fly ash blended cement composites. To overcome this limitation of low calcium class F fly ash, researchers have looked at various ways like; fly ash particle size reduction [12], use of hydrated lime [13, 14], set accelerator [15], silica fume [16, 17] and metakaolin [18]. All of these methods have considerably contributed in their individual capacity in increasing the use of fly ash as a cement replacement material. Lime is the most crucial additive required for the pozzolanic reaction of amorphous silica present in low calcium class F fly ash, to produce strength forming C-S-H gel [13, 19]. Bharbhuia et al. (2009) studied the effect of hydrated lime on the reactivity of fly ash. They observed that the addition of hydrated lime accelerated the pozzolanic reaction resulting in a considerable improvement in the compressive strength of fly ash blended concrete. The difference in strength gain between hydrated lime modified and non-modified fly ash concrete increased with the increase in fly ash content [13]. Although hydrated lime has proved to be highly effective in improving the pozzolanic reaction but the increase in pozzolanic reaction does not always help in improving the strength development in the blended cement composites. Roychand et al. (2016) studied the effect of hydrated lime in combination with silica fume and nano slice on high volume fly ash cement composites. They observed that when hydrated lime powder was used in conjunction with silica fume in HVFA cement mortar, there was a

considerable increase in 7 and 28 day compressive strength compared to that of silica fume modified HVFA cement mortar not containing hydrated lime powder. However, when they used hydrated lime in combination with nano-silica in HVFA cement mortar, they noticed a considerable increase in early age micro cracking followed by a considerable reduction in compressive strength compared to the nano silica modified HVFA cement mortar not containing hydrated lime [17].

Oner et al. (2007) studied the effect of GGBFS on blended concrete at various cement replacement levels. They found that the early age strengths of all replacement levels were lower than that of the control mix because of the low pozzolanic activity of GGBFS. However, they found that with the increase in the curing age, the compressive strength of GGBFS concrete increases with the increase in GGBFS content up to an optimum replacement level. With the further increase in GGBFS beyond the optimum content, the strength decreases with the increase in GGBFS content. They found that 55–59% of GGBFS was the optimum content that provided the maximum improvement in compressive strength [20]. Another study by Hogan et al. (1981) reports the similar slow strength development of GGBFS blended concrete during the first three days of hydration. However, they found the optimum content of GGBFS to be 40% [21]. This reinforces the observation by Pal et al. (2003) that the reactivity of GGBFS depends on many factors like glass content, chemical composition and Blaine's fineness which varies with the source of GGBFS.

As the quest for the increase in the cement replacement levels is growing, the research focus is shifting towards the use of nanomaterials, because of their high reactivity and large surface area. Researchers have looked at the effect of nano silica [22, 23], nano alumina [24], nano calcium carbonate [25], nano iron oxide [26] and nano titanium oxide [24] on the properties of FA blended cement composites. Among the studies conducted on the effect of various nanomaterials on HVFA cement composites, nano silica has proved to be the most effective nanomaterial that significantly improves the properties of HVFA cement composites. Hou et al. (2012) studied the effect of 0, 2.25 and 5 % colloidal nano-silica (CNS) on 60 % FA blended cement composite. They observed that the compressive strength of the mortar samples at 7 and 28 days increased with the increasing amount of CNS, with the maximum increase observed at 5% CNS concentration. The addition of 5% CNS increased the compressive strength of HVFA cement blend by 60 and 33% at 7 and 28 days respectively. Roychand et al. (2016) studied the effect of 5 and 7.5% of nano silica on high volume

ultrafine fly ash (HV-UFFA) cement mortar containing 75% of FA. They also looked at the effect of the addition of HL powder to the nano silica modified HV-UFFA cement blend. They observed that the best results in the improvement of compressive strength were achieved with the addition of 5% nS and without the use of externally added HL powder. They noticed an improvement in compressive strength by 918 and 567% at 7 and 28 day compared to the HV-UFFA cement blend not containing nano silica. The compressive strength achieved at 28 days was comparable to that of OPC [17]. This shows that the amorphous nano silica holds a great potential for the development of zero cement composite having mechanical properties at par or better than that of OPC. Therefore this study was undertaken to develop a cement composite, replacing 100% of cement, incorporating nano silica, fly ash, slag, and hydrated lime. Compressive strength tests were undertaken to identify the mechanical properties of the blended mortar samples. In addition, to investigate the various physicochemical changes taking place within the cement matrix of various hydrated paste samples, scanning electron microscopy (SEM), thermogravimetric (TG) and x-ray diffraction (XRD) analysis in conjunction with quantitative phase analysis were undertaken to formulate strategies for its further development.

2. Materials and Experimental Procedure

2.1 Materials and mix design

The materials used in this study were; ordinary portland cement, ground granulated blast furnace slag (slag), low calcium class F fly ash, nano silica, and polycarboxylic ether based superplasticizer “Glenium 79” having a water content of 55%. The chemical composition of OPC, Slag, FA and nS is shown in Table 1. The crystalline and amorphous mineral composition of OPC and slag is presented in Table 2 and that of FA is presented in Table 3, as determined with the help XRD rietveld refinement method. To calculate the amount of amorphous silica, quartz and the crystalline component of silica present in mullite was deducted from the total silica present in FA as shown in Table 1. Similarly, the crystalline component of alumina present in mullite was deducted from the total alumina present in the FA to calculate the amount of amorphous alumina. Particle size distribution of OPC, Slag and FA obtained with the help of laser diffraction particle size analyser “Malvern Mastersizer 3000” is presented in Table 4 in addition to the mean particle size of nano silica provided by the chemical supplier.

Table 1: Chemical composition of OPC, SLAG, FA, MFA and nS

Oxides	OPC (%)	SLAG (%)	FA (%)	nS (%)
SiO_2	19.7	29.9	72.9	99.9
CaO	63.1	47.8	0.3	-
Al_2O_3	4.8	12.9	22.3	-
Fe_2O_3	3.2	0.4	1.1	-
SO_3	2.5	2.0	0.2	-
MgO	2.1	4.5	0.3	-
Na_2O	0.2	0.4	0.2	-
K_2O	0.4	0.5	0.3	-
TiO_2	0.1	0.6	1.2	-
LOI	2.8	0.8	1.2	-

Table 2: Crystalline and amorphous mineral composition of OPC and Slag

	C_3S	C_2S	C_3A	C_4A	CH	CC	$C\bar{S}$(G)	$C\bar{S}$(B)	MgO	Qz	Amorphous
OPC	62.1%	6.2%	7.7%	7.2%	1.8%	7.5%	3.9%	1.1%	2.0%	0.5%	-
Slag	-	2.6%	-	-	-	3.2%	4.4%	-	-	-	89.8%

* Amorphous content may include possible crystalline phases which were below the XRD detection limit

Table 3: Crystalline and amorphous mineral composition of FA

	Quartz	Mullite	Magnetite	Rutile	Amorphous Silica	Amorphous Alumina
FA	22.8%	29.9%	1.4%	1.0%	42.9%	0.5%

Table 4: Particle size distribution of OPC, FA, SLAG and nS

Material	D[4,3] Mean	d_{10}	D_{25}	D_{50}	D_{75}	D_{90}
OPC	24.6 μm	2.7 μm	6.5 μm	15.4 μm	28.3 μm	44.2 μm
FA	28.7 μm	2.3 μm	5.8 μm	14.0 μm	33.1 μm	75.2 μm
SLAG	16.4 μm	2.8 μm	6.7 μm	14.1 μm	23.6 μm	33.5 μm
nS*	7 nm	-	-	-	-	-

* Particle size is shown in nanometers as provided by the chemical supplier

Figure 1 shows XRD diffractograms of OPC, Slag, FA and nS along with their respective identified crystalline phases. The predominant crystalline phase present in slag was gypsum in addition to the presence of other minor phases of aragonite and calcite. Fly ash shows the major crystalline phases of quartz and mullite in addition to the minor peaks of rutile and maghemite. Nano silica showed a broad hump centered around 22° 2-theta, which is a typical characteristic of amorphous silica content.

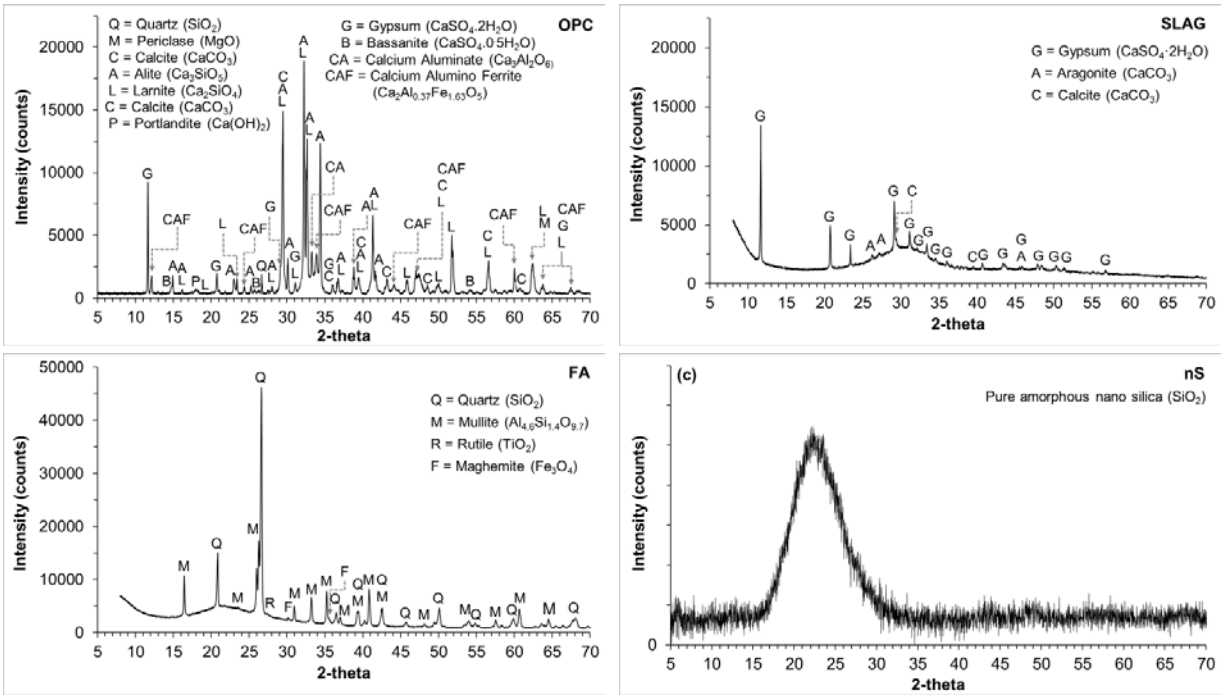

Figure 1: XRD diffractograms of OPC, Slag, FA and nS

Tables 5 and 6 summarize the various mortar mix designs tested. OPC, Slag, FA and nS were added as a percentage mass of the total binding material. HL was added as an additive, as a percentage of the total binder content. The amount of superplasticizer requirement for each mix design was calculated in the trial work, to get an approximately similar consistency for the self-consolidation of the mortar samples. The water content of SP was adjusted in the total w/b ratio. TGA and XRD were conducted on the hydrated binder paste, and SEM was performed on the mortar samples.

Table 5: Mortar mix design

Mix	Binder (%)				HL (% of binder)	S/B (by weight)	W/B (by weight)	SP
	OPC	FA	Slag	nS				
M1	25	75	0	0	0	2.4	0.3	9
M2	0	75	25	0	0	2.4	0.3	50
M3	0	75	25	0	10	2.4	0.3	27
M4	0	72.5	25	2.5	10	2.4	0.3	50
M5	0	70	25	5.0	10	2.4	0.3	58
M6	0	67.5	25	7.5	10	2.4	0.3	132
M7	0	72.5	25	2.5	15	2.4	0.3	45
M8	0	70	25	5.0	15	2.4	0.3	52
M9	0	67.5	25	7.5	15	2.4	0.3	110

B = binder; S = sand; W = water; SP = superplasticizer (mL kg^{-1} binder)

2.2 Sample preparation, curing & testing

2.2.1 TGA and XRD of binder raw material

Thermogravimetric analysis was conducted on OPC and slag powder sample to ascertain the presence of $CaCO_3$ since it has XRD peak overlap with Alite and Larnite. TGA also helped in identifying the presence of $Ca(OH)_2$ in OPC. Thermogravimetric analysis was conducted using PerkinElmer STA 6000 thermal analyser in a nitrogen environment with a flow rate of 19.8 mL min^{-1}. 20 - 30 mg of powdered samples were initially heated at 40^0C for 5 minutes to expel any moisture caught by the samples while handling. Then the samples were heated from 40 – 550 ^{0}C with the heating rate of 20 ^{0}C min^{-1}.

X-ray diffraction was conducted on all the raw materials using a Bruker AXS D4 Endeavour system with Cu-Kα radiation operated at 40 kV and 40 mA and a Lynxeye linear strip detector. The samples were tested between 5° and 90° 2-theta (2θ) with a step size of 0.01° and counting time of 1s per step.

2.2.2 Compressive strength of mortar

All the raw materials were dry mixed at low speed in the mortar mixer for 1 min to obtain a homogenous mix. Then water and SP were added and mixed for 3 min, followed by a final high speed mixing for another 1 min. Mortar samples were then poured into 50 mm x 50 mm

x 50 mm moulds. The samples were covered with a plastic sheet, cured at room temperature for 24 hrs, de-moulded and then further cured in water at room temperature as per ASTM C109 until the time of testing. The samples were taken out of water, wiped and surface dried after 7 and 28 days of curing. Compressive strength of the mortar samples was measured as per ASTM C109 with a loading rate of 0.36 MPa/s. For every mix at each curing age, three replicates were tested.

2.2.3 TGA and XRD of hydrated paste samples

Mixing procedure and curing method were kept the same for hydrated paste samples for TGA and XRD. The samples at a particular curing age were taken out of the curing tank, surface dried, ground and sieved through 45 μm sieve. To stop hydration and to remove physically bound water the solvent exchange method was adopted using acetone. A 100 mL of acetone was added to 30 g of the sieved sample in a plastic bottle, mixed vigorously by hand for about 3 mins and then kept on table for about a minute. Excess acetone was drained out and the process was repeated. The samples were then dried overnight in an oven at 40 °C temperature. The dried samples were collected and stored in a sealed plastic container till the time of testing. TGA and XRD were conducted on all the hydrated paste samples at 7 and 28 days of curing, using method described in section 2.3.1

2.2.4 SEM of hydrated mortar samples

For SEM, a small thin section of the hardened mortar sample was cut out from the internal part of the specimen. It was then embedded in epoxy, ground, polished, mounted on a steel stub and gold coated. FEI Quanta 200 SEM was used to study the microstructure of the hardened paste samples. The accelerating voltage of the beam was 20 Kv and the electron images were acquired at 10mm working distance and 5000x magnification.

3. XRD and TGA Data analysis

Calcium silicate hydrate, the main phase responsible for the strength development in a cement matrix is difficult to identify, both in XRD and TGA data individually. In X-ray diffraction data, C-S-H phase don’t show sharp crystalline peaks because of their near amorphous nature [27]. Large amorphous hump present in XRD diffraction data of hydrated samples containing SCM, can have any combination of un-hydrated amorphous material and C-S-H gel. Therefore, XRD data poses a big challenge to correctly identify the amount of C-

S-H gel. In TGA, the thermal breakdown temperature of chemically bound water of C-S-H has an overlap with ettringite, gypsum, mono-carboaluminate, hemi-carboaluminate and mono-sulfoaluminate phases between 50 to ~350 °C temperature range as described in [28]. This again makes it difficult to quantify the amount of C-S-H gel formation from the TGA data. Therefore, to estimate the proportion of the main strength forming C-S-H gel in the hydrated cement paste, TGA was combined with XRD quantitative phase analysis. The quantitative phase analysis on XRD data was undertaken using rietveld refinement external standard method as described in [28]. The external standard used was 99.9% pure quartz powder having particle size less than 45µm. Chemically bound water was calculated from the percentage proportion of the identified ettringite, gypsum, mono-carbonate and hemi-carbonate phases using table 6. The chemically bound water, so obtained from the XRD data, was deducted from the total mass loss between (i) 50 to ~250 °C for the group of phases containing C-S-H, ettringite and gypsum and (ii) 50 to ~350 °C for the group of phases containing C-S-H, ettringite, gypsum, mono-carboaluminate and hemi-carboaluminate phases, to calculate the amount of C-S-H bound water. The exact boundaries of the mass loss due to various phases or group of phases were identified with the help of TG derivative curve.

Table 6: Chemically bound water and CO_2 contents of mineral phases of hydrated cement paste samples

Mineral	Chemical formula	Bound water (Wt. %)
Ettringite	$Ca_6Al_2(SO_4)_3(OH)_{12}\cdot 26H_2O$	52.64
Hemi-carboaluminate	$Ca_4Al_2(CO_3)_{0.5}(OH)_{13}\cdot 5.5H_2O$	38.30
Mono-carboaluminate	$Ca_4Al_2(CO_3)(OH)_{12}\cdot 5H_2O$	34.86
Gypsum	$CaSO_4\cdot 2H_2O$	20.93

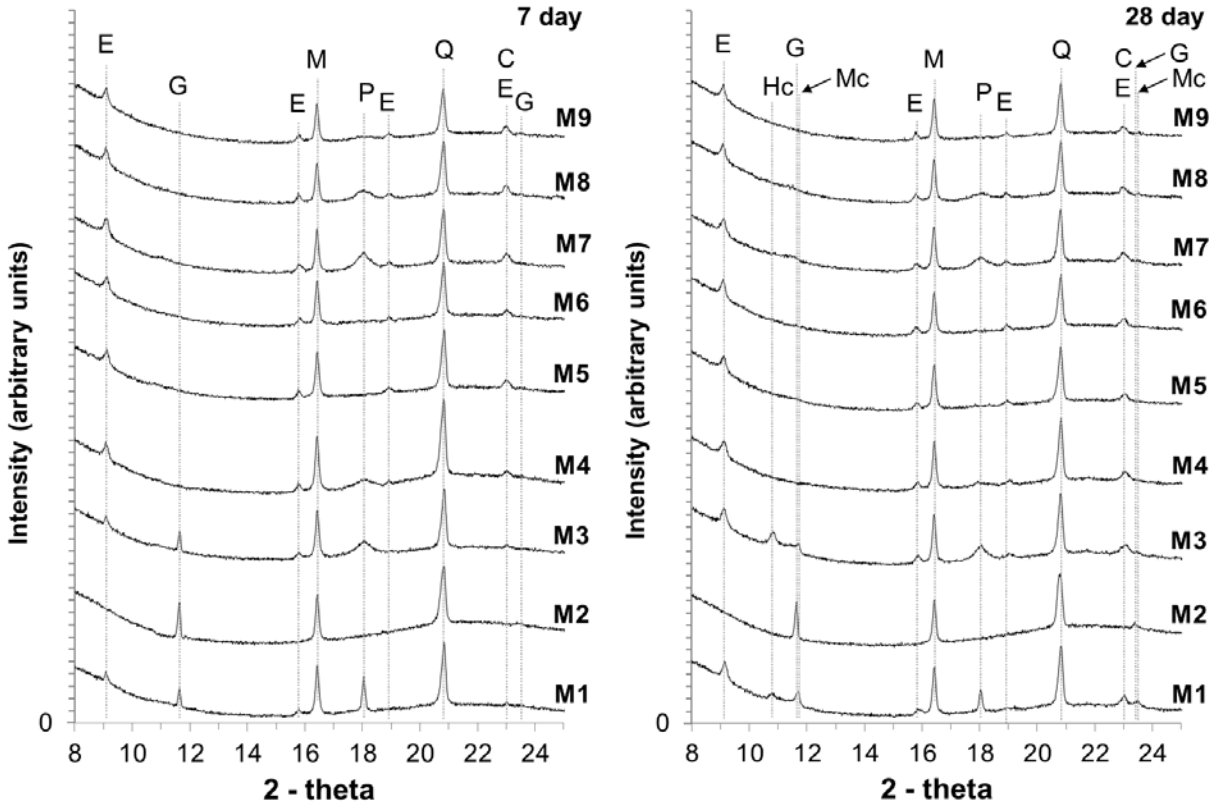

Figure 2: X-ray diffractograms of hydrated paste samples at 7 and 28 days of curing

X-ray diffraction data of hydrated paste samples at 7 and 28 days of curing is shown in Figure 2. The primary quartz peak from the fly ash present in the samples, located at ~26.7° 2**θ** had a very high intensity and was overshadowing the low intensity hydrated phases used in the analysis. Therefore, for the clarity in the presentation of the crystalline phases used in the combined XRD and TGA analysis, the XRD data is presented from 8° to 25° 2-theta. The various phases identified in the XRD patterns were ettringite (E), gypsum (G), hemi-carboaluminate (H_c), monocarbonate (M_c), mullite (M), portlandite (P), quartz (Q) and calcite (C).

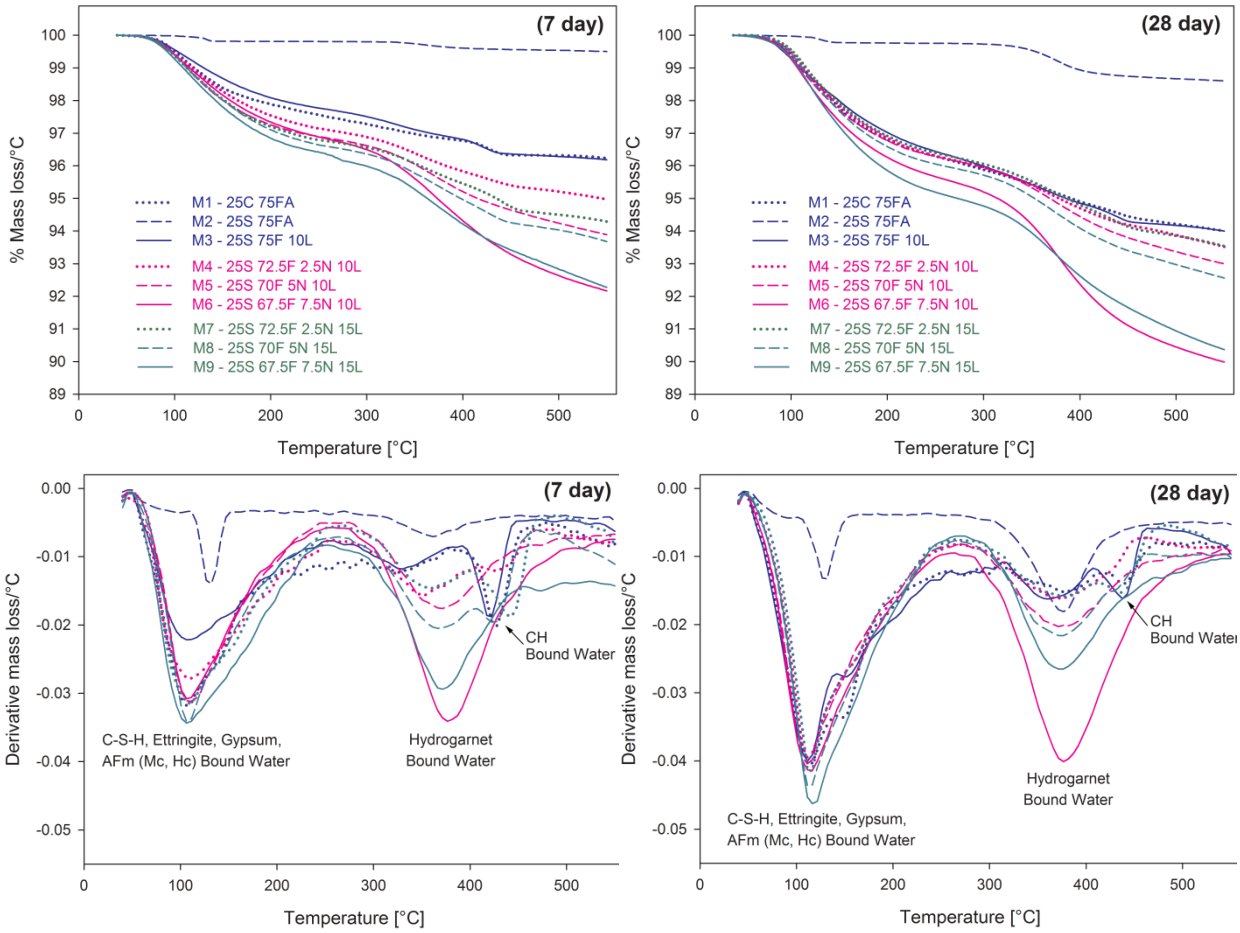

Figure 3: TG and DTG curves of hydrated paste samples at 7 and 28 days of curing

Note: C-S-H= calcium silicate hydrate, Mc = mono-carbonaluminate, Hc = hemi-carboaluminate, CH = calcium hydroxide

Figure 3 above presents the thermogravimetric mass loss and derivative curves of hydrated paste samples at 7 and 28 days of curing. Derivative curves help in identifying the exact boundaries of the mass loss of individual (having no thermal mass loss overlap) or a group of phases. The thermal breakdown temperature of chemically bound water of ettringite, C-S-H, C-A-S-H, gypsum, mono-carbonate, hemi-carbonate and mono-sulphate phases have an endothermic peak overlap between 50 and ~300 °C temperature range as described in [28]. Therefore, to identify the proportion of the main strength forming C-S-H/C-A-S-H gel in cement, TGA was combined with XRD quantitative phase analysis. The quantitative phase analysis on XRD data was undertaken using the rietveld refinement external standard method as described in [28]. The external standard used was 99.9% pure quartz powder having particle size less than 45µm. Chemically bound water was calculated from the percentage proportion of the identified ettringite, gypsum, mono-carbonate and hemi-carbonate phases using table 6. The chemically bound water, so obtained from the XRD data, was deducted from the total mass loss between 50 to ~300 °C from TGA data, to calculate the mass from

C-S-H and C-A-S-H phases. The exact boundaries of the mass loss due to various phases or group of phases were identified with the help of TG derivative curve (DTG) as shown in the figures 3(a) and (b). The second endothermic peak is associated with a hydrogarnet phase which shows an endothermic peak varying between ~310 to ~450 °C temperature [28-32]. The various phases that come under hydrogarnet family are non-siliceous hydrogarnets $Ca_3(Al_xFe_{1-x})_2(OH)_{12}$ and siliceous hydrogarnets $Ca_3(Al_xFe_{1-x})_2(SiO_4)_y(OH)_{4(3-y)}$ [32-35]. Previous studies show that some siliceous hydrogarnets show very poor crystalline [36-38]. The third endothermic peak associated with the thermal decomposition of portlandite lies between ~400 and ~500 °C temperature [28]

Table 7 below presents the combined TGA and XRD analysis of chemically bound water of hydrated paste samples. Column (a) shows the mass loss of chemically bound water of C-S-H/C-A-S-H, Ettringite, Hc, Mc and Gypsum, obtained from the thermo-gravimetric analysis and expressed as a percentage of dried mass of the powder sample at 50 °C. Columns (b) to (e) present the chemically bound water of the crystalline phases quantified with the help of XRD rietveld refinement external standard method and expressed as the percentage of dried powder sample.

Table 7: Combined TGA and XRD analysis of chemically bound water of hydrated paste samples

Mix	C-S-H/C-A-S-H + Ettringite + Hc + Mc + Gypsum (a)		Ettringite (b)		Gypsum (c)		Hc (d)		Mc (e)		C-S-H/C-A-S-H = a - (b+c+d+e)	
	7d	28d	7d	28d	7d	28d	7d	28d	7d	28d	7d	28d
M1	2.18	4.17	0.60	1.18	0.10	-	-	0.21	-	0.35	1.48	2.43
M2	0.20	0.22	-	-	0.24	0.21	-	-	-	-	-0.04	0.01
M3	2.23	4.10	0.58	1.13	0.13	-	-	0.40	-	0.18	1.52	2.39
M4	2.85	3.93	1.16	1.10	-	-	-	-	-	-	1.69	2.83
M5	3.08	4.27	1.08	1.12	-	-	-	-	-	-	2.00	3.15
M6	3.12	4.33	1.00	1.10	-	-	-	-	-	-	2.12	3.23
M7	3.20	4.50	1.10	1.16	-	-	-	-	-	-	2.10	3.34
M8	3.36	4.83	1.08	1.12	-	-	-	-	-	-	2.28	3.71
M9	3.57	5.37	1.14	1.08	-	-	-	-	-	-	2.43	4.29

Table 8 presents the mass loss of chemically bound water of hydrogarnet phase and the portlandite content of the hydrated paste samples expressed as CH (residual) and CH (consumed). . Equations (1) and (2) show the calculations of CH (residual) and CH (consumed), expressed as percentage of the mass of dry sample at 50 °C (M_{50}).

$$CH(residual) = \frac{\mathrm{M}^{\mathrm{S}}_{\mathrm{H2O\,CH}} * \frac{74}{18}}{M_{50}} * 100\ [\%] \quad (1)$$

$$CH(consumed) = \left[\frac{\mathrm{M}^{\mathrm{S}}_{\mathrm{H2O\,CH}} * \frac{74}{18}}{M_{50}} * 100\ [\%]\right] - \left[\frac{CH_{Add}}{100 + CH_{Add}} * 100\ [\%]\right] \quad (2)$$

$\mathrm{M}^{\mathrm{S}}_{\mathrm{H2O\,CH}}$ is mass loss due to the dehydroxylation of calcium hydroxide present in the hydrated cement paste. The fraction $\frac{74}{18}$ is used to convert CH bound water to CH mass, where 74 is the molar mass of $Ca(OH)_2$ and 18 is the molar mass of H_2O. $\mathrm{CH_{Add}}$ represents the percentage of calcium hydroxide powder added to the mix design.

Table 8: Mass loss due to hydrogarnet chemically bound water, residual and consumed portlandite content, and total chemically bound water, expressed as % of initial dried mass

Mix	Hydrogarnet bound water (%)		CH (residual) (%)		CH (consumed) (%)		Total chemically bound water (%)	
	7d	28d	7d	28d	7d	28d	7d	28d
M1	0.50	1.00	2.16	1.97	-	-	3.67	5.84
M2	0.24	1.02	-	-	-	-	0.47	1.31
M3	0.91	1.08	2.55	2.30	6.55	6.80	3.72	5.85
M4	1.40	1.68	1.56	0.52	7.54	8.58	4.73	5.89
M5	2.25	2.38	-	-	9.10	9.10	5.68	6.71
M6	3.65	4.72	-	-	9.10	9.10	7.47	9.89
M7	1.26	1.76	3.69	3.00	9.35	10.04	5.46	6.08
M8	1.67	2.34	2.98	1.94	10.06	11.10	5.83	7.11
M9	2.84	3.84	1.71	-	11.33	13.04	7.04	9.17

4. Results and discussion

Table 7 shows the C-S-H/C-A-S-H bound water of the control mix M1 was 1.48% which increased to 2.43% at 28 days, but the relative reduction in the CH content was considerably small. This is most likely because of the increase in the degree of hydration of calcium silicate phases present in OPC that released more CH content into the system, thereby making it available for further reaction with the amorphous silica present in FA. This increase in the C-S-H/C-A-S-H content from 7 to 28 days was also reflected in the corresponding improvement in its 28 day strength as shown in figure 4. The x-ray diffraction data in figure 3 shows the partial conversion of gypsum to ettringite at 7 days and the complete conversion taking place by 28days. In addition, Hc and Mc phases were also observed at 28 days of curing. Since the amount of ettringite formed was the maximum that can be produced from available gypsum based on mass balance and no other sulfate bearing phase was observed in the XRD data, the formation of Hc and Mc phases is less likely due to the substitution of sulfate with the carbonate ions. This indicates that the presence of Hc and Mc phases at 28days were most likely produced due to the reaction of calcium aluminate hydrate with the $CaCO_3$ present in OPC.

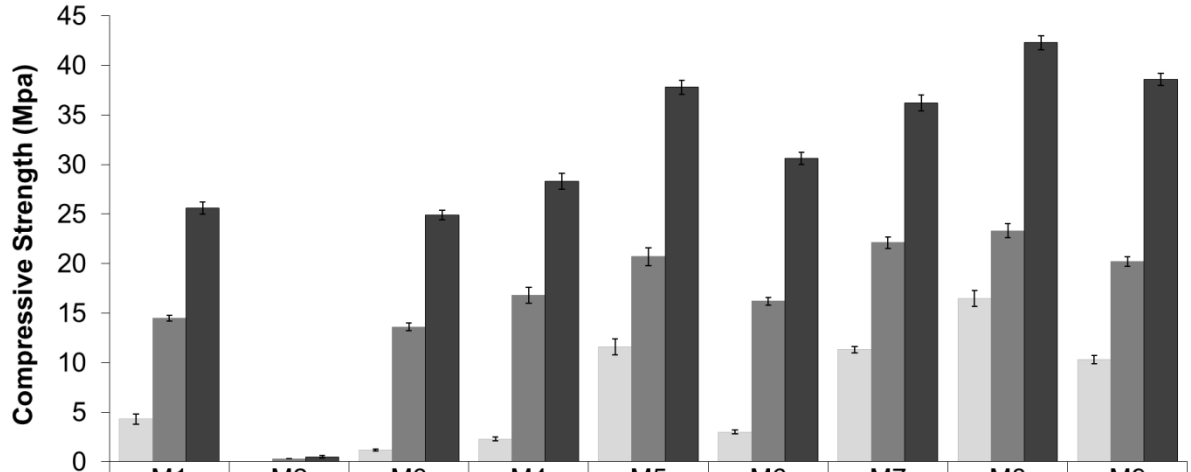

	M1	M2	M3	M4	M5	M6	M7	M8	M9
3 day	4.3	0.0	1.2	2.3	11.6	3.0	11.3	16.5	10.3
7 day	14.5	0.3	13.6	16.8	20.7	16.2	22.1	23.3	20.2
28day	25.6	0.5	24.9	28.3	37.8	30.6	36.2	42.3	38.6

Figure 4: Compressive strength of mortar samples at 7 and 28 days of curing

In mix M2, OPC present in M1 was replaced with slag. No C-S-H/C-A-S-H gel was formed at both 7 and 28 days of curing. There was no change in the gypsum content at both curing ages, but a small amount of hydrogarnet phase was present which showed a considerable increase by 28 days of curing. No xrd peak reflection of the hydrogarnet phase was visible in

the x-ray diffraction data indicating that it is most likely a siliceous hydrogarnet phase which shows very poorly crystalline or amorphous characteristics [36-38]. Fly ash contains negligible content of amorphous alumina, but it is present in large amount in slag. The presence and increase in the siliceous hydrogarnet phase from 7 to 28 days could possibly be because of the hydration reaction of CaO, alumina, and silica present in the amorphous component of the slag. There was a negligible development of compressive strength at 3, 7 and 28 days of curing and the little strength that was observed could possibly be imparted by the calcium aluminate hydrate phase present in the cement matrix. SEM image of M2 shows very little amount of gel formation, which is most likely from the formation of siliceous hydrogarnet phase.

With the addition of 10% HL to the FA and slag blend in M3, there was a small increase in 3 day strength, and a significant improvement at 7 and 28 days of curing, indicating that an alkaline activator was necessary to initiate a pozzolanic reaction in the FA and slag blended composite. The calcium hydroxide powder added externally was instrumental in significantly improving the pozzolanic reaction of the fly ash and slag blend. This further shows that the CaO content present in the amorphous content of the slag is not present as an independent component but is most likely present in combination with alumina or with alumina and silica. The reason being, if CaO were present as an independent elemental oxide, on reacting with water would have provided enough alkalinity for the production of C-S-H/C-A-S-H gel, which wasn't formed in mix M1. Therefore, the amorphous content (CaO, Al_2O_3, SiO_2) of slag is most likely present in the form of calcium aluminate or calcium aluminosilicate phase. The increase in the pozzolanic reaction in M3 at both 7 and 28 days compared to that of M2 was clearly visible in the formation of a considerable amount of C-S-H/C-A-S-H gel as shown in Table 7 and the SEM images are shown in figure 5. The development of C-S-H/C-A-S-H gel can also be corroborated with the consumption of 7.45% $Ca(OH)_2$ out of the total 10% added to the mix. Although M3 showed a significant increase in strength between 7 and 28 days with the corresponding increase in C-S-H/C-A-S-H gel, the increase in the consumption of Ca(OH)2 was very small, and there was a little increase in the hydrogarnet phase. This indicates that the increase in the C-S-H/C-A-S-H gel was most likely due to the internal pozzolanic reaction of the amorphous CaO, Al_2O_3 and the SiO_2 content present in the slag. Since this reaction was not visible in M2, it indicates that Ca(OH)2 present in the pore solution was instrumental in the activation and the resultant pozzolanic reaction of the amorphous CaO, Al_2O_3 and the SiO_2 content present in the slag.

When 2.5% nS was added to the slag, FA and HL blend, in M4, there was an increase in compressive strength of 91.6%, 23.5% and 13.6% at 3, 7 and 28 days respectively. Nano silica is highly reactive in nature because of its amorphous nature and very high surface area compared to that of FA and slag. This results in the increase in the production of additional C-S-H/C-A-S-H gel at both 7 and 28 days of curing compared to that of M3, as can be observed in Table 7, thereby improving its compressive strength at all curing ages. This increase in the production of C-S-H/C-A-S-H gel was also supported by the increase in the consumption of $Ca(OH)_2$ in M4 compared to that of M3. An increase in the hydrogarnet phase in M4 was also noticed at both 7 and 28 days of curing compared to that of M3. But the x-ray diffraction data does not show any peak reflection associated with any hydrogarnet phase. Carlson, E.T. (1956) in his study on the formation of hydrogarnets found that some forms of siliceous hydrogarnets show very poor crystallinity [36]. He also found that the hydrogarnets containing increasing amounts of silica underwent the same type of decomposition at progressively higher temperatures. Typically, thermal decomposition of Katoite (C_3AH_6) a non-siliceous hydrogarnet has an endothermic peak located between ~300 to ~330 °C temperature [28, 39, 40], the hydrogarnet phase in M4 containing 2.5% of amorphous nano silica, showed an endothermic peak centered around ~352 °C. This indicates that the hydrogarnet so formed in M4 is most likely a siliceous hydrogarnet with very low crystallinity, which makes it difficult to identify from the x-ray diffraction data. The SEM image of M4 shows a considerable amount of micro-cracking formed within the cement matrix. A large increase in the chemically bound water was observed in M4 at 7 days indicating a considerable reduction in its internal relative humidity, compared to that of M3. This indicates that the presence of micro-cracking could possibly be because of the self-desiccation effect which increases with the increase in hydration/pozzolanic reaction in low water/cement ratio mixes [41].

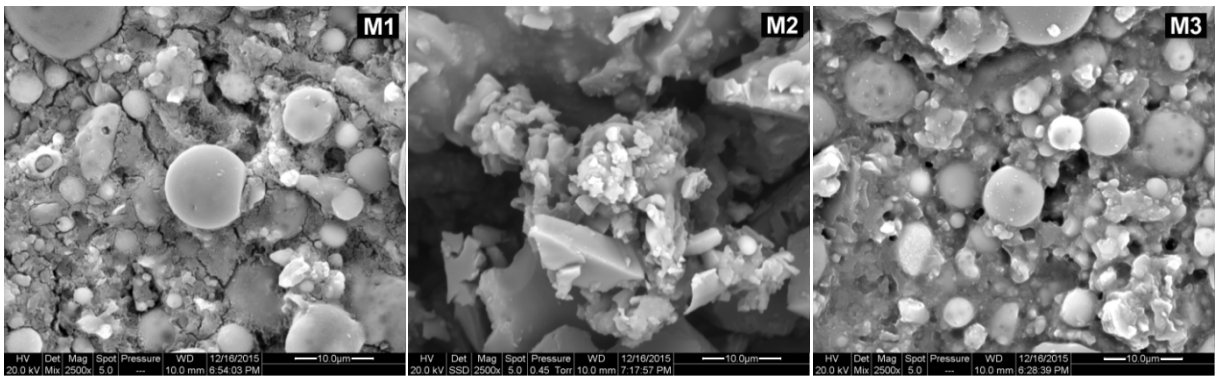

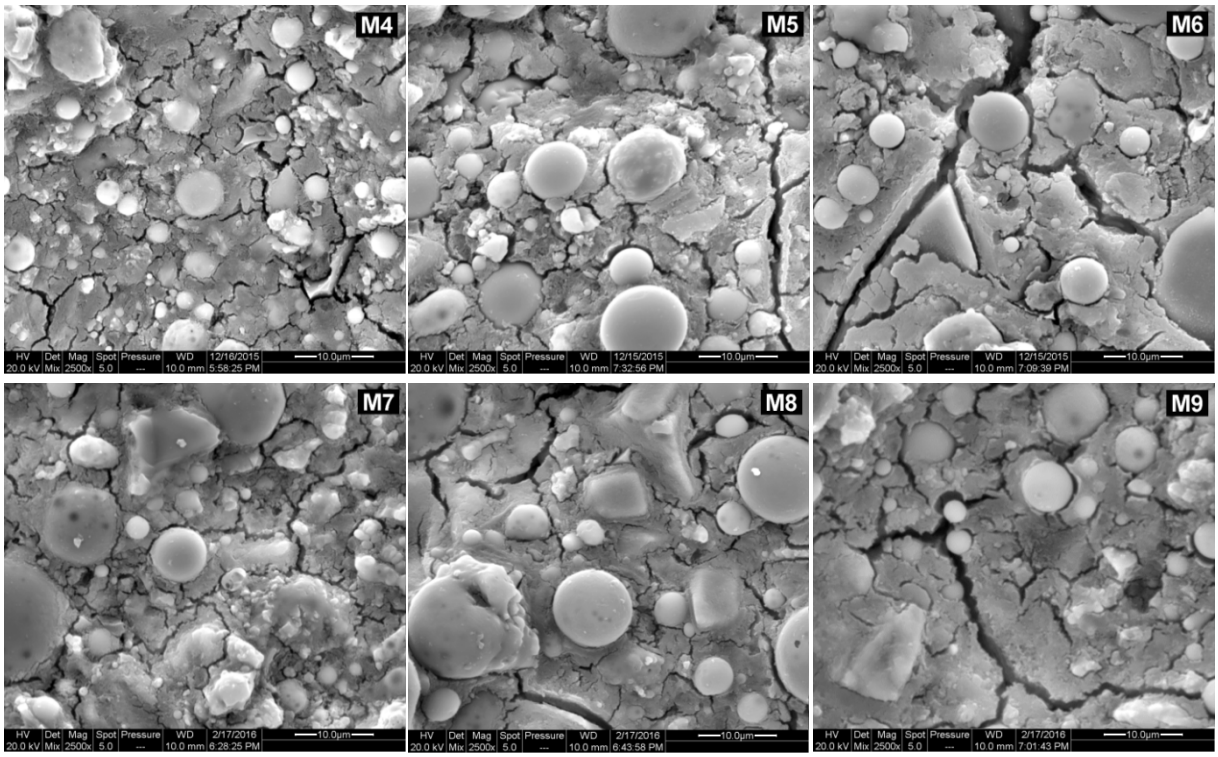

Figure 5: Scanning electron microscopy images of hydrated samples at 28 days of curing

With the increase in nS content to 5% in M5, there was a significant increase in 3 day compressive strength followed by a considerable improvement at 7 and 28 days strengths compared to that of M4. Table 7 shows a considerable improvement in the pozzolanic reaction of M5 as reflected in the increase in C-S-H/C-A-S-H gel at both 7 and 28 days of curing, compared to that of M4. Table 8 shows that the available portlandite was totally consumed at 7 days and there was no other source of production of additional portlandite. In spite of having no availability of portlandite, there was a considerable increase in the C-S-H/C-A-S-H gel between 7 and 28 days. This indicates that there was an internal pozzolanic reaction of the amorphous CaO, Al_2O_3 and SiO_2 content to produce an additional C-A-S-H gel that subsequently improved the 28 day compressive strength of M5 compared to that of M4. There was a considerable increase in the hydrogarnet phase in M5 at both 7 and 28 days of curing compared to that of M4. In addition the TG endothermic peak of the hydrogarnet phase shifted towards a higher temperature indicating an increase in its thermal stability. Moreover, no xrd peak reflection was observed at both 7 and 28 days of curing. This again indicates the formation of siliceous hydrogarnet with very poor crystallinity but increased thermal stability. The SEM image of M5 showed an increase in micro-cracking compared to that of M4, which again could be attributed to the increase in the self-desiccation effect due to the increase in the pozzolanic reaction.

On further increasing the nS content to 7.5% in M6, a 74% reduction in 3 day compressive strength was observed, followed by a 22% and 19% reduction at 7 and 28 days respectively, compared to that of M5. Interestingly, M6 showed a marked increase in the C-S-H/C-A-S-H gel compared to M5, at both 7 and 28 days of curing. The available portlandite was totally consumed at 7 days by the pozzolanic reaction in M6, similar to that in M5 containing 5% nS. This indicates that the increase in C-S-H gel at both 7 and 28 days in M6 compared to that of M5 is most likely due to the internal pozzolanic reaction of the amorphous content present in slag. This also shows that the internal pozzolanic reaction of the amorphous content in the slag increases with the increase in nano silica content. The SEM image of M6 shows an increase in size and density of micro-cracking within the cement matrix, compared to that of M5. This reinforces our earlier observation and also reported by [41], that the self-desiccation effect in low water/cement ratio mixes increases with the increase in pozzolanic reaction resulting in the increase in micro-cracking within the cement matrix. This indicates that the effect of increase in micro-cracking in M6 was more prominent than the increase in the C-S-H/C-A-S-H gel, which negatively impacted its strength development, resulting in the reduction in its compressive strength compared to that of M5. Mix M6 showed a significant increase in the formation of hydrogarnet phase at both 7 and 28 days of curing. Similar to that in M4, this hydrogarnet phase does not show any clearly defined xrd peak reflection and has a TG endothermic peak centered around ~361 °C, indicating that it is most likely a very poorly crystalline siliceous hydrogarnet [36].

Mix M7 had a similar concentration of 2.5% nS, 72.5% FA, and 25% slag as that of M4 but the HL content was increased to 15%. This increase in HL improved its 3 day compressive strength by 404%, followed by a 31.5% and 28% increase in strength at 7 and 28 days of curing, compared to that of M4 containing 10% HL. A considerable increase in the formation of C-S-H/C-A-S-H gel followed by a marked increase in the portlandite consumption was observed at both 7 and 28 days, compared to that of M4. This increase in the C-S-H/C-A-S-H gel was also reflected in a considerable increase in its 7 and 28 day compressive strength compared. A marked reduction in the formation of siliceous hydrogarnet was observed at 7 days, but at 28 days it showed a small increase compared to that of M4. This indicates that at high portlandite concentration the formation of siliceous hydrogarnet slows down, and as the portlandite gets consumed by the amorphous silica present in the mix, the formation of siliceous hydrogarnet accelerates, eventually showing a small increase at 28 days, compared to that of M4. SEM image of M7 shows a similar size and density of micro-cracks compared

to that of M4, but they reduced considerably compared to that of M6. The total chemically bound water of M7 was considerably lower than that of M6 and slightly higher than that of M4, indicating a much higher internal relative humidity in M7 compared to that of M6 and slightly lower than that of M4. Therefore no noticeable difference in micro-cracking in M7 compared to that of M4 in spite of a small decrease in internal relative humidity can be attributed to a considerable increase in C-S-H/C-A-S-H gel, which increases the tensile capacity of the cement matrix that can resist internal stresses. The significant decrease in micro-cracking in M7 compared to that of M6 can be attributed to the formation of slightly higher C-S-H/C-A-S-H gel at 28 days and the presence of considerably higher internal relative humidity at both 7 and 28 days in M7.

When the HL content in mix M8 containing 5% nS, 70% FA and 25% slag (similar to that of M5) was increased to 15%, a considerable increase in the formation of C-S-H/C-A-S-H gel was observed followed by a marked increase in the portlandite consumption both at 7 and 28 days compared to that of M5. This increase in C-S-H gel is also reflected in the corresponding increase in 7 and 28 days compressive strength compared to that of M5. Mix M8 showed a similar trend in the formation of poorly crystalline siliceous hydrogarnet as was observed in M7. There was a considerable decrease in the formation of siliceous hydrogarnet at 7 days compared to that of M5, but this reduction was more pronounced in M8 compared to that in M7. Beyond 7 days the formation of siliceous hydrogarnet accelerated, and was slightly less than that of M5 at 28 days. As a significant amount of the portlandite was consumed by 7 days, the acceleration in the formation of siliceous hydrogarnet is most likely due to the presence of low portlandite concentration and high amorphous silica content within the cement matrix. SEM image of M8 shows an increase in micro-cracking compared to that of M7. This is most likely because of the increase in self-desiccation effect in M8 due to the reduction in internal relative humidity compared to that of M7, which played a more dominant role on the increase in crack formation than the improvement in tensile capacity from the increase in C-S-H/C-A-S-H gel.

Mix M9 had a similar concentration of 7.5% nS, 67.5% FA, and 25% slag as that of M6 but the HL content was increased to 15%. This increase in HL considerably increased the formation of C-S-H/C-A-S-H gel at both 7 and 28 days compared to that of M8 containing a lower concentration of nS and that of M6 containing a lower concentration of HL. This increase in C-S-H/C-A-S-H gel formation was supported by a considerable increase in the

portlandite consumption compared to that of M6 and M8. This indicates that the increase in amorphous silica content increases the potential of the pozzolanic reactivity and demands an increase in the portlandite concentration. Although, the C-S-H/C-A-S-H gel formation in M9 showed a considerable increase compared to that of M8, the compressive strength showed a marked decrease at both 7 and 28 days. The SEM image of M9 shows an increase in width of micro-cracking most likely because of the self-desiccation effect due to a significant decrease in the internal relative humidity of M9 compared to that of M8. The wider the cracks, the deeper they are resulting in the development of a much weaker cement matrix compared to that with a smaller size cracks. Therefore, the reduction in the compressive strength of M9 compared to that of M8 is most likely because of a considerable increase in micro-cracking in M9. A similar trend in the reduction of compressive strength in spite of the increase in C-S-H/C-A-S-H gel was observed in M6 compared to that of M5, which also showed an increase in micro-cracking in M6 compared to that of M5. This shows that 5% is the optimum content of nS for the given set of mix designs of this experiment. However, the increase in HL showed a positive correlation with the increase in pozzolanic reaction and the subsequent increase in the development of compressive strength. There was a considerable decrease in the formation of siliceous hydrogarnet in M9 at both 7 and 28 days compared to that of M6, but it was higher than that of M8 at both curing ages. This indicates that at high portlandite content the increase in amorphous silica accelerates the formation of C-S-H/C-A-S-H gel and hinders the development of poorly crystalline siliceous hydrogarnet. This effect of the increase in C-S-H/C-A-S-H gel followed by the decrease in the formation of hydrogarnet phase increases with the increase in amorphous silica content at high portlandite concentration.

5. Conclusions

Based on the findings of this research, the following conclusions can be drawn:

i) The addition of nano silica can help in achieving an environmental friendly zero cement composite without the need of any heat treatment.

ii) The optimum content of nano silica in a high volume fly ash, slag, and HL blend is 5%. With a further increase in nano silica content although the pozzolanic reaction and the resulting C-S-H/C-A-S-H gel formation increases but it also increase the micro-cracking due to self-desiccation effect in the cement matrix, resulting in negatively impacting the strength development.

iii) Both slag and fly ash require portlandite as an external alkaline activator to initiate a pozzolanic reaction within the cement matrix. Although the slag has high lime (CaO) content, it is not present as free lime that can provide portlandite for an internal pozzolanic reaction.

iv) The portlandite added externally in the form of $Ca(OH)_2$ powder, to the nS modified SCM blend, activates the pozzolanic reaction which increases with the increase in portlandite content.

v) The siliceous hydrogarnet formed due to the pozzolanic reaction of amorphous silica (FA, slag, nS) with the calcium aluminate present in the slag, shows very poor crystallinity with no visible peak reflection in x-ray diffraction data.

vi) The formation of siliceous hydrogarnet increases with the increase in amorphous nano silica but decreases with the increase in hydrated lime concentration within cement matrix.

6. Acknowledgement

The authors fully acknowledge the scientific and technical support provided by the Microscopy & microanalysis facility, Rheology and material characterisation facility and the X-ray facility at RMIT University. The authors would like to thank Cement Australia for providing the material support to carry out this research.

References

[1] Heidrich C, Feuerborn H-J, Weir A. Coal Combustion Products: a Global Perspective. WOCA; 2013.

[2] Malhotra V. Fly ash, slag, silica fume, and rice-husk ash in concrete: a review. Concrete International. 1993;15(4).

[3] Helmuth R. Fly ash in cement and concrete1987.

[4] Malhotra V. High-performance high-volume fly ash concrete. Concrete International. 2002;24(7):30-4.

[5] V.D. G. Ancient, Modern and Future Concretes, Durability of Concrete, Aspect of admixtures and industrial products. Swedish Council for Building Research, Gothengurg, Sweden. 1989:53-62.

[6] Swamy RN. Cement replacement materials: Surrey University Press; 1986.

[7] The Future of Ferrous Slag to 2022. UK: Smithers Apex; 2012.

[8] Rangan BV. Fly ash-based geopolymer concrete. Your Building Administrator. 2008;2.

[9] Wang S, Li VC. Engineered cementitious composites with high-volume fly ash. ACI Materials Journal. 2007;104(3).

[10] Şahmaran M, Yaman İÖ, Tokyay M. Transport and mechanical properties of self consolidating concrete with high volume fly ash. Cement and concrete composites. 2009;31(2):99-106.

[11] Liu M. Self-compacting concrete with different levels of pulverized fuel ash. Construction and Building Materials. 2010;24(7):1245-52.

[12] Paya J, Monzo J, Peris-Mora E, Borrachero M, Tercero R, Pinillos C. Early-strength development of Portland cement mortars containing air classified fly ashes. Cement and concrete research. 1995;25(2):449-56.

[13] Barbhuiya S, Gbagbo J, Russell M, Basheer P. Properties of fly ash concrete modified with hydrated lime and silica fume. Construction and Building Materials. 2009;23(10):3233-9.

[14] Jayakumar M, Abdullahi MS. Experimental Study on Sustainable Concrete with the Mixture of Low Calcium Fly Ash and Lime as a Partial Replacement of Cement. Advanced Materials Research. 2011;250:307-12.

[15] Thomas MD. Optimizing Fly Ash Content for Sustainability, Durability, and Constructability. Proc of Coventry University and The University of Wisconsin, Milwaukee Centre for By-Products Utilization Second International Conference on Sustainable Construction Materials and Technologies, Universita Politecnica Delle Marche, Ancona, Italy Np: np, nd N pag2010.

[16] El-Chabib H, Syed A. Properties of self-consolidating concrete made with high volumes of supplementary cementitious materials. Journal of Materials in Civil Engineering. 2012;25(11):1579-86.

[17] Roychand R, De Silva S, Law D, Setunge S. Micro and nano engineered high volume ultrafine fly ash cement composite with and without additives. International Journal of Concrete Structures and Materials. 2016;10(1):113-24.

[18] Wei X, Zhu H, Li G, Zhang C, Xiao L. Properties of high volume fly ash concrete compensated by metakaolin or silica fume. Journal of Wuhan University of Technology-Mater Sci Ed. 2007;22(4):728-32.

[19] Oner A, Akyuz S, Yildiz R. An experimental study on strength development of concrete containing fly ash and optimum usage of fly ash in concrete. Cement and Concrete Research. 2005;35(6):1165-71.

[20] Oner A, Akyuz S. An experimental study on optimum usage of GGBS for the compressive strength of concrete. Cement and Concrete Composites. 2007;29(6):505-14.

[21] Hogan F, Meusel J. Evaluation for durability and strength development of a ground granulated blast furnace slag. Cement, Concrete and Aggregates. 1981;3(1):40-52.

[22] Shaikh F, Supit S, Sarker P. A study on the effect of nano silica on compressive strength of high volume fly ash mortars and concretes. Materials & Design. 2014;60:433-42.

[23] Roychand R, De Silva S, Law D, Setunge S. High volume fly ash cement composite modified with nano silica, hydrated lime and set accelerator. Materials and Structures. 2016;49(5):1997-2008.

[24] Mohseni E, Miyandehi BM, Yang J, Yazdi MA. Single and combined effects of nano-SiO_2, nano-Al_2O_3 and nano-TiO_2 on the mechanical, rheological and durability properties of

self-compacting mortar containing fly ash. Construction and Building Materials. 2015;84:331-40.

[25] Shaikh FU, Supit SW. Mechanical and durability properties of high volume fly ash (HVFA) concrete containing calcium carbonate ($CaCO_3$) nanoparticles. Construction and building materials. 2014;70:309-21.

[26] Oltulu M, Şahin R. Effect of nano SiO_2, nano Al_2O_3 and nano Fe_2O_3 powders on compressive strengths and capillary water absorption of cement mortar containing fly ash: a comparative study. Energy and Buildings. 2013;58:292-301.

[27] HUNNICUTT WA. Characterization of Calcium-silicate-hydrate and Calcium-alumino-silicate-hydrate, University of Illinois at Urbana-Champaign; 2013.

[28] Scrivener K, Snellings R, Lothenbach B. A Practical Guide to Microstructural Analysis of Cementitious Materials: Crc Press; 2016.

[29] Madej D, Szczerba J, Pięta A, Śnieżek E, Prorok R. Reactions in the system CaO-Al_2O_3-H_2O. Selected Aspects of Modern Engineering: Wydawnictwa AGH; 2013. p. 113-25.

[30] Cardoso FA, Innocentini MD, Akiyoshi MM, Pandolfelli VC. Effect of curing time on the properties of CAC bonded refractory castables. Journal of the European Ceramic Society. 2004;24(7):2073-8.

[31] Schmitt N, Hernandez J-F, Lamour V, Berthaud Y, Meunier P, Poirier J. Coupling between kinetics of dehydration, physical and mechanical behaviour for high alumina castable. Cement and concrete research. 2000;30(10):1597-607.

[32] Dilnesa BZ, Lothenbach B, Renaudin G, Wichser A, Kulik D. Synthesis and characterization of hydrogarnet $Ca_3(Al_xFe_{1-x})_2(SiO_4)_y(OH)_{4(3-y)}$. Cement and Concrete Research. 2014;59:96-111.

[33] Passaglia E, Rinaldi R. Katoite, a new member of the $Ca_3Al_2(SiO_4)_3$-$Ca_3Al_2(OH)_{12}$ series and a new nomenclature for the hydrogrossular group of minerals. Bull Mineral. 1984;107:605-18.

[34] De Jong J, Stein H, Stevels J. Influence of amorphous silica on the hydration of tricalcium aluminate. Journal of Applied Chemistry. 1969;19(1):25-8.

[35] Dilnesa BZ. Fe-containing hydrates and their fate during cement hydration: thermodynamic data and experimental study, ÉCOLE POLYTECHNIQUE FÉDÉRALE DE LAUSANNE; 2011.

[36] Carlson ET. Hydrogarnet Formation in the System Lime-AI flumina-Silica-Water. Journal of Research of the National Bureau of Standards. 1956;56(6).

[37] Dilnesa B, Wieland E, Lothenbach B, Dähn R, Scrivener K. Fe-containing phases in hydrated cements. Cement and Concrete Research. 2014;58:45-55.

[38] Vespa M, Wieland E, Dähn R, Lothenbach B. Identification of the Thermodynamically Stable Fe-Containing Phase in Aged Cement Pastes. Journal of the American Ceramic Society. 2015;98(7):2286-94.

[39] George C. Industrial Aluminous Cements in: Structure and performance of cements, S. 415 ff.; edited by P. Barnes. Applied Science Publishers; 1983.

[40] Fryda H, Scrivener K, Chanvillard G, Féron C. Relevance of laboratory tests to field applications of calcium aluminate cement concretes. International conference on calcium aluminate cements2001. p. 227-46.

[41] Persson B. Self-desiccation and its importance in concrete technology. Materials and Structures. 1997;30(5):293-305.

Chapter 7

7. Conclusions and recommendations for further research

7.1. Conclusions

This research investigated the effect of various micro and nano materials in combination with different cement additives on low calcium class F high volume fly ash with or without the use of GGBFS. The major conclusions of this research are summarised below:

i) Silica fume, when used in conjunction with SA or HL considerably improves the pozzolanic reaction of HV-UFFA cement composite resulting in the improvement of its compressive strength. But, when both SA and HL are used in conjunction with the SF, the combined effect provides the best performance in accelerating the pozzolanic reaction resulting in a significant improvement in its compressive strength.

ii) Use of silica fume considerably reduces the development of micro cracks but when it is combined with the SA or HL increases the formation of micro cracks due to the combined effect of disjoining pressure and self-desiccation effect. The highest stresses are induced when both the SA and the HL are combined with SF resulting in a significant increase in crack formation. However, this mix presented the best compressive strength because the increase in the production of C-S-H gel from the accelerated pozzolanic reaction resulted in counterbalancing the effect of increased cracking, thereby, improving its compressive strength.

iii) Nano silica, when used in conjunction with the SA or the HL considerably improves the pozzolanic reaction of HV-UFFA cement composite resulting in the improvement of its 1 day compressive strength. However, the formation of micro cracks due to the disjoining pressure and self-desiccation effect hinders the development of its later age strengths inspite of the increase in pozzolanic reaction. When both SA and HL are used in conjunction with the nS, the combined effect further accelerates the pozzolanic reaction, resulting in considerably improving its 1 day strength. But at later ages their combined effect significantly increases the formation of early age micro cracks resulting in considerably hindering the development of 7 and 28 day strengths, inspite of the increase in pozzolanic reaction.

iv) Ultra-fine fly ash when combined with nano silica can help in achieving 80% replacement of cement, having comparable mechanical properties to that of OPC.

v) Addition of set accelerator considerably increases the formation of delayed ettringite content. This increase in delayed ettringite content had a detrimental impact on the compressive strength of nano silica modified HVFA blends. The effect of ettringite content at 7 days was inversely proportional to the the percentage of nano silica content. Since, higher nano silica content results in higher early strength, the detrimental effect of the expansive forces of delayed ettringite was reduced, thereby resulting in higher strength in 7.5% nS blended mix as compared to the one containing 5% nano silica.

vi) The optimum quantity of nano silica in a mix design is highly dependent on the quantity of portlandite availability in the mix design. Mix designs containing higher portlandite content (as shown in chapters 3, 4 and 6) either due to the presence of higher OPC content or due to externally added $Ca(OH)_2$ showed 5% nano silica to be the optimum content. However at lower OPC content (as shown in chapters 5) where there is no externally added $Ca(OH)_2$ and even the content of OPC is the lowest of all experiments, which produces lower portlandite, shows an increase in compressive strength even at 7.5% of nano silica content. This indicates that the disjoining pressure induced by the increase in pore solution concentration of calcium ions (Ca^+, $CaOH^+$) in conjunction with the self-desiccation due to the increase in pozzolanic reaction combine together at higher concentrations of nano silica thereby resulting in the reduction of compressive strength at higher nano silica content i.e. 7.5%.

vii) The addition of nano silica to class F low calcium HVFA cement composite considerably increases the formation and thermal stability of silica-rich hydrogarnet phase, which increases with the increase in nano silica content.

viii) The addition of both 2.5% and 5% nCC content show no increase in the pozzolanic reaction at 7 days of curing, but shows a small increase in compressive strength, which increases with the increase in nCC content. This could possibly be attributed to dense particle packing effect provided by nCC to the cement matrix. The improvement in the reactivity of fly ash due to the addition of nCC is evident at 28 days of curing from the increase in C-S-H gel and corresponding increase in compressive strength. This increase in the formation of C-S-H gel and the commensurate increase in 28 day strength increases with the increase in nCC content.

ix) The addition of nano alumina helps in improving the mechanical properties of VHVFA cement composite, only if added in small quantity i.e. 2.5% or possibly lower. At

higher concentration the hydration/pozzolanic reaction is severely inhibited due to the formation of large amounts of $Al(OH)_3$ gel resulting in negligible formation of C-S-H/C-A-S-H gel (if any), leading to a significant reduction in the compressive strength results, compared to that of M6 having lower nA content.

x) The addition of nano silica can help in achieving an environmental friendly zero cement composite without the need of any heat treatment.

xi) The optimum content of nano silica in a high volume fly ash, slag, and HL blend is 5%. With a further increase in nano silica content although the pozzolanic reaction and the resulting C-S-H/C-A-S-H gel formation increases but it also increase the micro-cracking due to self-desiccation effect in the cement matrix, resulting in negatively impacting the strength development.

xii) Both slag and fly ash require portlandite as an external alkaline activator to initiate a pozzolanic reaction within the cement matrix. Although the slag has high lime (CaO) content, it is not present as free lime that can provide portlandite for an internal pozzolanic reaction.

xiii) The portlandite added externally in the form of $Ca(OH)_2$ powder, to the nS modified SCM blend, activates the pozzolanic reaction which increases with the increase in portlandite content.

xiv) The siliceous hydrogarnet formed due to the pozzolanic reaction of amorphous silica (FA, slag, nS) with the calcium aluminate present in the slag, shows very poor crystallinity with no visible peak reflection in x-ray diffraction data.

xv) The formation of siliceous hydrogarnet increases with the increase in amorphous nano silica but decreases with the increase in hydrated lime concentration within cement matrix.

xvi) Overall it is concluded that the compressive strength development in cement composites containing supplementary cementitious materials predominantly depends upon the following:

- Particle size: smaller the particle size, higher is the pozzolanic rate resulting in the increase in compressive strength. This was demonstrated by the improvement in compressive strength in the following order: nano silica > silica fume > ultrafine fly ash > raw fly ash.

- Amorphous silica content: higher the amorphous silica, higher is the formation of C-S-H gel resulting in the increase in compressive strength which is in the following order: nano silica > silica fume > fly ash
- Internal relative humidity: the rate of decrease in internal relative humidity at early ages due to the increase in pozzolanic reaction significantly affects the strength development due to the increase in self-desiccation effect and formation of micro-cracks. The strength development depends upon the counterbalancing role of the formation of C-S-H gel (positive effect) and the formation of micro-cracks due self-desiccation (negative effect). The development of compressive strength depends upon the factor that shows dominant effect in the cement microstructure. If the formation of C-S-H gel shows the dominant effect the self-desiccation effect does not show adverse effect in considerably hindering the development of compressive strength. However, in place of C-S-H gel, the increase in pozzolanic reaction shows the dominant effect in the formation of C-A-H along with a significant reduction in the internal relative humidity, they both combine to significantly hamper the development of compressive strength.

7.2. Recommendations for further research

i) The scope of this research was limited to only one type of fly ash. Therefore, further investagations need to be undertaken on various different fly ashes using the same treatments, to study the variation in the results of the physicochemical properties of the blended cement/cementitious material composites.

ii) Due to the cost of nano silica used this research was undertaken on mortar samples only. Further research needs to be undertaken on concrete so that possible industrial applications could be explored based on the achieved results.

iii) This study looked at only the mechanical properties to optimise the use of various micro/nano materials and cement additives to develop a cement composite replacing 70 - 100% cement. Further investigations need to be undertaken to study the durability properties of the various optimised cement composites.

iv) The addition of both SA and HL to the nano silica modified HVFA cement composites show a significant increase in its pozzolanic reaction, but a considerable reduction in its compressive strength. This effect of reduction in strength in spite of the increase in

pozzolanic reaction is due to a considerable increase in the formation of micro cracks induced by the self-desiccation effect and disjoining pressure. There is a great potential of tapping the benefits of the accelerated pozzolanic reaction to further improve the mechanical properties if the formation of micro cracks are controlled, which can be studied in the future research.

v) Nano silica modified HVFA cement composites show a very dense cement matrix as observed in the SEM images. If suitable high tensile strength fibers are incorporated into nano silica modified HVFA cement composites, they can help in improving its flexural strength by providing a strong anchorage to the fibers within the cement matrix. This can be further explored in the future research.

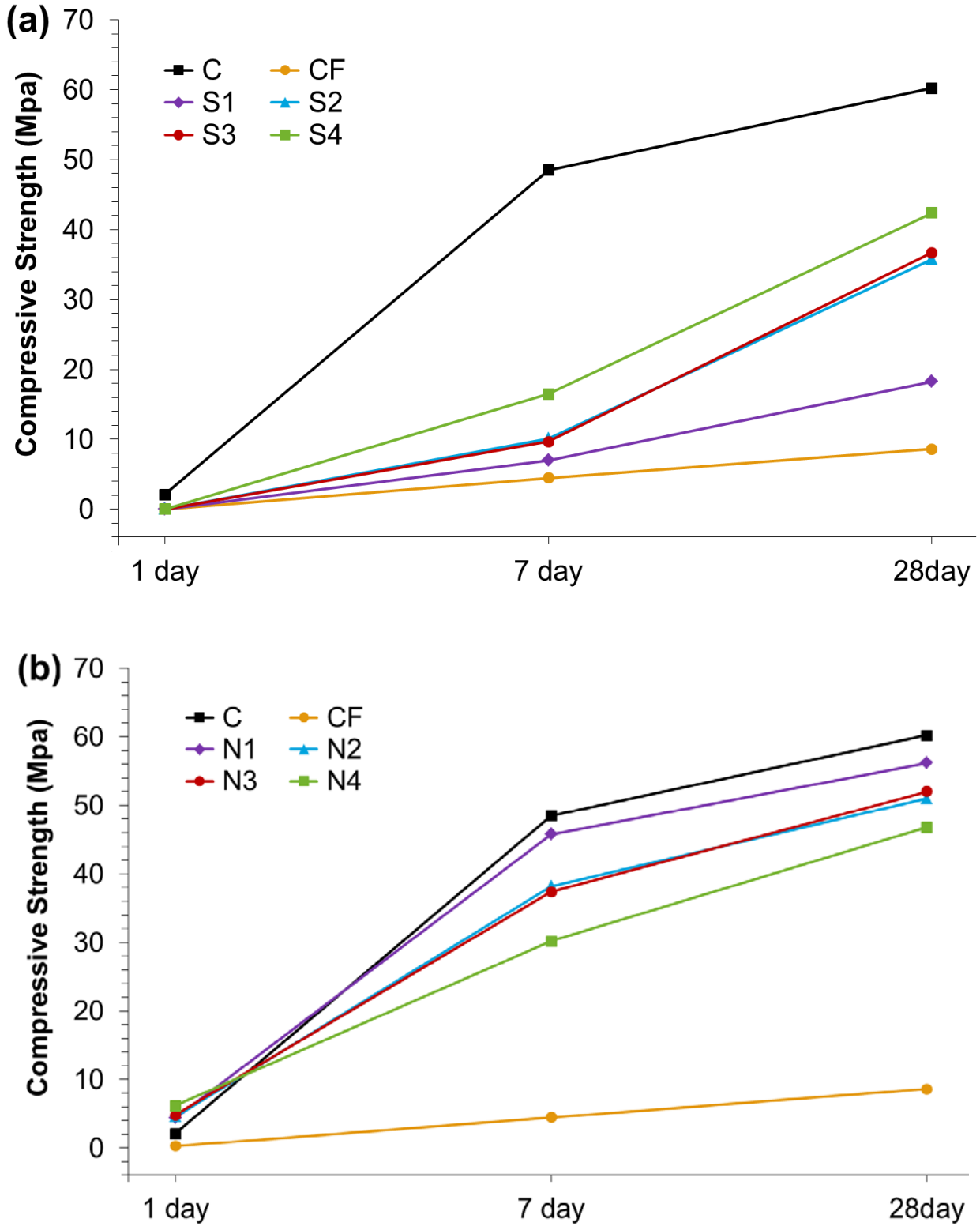

Figure 2 (Chapter 3): Compressive strength of mortar samples (a) containing silica fume (b) containing nano silica at 1, 7 & 28 days of curing

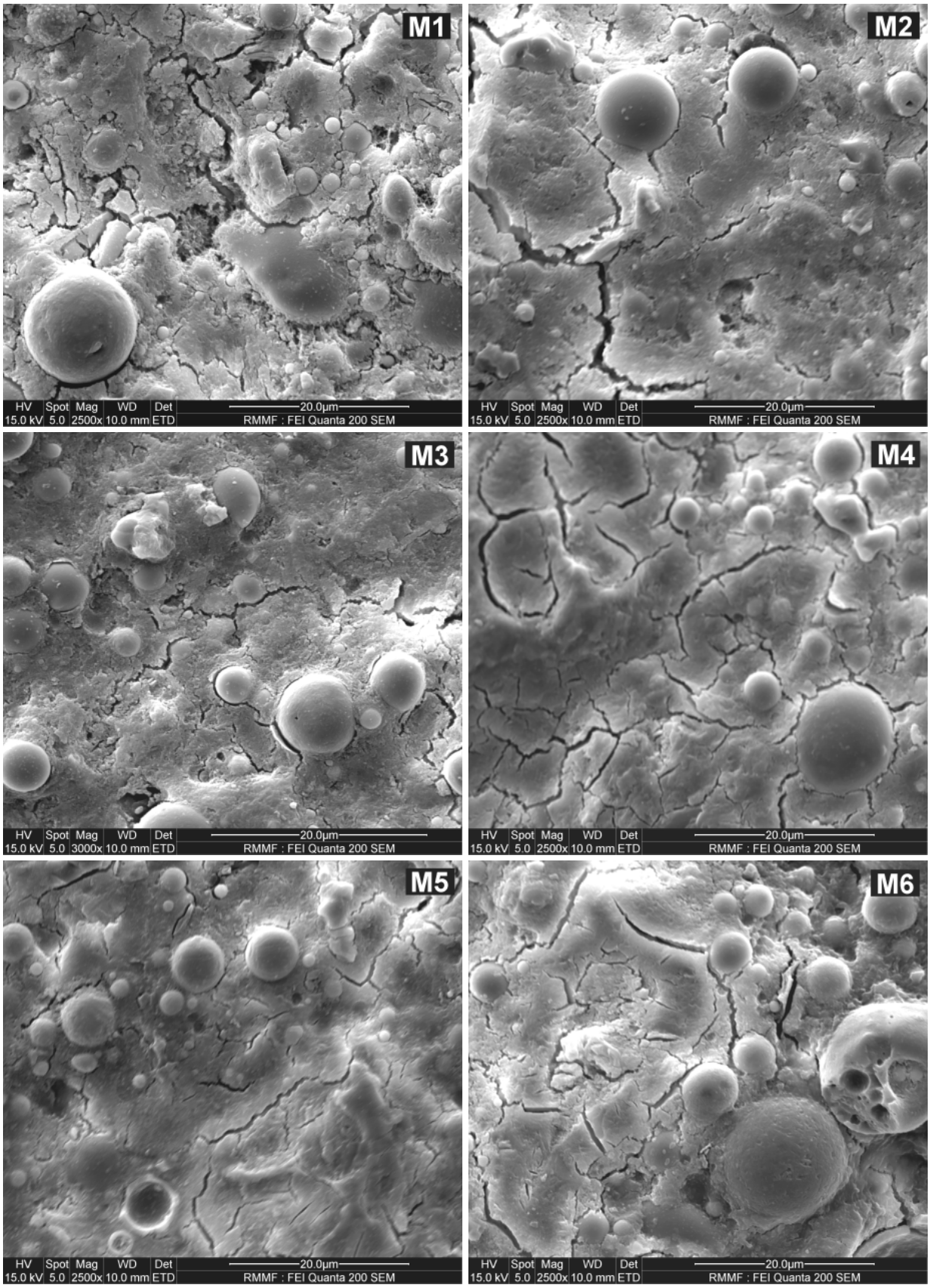
M1
HV Spot Mag WD Det
15.0 kV 5.0 2500x 10.0 mm ETD
20.0µm
RMMF : FEI Quanta 200 SEM
M2
HV Spot Mag WD Det
15.0 kV 5.0 2500x 10.0 mm ETD
20.0µm
RMMF : FEI Quanta 200 SEM
M3
HV Spot Mag WD Det
15.0 kV 5.0 3000x 10.0 mm ETD
20.0µm
RMMF : FEI Quanta 200 SEM
M4
HV Spot Mag WD Det
15.0 kV 5.0 2500x 10.0 mm ETD
20.0µm
RMMF : FEI Quanta 200 SEM
M5
HV Spot Mag WD Det
15.0 kV 5.0 2500x 10.0 mm ETD
20.0µm
RMMF : FEI Quanta 200 SEM
M6
HV Spot Mag WD Det
15.0 kV 5.0 2500x 10.0 mm ETD
20.0µm
RMMF : FEI Quanta 200 SEM

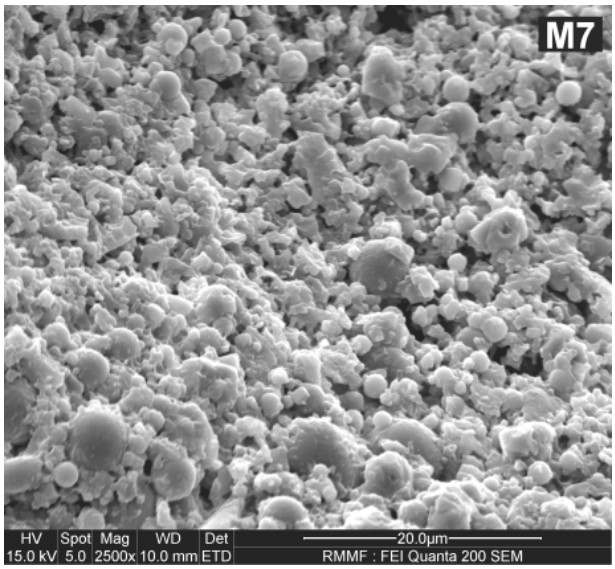

Figure 6 (Chapter 5): Scanning electron microscopy images of hydrated samples at 28 days of curing (High resolution)

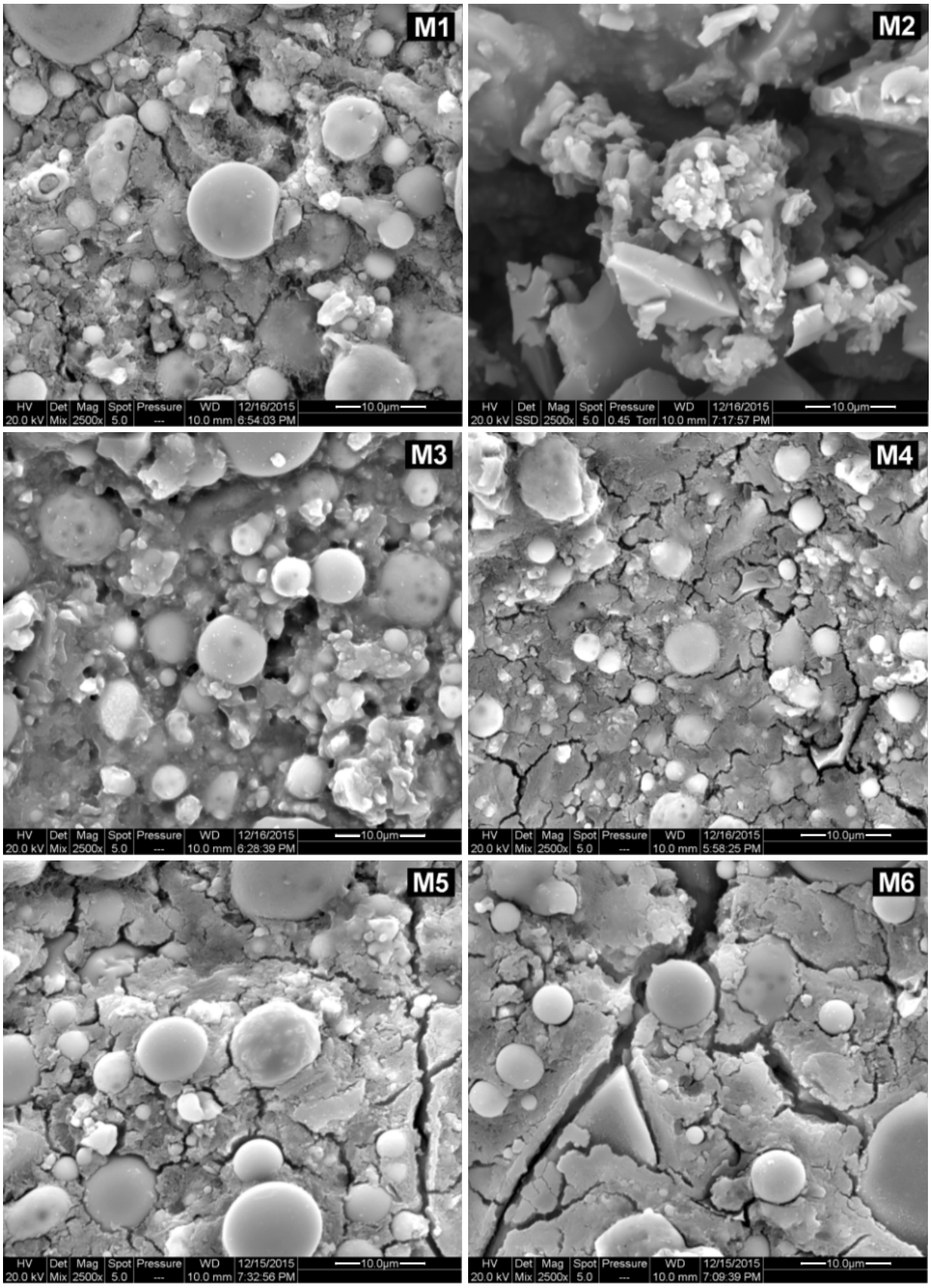
M1
HV Det Mag Spot Pressure WD 12/16/2015
20.0 kV Mix 2500x 5.0 --- 10.0 mm 6:54:03 PM
10.0µm
M2
HV Det Mag Spot Pressure WD 12/16/2015
20.0 kV SSD 2500x 5.0 0.45 Torr 10.0 mm 7:17:57 PM
10.0µm
M3
HV Det Mag Spot Pressure WD 12/16/2015
20.0 kV Mix 2500x 5.0 --- 10.0 mm 6:28:39 PM
10.0µm
M4
HV Det Mag Spot Pressure WD 12/16/2015
20.0 kV Mix 2500x 5.0 --- 10.0 mm 5:58:25 PM
10.0µm
M5
HV Det Mag Spot Pressure WD 12/15/2015
20.0 kV Mix 2500x 5.0 --- 10.0 mm 7:32:56 PM
10.0µm
M6
HV Det Mag Spot Pressure WD 12/15/2015
20.0 kV Mix 2500x 5.0 --- 10.0 mm 7:09:39 PM
10.0µm

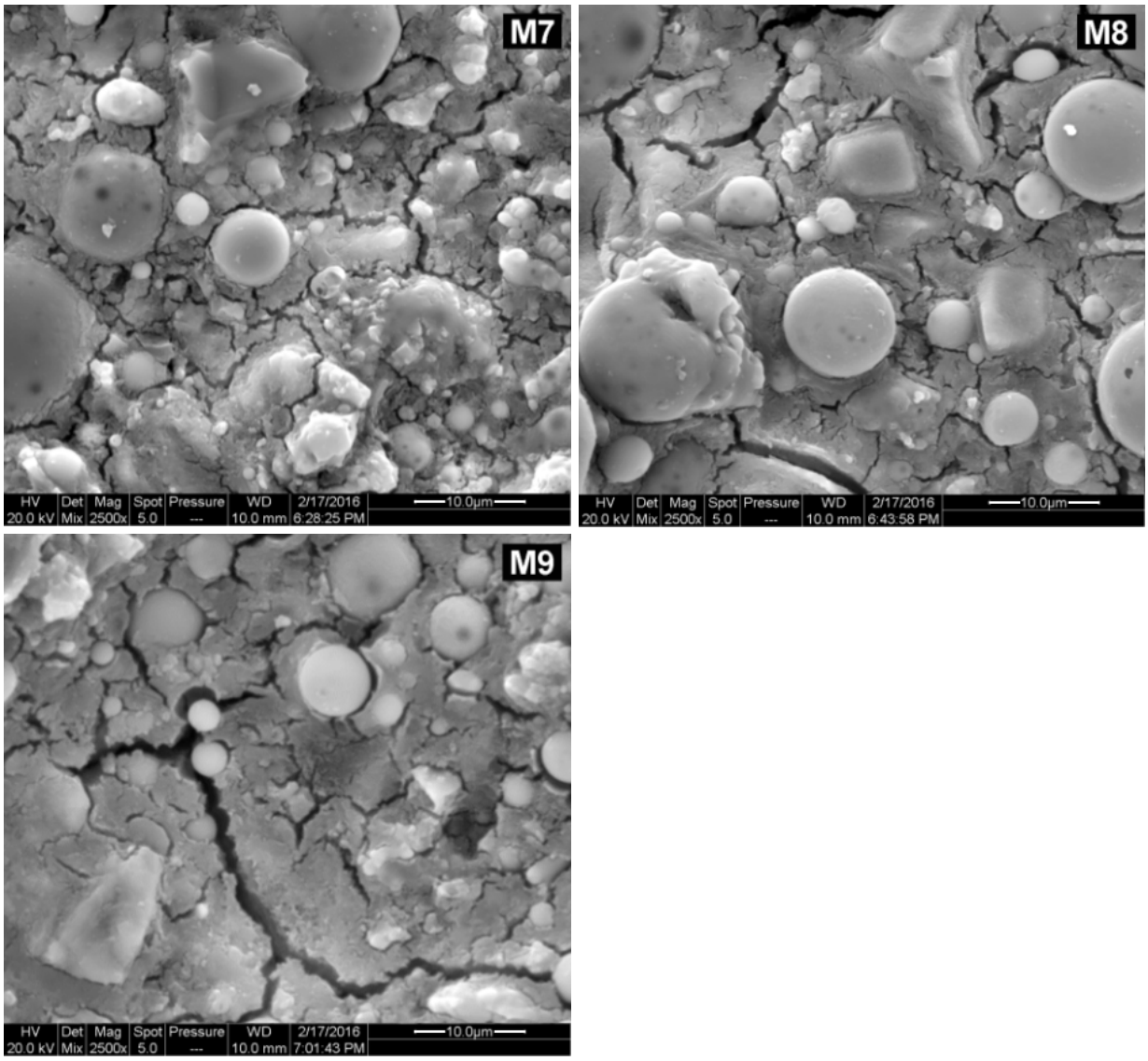

Figure 5 (Chapter 6): Scanning electron microscopy images of hydrated samples at 28 days of curing (High resolution)